

**Interactive effects of CO₂ enrichment and drought stress on photosynthesis
and productivity in field grown short rotation coppice mulberry (*Morus* Spp.),
a potential bio-energy tree species**

Submitted for the award of

Doctor of Philosophy

By

Kalva Madhana Sekhar

(10LPPH05)

Supervisor: Professor Attipalli R. Reddy



Department of Plant Sciences

School of Life Sciences

University of Hyderabad

Hyderabad 500046, India



**Department of Plant Sciences
School of Life Sciences
University of Hyderabad
Hyderabad-500046**

DECLARATION

I, Kalva Madhana Sekhar, hereby declare that this thesis entitled “**Interactive effects of CO₂ enrichment and drought stress on photosynthesis and productivity in field grown short rotation coppice mulberry (*Morus Spp.*), a potential bio-energy tree species**” submitted by me under the supervision of **Prof. Attipalli R. Reddy** is an original and independent research work. I also declare that it has not been submitted previously in part or in full to this University or any other University or Institution for the award of any degree or diploma. The particulars given in this thesis are true to the best of my knowledge and belief.

Date:

Name: Kalva Madhana Sekha

Signature:

Regd. No: 10LPPH05

ACKNOWLEDGEMENTS

*I express my overwhelming sense of gratitude to my supervisor **Prof. Attipalli R. Reddy** for accepting and allowing me to work in his lab. His continuous encouragement, stimulating guidance and moral support enabled me to complete research work successfully. The blessings, help and advice given by him time to time shall carry me a long way in the journey of life on which I am about to embark.*

*I would like to thank Doctoral Committee members, **Prof. A. S. Raghavendra** and **Prof. K.P.M.S.V. Padmasree**, for their cordial support, valuable suggestions and guidance throughout my research work.*

*I extend my sincere and heartfelt gratitude to Head of the Department of Plant Sciences, **Prof. Ch. Venkata Ramana** and former Head **Prof. A. R. Reddy** for providing the necessary departmental facilities for the smooth conduction of research work.*

*I am thankful to the Dean **Prof. P Reddanna** and former Deans **Prof. M. Ramanadham**, **Prof. A. S. Raghavendra**, **Prof. AparnaDutta Gupta** for extending facilities available in the school for my research work.*

*I extend my sincere thanks to all the **faculty members** of School of Life Sciences, for permitting me to use the research facilities.*

*My greatest gratitude goes to my beloved teacher **Dr. Sreenivasa Rao**, who taught me just not science, also ethics and morals in life.*

*I am so grateful to my seniors **Dr. Chalapathi**, **Dr. Girish**, **Dr. Debashree** and **Dr. Anirban Guha** for their help and support. I specially thank **Dr. Debashree** for her suggestions and help.*

*I thank my present lab mates Chaitnaya, Sumit, Shalini, Harsha, Suresh, Sitaram, Tamna and Divya for maintaining a cheerful environment in the lab. I specially thank **Shalini**, **Harsha** and **Sitaram** for their help and support during my PhD tenure.*

*I am thankful to our field assistants **Mr. Lakshman**, **Mr. Ashok**, **Mr. Satish** for their help in maintaining the plants and lab work. I specially thank **Lakshman** for his help during my PhD period for maintaining my plants.*

*I thank all the **non-teaching staff** members of Department of Plant Sciences and School of life Sciences for their help.*

*I thank **DBT**, **DST**, **CSIR** and **DST-Nanotechnology** for funding the lab.*

*I thank **DST-FIST**, **UGC-SAP** and **DBT-CREBB** for the facilities in the Department/School.*

*I am so grateful to my friends and well wishers **Dr. Krishnarjuna**, **Dr. Gangadhar**, **Dr. Ramesh**, **Dr. A. Venugopal**, **Dr. Sunil**, **Lakshmi Kanth** and **Pratap** for their encouragement, suggestions, care and help offered to me personally and professionally during my Ph.D.*

My heartfelt thanks to all my HCU friends for their care, support and encouragement throughout research work.

*I extend my sincere and heartfelt thanks to my brother-in-law **Lakshmi Sekhar**, my sister **Maheswari** and niece **Lakshmi Thanmayi** for their co-operation, love and support throughout my life. I never forget his help and support during my difficulties.*

*My deepest gratitude goes to my brother and family (**Kalva Mahesh, Lakshmi, Cherry and Aradhya**) for their co-operation, love and support throughout my life.*

*I express my overwhelming sense of gratitude to my better half (wife) **Dr. Lakshmi** and my son's **K. Madhava Sai Krish (Apple)** and **K. Mahaswin Sai Bahuleya (Bahu)** for their love and affection. Understanding me best as a Ph.D. herself, **Dr. Lakshmi** has been my best friend and great companion, loved, supported, encouraged, entertained, and helped me get through this agonizing period in the most positive way. Her tolerance of my occasional vulgar moods is a testament in itself of her unyielding devotion and love.*

*I have no words to put across gratefulness to **my parents**; this work should serve as a small token for their unconditional love, encouragement and support. I never would have made it this far without them. I would also like to apologize for all the inconvenience caused to them during my research work.*

I am thankful to one and all, who helped me directly or indirectly at every stage of my research work.

*All that I cherish today is the grace of God. I thank the **Almighty God** for answering my prayers, for granting me the strength, wisdom, knowledge and showering his blessings upon me during research work.*

I dedicate this thesis to my parents and kalva family members

Kalva Madhana Sekhar

LIST OF CONTENTS

Contents	Pages
Chapter-1: Introduction	1-24
1.1 <i>Climate change: the world's most burning problem</i>	1-4
1.2 <i>Effect of elevated atmospheric [CO₂] on plant growth and photosynthetic physiology</i>	4-5
1.3 <i>Impact of elevated [CO₂]-drought interaction on photosynthetic performance and oxidative stress response of plants</i>	6-7
1.4 <i>Correlation of hydraulic conductivity and photosynthetic performance under elevated CO₂ and drought</i>	7-11
1.5 <i>Role of aquaporins (AQPs) in regulating hydraulic conductivity and photosynthesis under elevated [CO₂] and drought conditions</i>	11-13
1.6 <i>Importance of woody tree species as bio-energy resources and potential carbon sinks under future climate conditions</i>	13-14
1.7 <i>Important woody tree species for SRC, acting as potential bio-energy sources and carbon sinks</i>	14-16
1.8 <i>Mulberry: a potential bio-energy tree species for SRC forestry</i>	16-20
1.9 <i>Objectives for the current study</i>	21
Chapter-2: Materials and Methods	22-41
2.1 <i>Experimental facility</i>	25
2.2 <i>Plant material and Experimental Layout</i>	22-26
2.3 <i>Photosynthetic leaf gas exchange physiology</i>	27
2.4 <i>Photosynthetic response (A) to increased photosynthetic photon flux density (Q) and intercellular CO₂ concentration (C_i)</i>	27-30
2.5 <i>Chlorophyll a fluorescence measurements</i>	30-31
2.6 <i>Scanning Electron Microscopy (SEM)</i>	31
2.7 <i>Specific leaf area (SLA) and leaf biochemistry</i>	31-32
2.8 <i>Antioxidant enzyme activities and gene expression</i>	32-36
2.9 <i>Estimation of oxidative stress parameters, osmolytes and molecular antioxidants</i>	37-38
2.10 <i>Measurements of leaf relative water content (RWC), plant hydraulic conductivity parameters and aquaporins (AQPs) gene expression</i>	38-39
2.11 <i>Changes in morphological characteristics, plant growth, destructive biomass yield and carbon sequestration potential</i>	39-41
2.12 <i>Statistical analysis</i>	41
Chapter-3: Results	42-96
3.1 <i>Variations in photosynthesis, growth and bio-mass yield responses of two contrasting drought tolerant (DT) mulberry cultivars under elevated [CO₂] atmosphere</i>	42-49

3.2	<i>Establishing the long term carbon sequestration potential of mulberry with coppice management practices under [CO₂] enriched environment</i>	50-64
3.3	<i>Exploring the dynamic changes of antioxidant systems in short rotation Coppice (SRC) mulberry in response to elevated [CO₂] and Drought individually as well as in their combination</i>	65-85
3.4	<i>Investigating the coordinate changes of hydraulic conductance and photosynthesis with particular reference to expression profiles of certain AQPs in short rotation coppice mulberry</i>	86-96

Chapter-4: Discussion	97-122
------------------------------	---------------

4.1	<i>Mulberry plants showed genotypic variations under [CO₂] enriched environment</i>	97-99
4.2	<i>Short rotation coppice (SRC) mulberry plants exhibited photosynthetic acclimation under long term [CO₂] enrichment</i>	100-103
4.3	<i>Elevated [CO₂] ameliorates drought induced negative effects in short rotation coppice (SRC) mulberry even under prolonged dry environments</i>	103-109
4.4	<i>SRC mulberry exhibited better photosynthetic performance and delayed drought- related symptoms even under prolonged drought conditions due to better hydraulic conductance</i>	109-112

Chapter-5: Summary and Conclusions	113-116
---	----------------

Chapter-6: Literature cited	117-131
------------------------------------	----------------

List of Publications

LIST OF FIGURES AND TABLES

Figures

Fig 1.1 Exponential rise in [CO₂] and temperature in the atmosphere from 18th to 21st century.

Fig 1.2 Different sources of anthropogenic emission of GHGs in to the atmosphere.

Fig 1.3 Cardinal symptoms of photosynthetic acclimation in plants grown under elevated [CO₂] environments due to source to sink imbalance under nutrient limiting conditions.

Fig 1.4 Schematic representation of enzymatic and non-enzymatic antioxidant defense mechanism in plants to combat the oxidative stress induced by different types of abiotic stress factors.

Fig 1.5 (A) Soil-plant-air continuum functioning in maintenance of water transport column
(B) Fine coordination between leaf gas exchange and whole plant hydraulic conductance (K_{plant}).

Fig 1.6 Aquaporins (PIPs and TIPs) facilitates the movement of both H₂O and CO₂ in different compartments as well as organelles of plant cells.

Fig 1.7 Schematic representation of carbon neutral renewable bio-energy production from short rotation coppice (SRC) forestry.

Fig 1.8 Rationale for selecting the mulberry as the model plant for the present study.

Fig 2.1 OTCs established in the botanical garden of University of Hyderabad for [CO₂] enrichment studies.

Fig 2.2 Infra red gas analyzer (IRGA) used for the measurements of photosynthetic leaf gas exchange physiology (A) and Handy PEA used for measuring PS-II efficiency (B) in mulberry.

Fig. 2.3 An ideal A/C_i curves showing changes in *in vivo* RuBP carboxylation (V_{cmax}) and its regeneration (J_{max}).

Fig 2.5 Measurements of *in situ* stem and leaf hydraulic conductance by hydraulic conductivity meter (HCM) in mulberry.

Fig 3.1 Photosynthetic rates in relation to photosynthetic photon flux density (PPFD) in S-13 and K-2 mulberry genotypes grown in ambient and elevated [CO₂].

Fig 3.2 Radar plot showing mean changes of chlorophyll *a* fluorescence JIP-test parameters in S-13 and K-2 grown under elevated and ambient [CO₂] atmosphere.

- Fig 3.3** Morphology and phenology of S-13 and K-2 mulberry genotypes grown under elevated (A) and ambient (B) [CO₂] atmosphere.
- Fig 3.4** Changes in biomass accumulation patterns in the two mulberry genotypes (S13 and K2) grown under ambient and elevated [CO₂] concentrations.
- Fig 3.4** Changes in A/C_i curves in SRC mulberry grown under elevated and ambient [CO₂] environments.
- Fig 3.5** Variations in parameters (V_{cmax} , J_{max} and A_{max}) deduced from A/C_i curves in mulberry grown under elevated and ambient [CO₂] environments.
- Fig 3.6** Changes in A/Q curves in SRC mulberry grown under elevated and ambient [CO₂] environments.
- Fig 3.7** Variations in parameters (A_{Sat} , AQE and LCP) deduced from A/Q curves in mulberry grown under elevated and ambient [CO₂] environments.
- Fig 3.8** Correlation between foliar nitrogen Vs V_{cmax} and J_{max} and V_{cmax} Vs J_{max} in mulberry grown under elevated and ambient [CO₂] environments
- Fig 3.9** SEM images of an abaxial surface of mulberry leaves grown under ambient and elevated [CO₂] grown plants to represent stomatal density and aperture.
- Fig 3.10** Morphological changes and destructive biomass yields from SRC-I to SRC-IV in both ambient and elevated [CO₂] grown mulberry plants.
- Fig 3.11** Biomass yields and carbon sequestration in SRC mulberry plants grown under both ambient and elevated [CO₂] atmosphere after one year of [CO₂] exposure
- Fig 3.12** Morphological changes between elevated and ambient [CO₂] grown SRC mulberry Plants (harvested for every 90 days) after 3 years of [CO₂] exposure.
- Fig 3.13** Cumulative biomass yields and the amount of carbon sequestered after three years of [CO₂] exposure in mulberry under both ambient and elevated CO₂ atmosphere.
- Fig 3.14** Morphological changes in mulberry plants grown under both elevated and ambient [CO₂] atmosphere at 30 days after stress (30DAS).
- Fig 3.15** ImageJ analysis showing changes in plant phenological characteristics, total chlorophyll content and above ground biomass yields at 30DAS in both elevated and ambient [CO₂] grown mulberry.
- Fig 3.16** Variations in photosynthetic leaf gas exchange physiology, chlorophyll a fluorescence characteristics and leaf relative water content (RWC).

Fig 3.17 Changes in antioxidant enzyme activities in mulberry.

Fig 3.18 Amplification of specific regions (200-300bp) from genes encoding key antioxidant enzymes using gene specific primers.

Fig 3.19 changes in transcript abundance of different antioxidant isoforms in mulberry.

Fig 3.20 Changes in oxidative stress characteristics, osmolyte content and molecular antioxidants in mulberry.

Fig 3.21 Variations in carbon assimilation rates (A) with increasing photosynthetic photon flux density (PPFD) , leaf water potential and parameters deduced from A/PPFD curves under well watered (WW) as well as after 30 days of drought (WS) between plants grown under elevated and ambient [CO₂] environments.

Fig 3.22 Changes in reciprocal instantaneous photosynthetic measurements between elevated and ambient [CO₂] grown plants in well watered (WW) and water stress environments (WS).

Fig 3.22 Variations in OJIP chl a fluorescence transients recorded in dark adapted mulberry plants grown in elevated and ambient [CO₂] conditions under control as well as drought environments.

Fig 3.23 Radar plot showing the mean changes of chlorophyll *a* fluorescence JIP-test parameters in mulberry between elevated and ambient [CO₂] grown plants under all the experimental conditions.

Fig 3.24 pipeline models showing the changes in phonological fluxes and number of open RCs per CSm in mulberry grown under elevated and ambient [CO₂] under WW as well as WS conditions

Fig 3.25 Changes in plant water status in SRC mulberry grown in elevated as well as ambient [CO₂] environments under WW as well as WS conditions.

Fig 3.26 Variations in plant hydraulic dynamics in mulberry grown in elevated as well as ambient [CO₂] environments under WW as well as WS conditions.

Fig 3.27 Correlation between K_S and photosynthetic leaf gas exchange physiology in mulberry grown in elevated as well as ambient [CO₂] environments under WW as well as WS conditions.

Fig 3.28 Correlation between K_L and photosynthetic leaf gas exchange physiology in mulberry grown in elevated as well as ambient [CO₂] environments under WW as well as WS

conditions.

Fig 3.29 Correlation between F and photosynthetic leaf gas exchange physiology in mulberry grown in elevated as well as ambient [CO₂] environments under WW as well as WS conditions.

Fig 3.30 Correlation between Ψ_{md} and photosynthetic leaf gas exchange physiology in mulberry grown in elevated as well as ambient [CO₂] environments under WW as well as WS conditions.

Fig 3. 31 Amplification of designed gene specific primes of both PIPs and TIPs in mulberry.

Fig 3.32 Expression profiles of both PIPs and TIPs in mulberry grown in elevated as well as ambient [CO₂] environments under WW as well as WS conditions

Tables

Table1.1 Studies including global change manipulations on SRC Poulas, salix and Eucalyptus spp.

Table.2.1 Selected chlorophyll a fluorescence JIP-test parameters

Table 2.2 Gene specific primers designed for antioxidant enzymes (Cyt- cytosolic, Chl- chloroplastic, Mit- Mitochondrial) and aquaporins (AQPs).

Table 3.1 Changes in photosynthetic leaf gas exchange characteristics and foliar biochemistry of two mulberry genotypes (S13 and K2) grown under elevated and ambient [CO₂] atmosphere.

Table 3.2 Statistical significance of photosynthetic leaf gas exchange characteristics, foliar biochemistry, destructive biomass and JIP test parameters between the treatments and genotypes.

Table 3.3 Changes in photosynthetic leaf gas exchange characteristics, chlorophyll a fluorescence parameters and foliar biochemistry in SRC mulberry grown under elevated and ambient [CO₂] atmosphere at 365 DAT and 1095 DAT.

Table 3.4 P-values representing significant changes in photosynthetic leaf gas exchange characteristics, chlorophyll *a* fluorescence, antioxidant enzyme activities, oxidative stress parameters and antioxidants in mulberry grown under both elevated, ambient [CO₂] atmosphere under well watered and WS conditions. Time has a significant effect for these parameters during drought in both elevated and ambient [CO₂] conditions.

Table 3.5 Changes in chlorophyll pigments in SRC mulberry grown under both elevated and ambient [CO₂] environments under WW as well as after 30 days of WS.

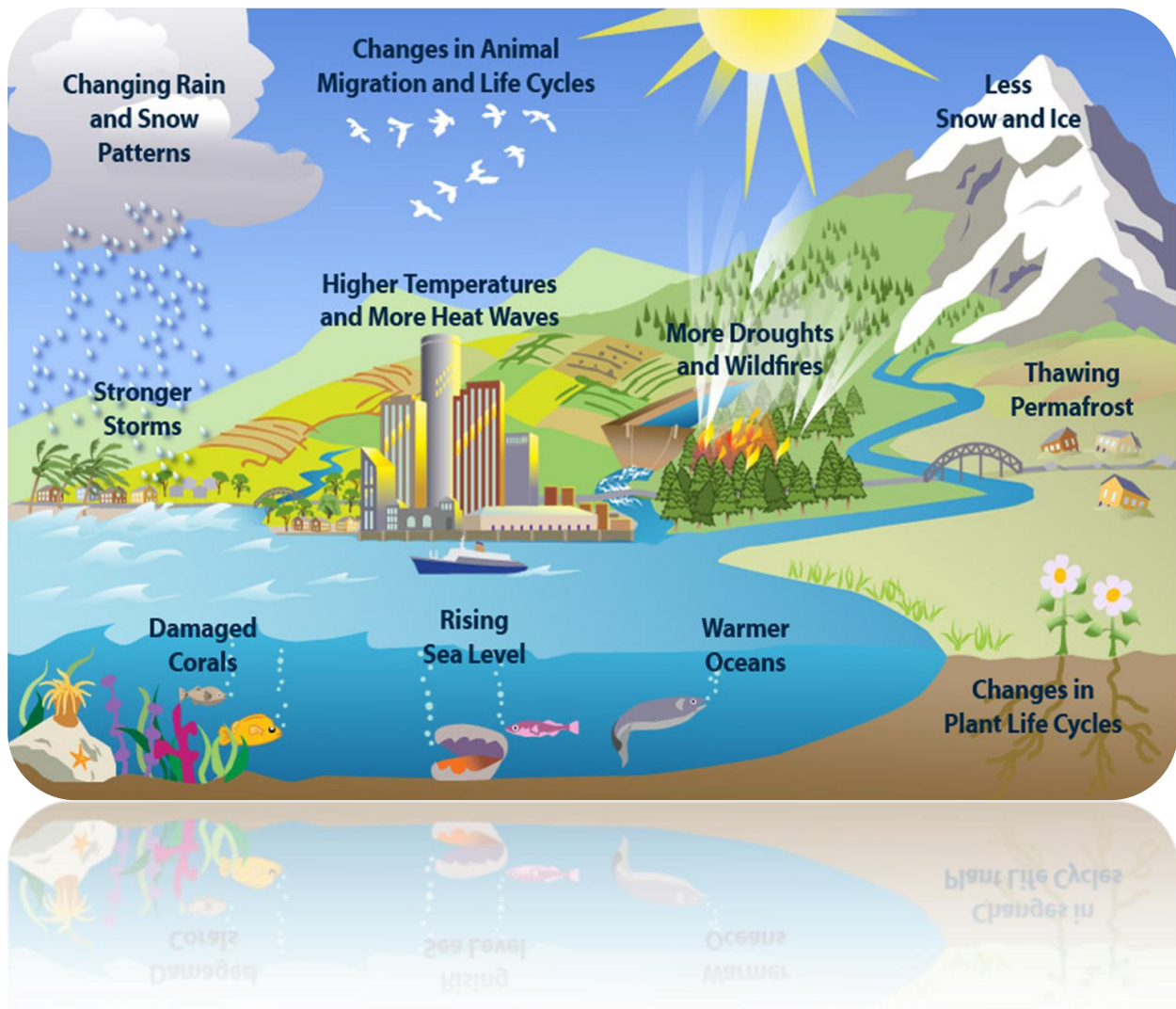
ABBREVIATIONS

2, 4-dinitrophenyl hydrazine	DNTPH
6 mM 5'-dithio-bis (2-nitrobenzoicacid)	DNTB
Analysis of variance	ANOVA
Apparent quantum efficiency	AQE
Aquaporins	AQPs
Ascorbate peroxidase	APX
Ascorbic acid	ASA
Catalase	CAT
Drought susceptible	DS
Drought tolerant	DT
Dry weights	DW
Endoplasmic reticulum	ER
Fresh weights	FW
Fructose-1,6-bisphosphatase	FBPase
Glutathione reductase	GR
Greenhouse gases	GHGs
Infrared CO ₂ /H ₂ O gas analyzer	IRGA
Leaf mass per area	LMA
Light compensation point	LCP
Malondialdehyde	MDA
Membrane intrinsic proteins	MIPs
Mono dehydro ascorbate reductase	MDHAR
NOD26-like intrinsic proteins	NIPs
Non dispersion infra-red	NDIR
Open top chambers	OTCs
P- nitro blue tetrazolium chloride	NBT
Phaspho ribulose kinase	PRK
Photosynthetic nitrogen use efficiency	PNUE
Photosynthetic photon flux density	PPFD

Photosystem-II	PS-II
Plasma membrane intrinsic proteins	PIPs
Reactive oxygen species	ROS
Relative water content	RWC
Ribulose 1, 5- bis phosphate	RuBP
Scanning Electron Microscopy	SEM
Sedoheptulose-1,7-bisphosphatase	SBPase
Short rotation coppice	SRC
Small intrinsic proteins	SIPs
Specific leaf area	SLA
Superoxide dismutase	SOD
Thiobarbituric acid	TBA
Tonoplast intrinsic proteins	TIPs
Total above ground dry weight	TAGDW
Total above ground fresh weight	TAGFW
Total leaf fresh weight	TLFW
Total phenolics	TPC
Total stem fresh weight	TSFW
Trichloroacetic acid	TCA
Water stress	WS
Water use efficiency	WUE _i

Chapter 1

Introduction



1.1 Climate change: the world's most burning problem

Climate change is now considered as one of the most crucial problem of the world as evident from observations including increased mean air temperatures, altered rain and snow -fall patterns, frequent and prolonged droughts along with widespread melting of snow/ice, leading to a considerable rise in the average sea level (IPCC, 2013). Increased emission of greenhouse gases (GHG's) through fossil fuel burning for industry, transportation and residential uses are the major causes for climate change. Major GHG's includes water vapour, carbon dioxide, methane, nitrous oxide, ozone and chlorofluorocarbons in the lower atmosphere, which absorb solar radiations and emit the same within the infrared range resulting in warming of earth's surface, a phenomenon termed as green house effect or global warming (NASA, 2014). Among all the GHG's, carbon dioxide (CO_2) constitutes a major proportion in the atmosphere and is the most important for both climate change in terms of greenhouse effect as well for human economy. It has been predicted that before industrialization, the concentration of CO_2 ($[\text{CO}_2]$) in the atmosphere was roughly $\sim 280 \mu\text{mol mol}^{-1}$, which by the end of the twentieth century the $[\text{CO}_2]$ reached to $\sim 369 \mu\text{mol mol}^{-1}$ and at present $[\text{CO}_2]$ is $400 \mu\text{mol mol}^{-1}$ (Fig. 1.1) . If this pace will continue, $[\text{CO}_2]$ is predicted to reach $\sim 560 \mu\text{mol mol}^{-1}$ by the year 2050 and $\sim 700 \mu\text{mol mol}^{-1}$ by the year 2100 (IPCC, 2013).

Natural sources of atmospheric $[\text{CO}_2]$ emissions includes, out gassing (slow release of absorbed or trapped gases) from volcanoes, combustion and natural decay of organic matter and respiration by aerobic organisms. These sources are balanced proportionally by a set of physical, chemical or biological processes called “sinks”, which tend to remove CO_2 from the atmosphere. Terrestrial plants constitute a potential biological sink, which takes up CO_2 through the process of photosynthesis and contributes in mitigating increased atmospheric $[\text{CO}_2]$ (Prentice et al., 2001; Solomon et al., 2007). Natural forests act as major sinks for CO_2 sequestration and contribute up to 70% of the global carbon sequestration. However, forest area has been reduced by almost 30 to 40% globally in the last 140 years and the present $[\text{CO}_2]$ sequestration rate of forests is not on par with the current scenario of increasing atmospheric $[\text{CO}_2]$ concentration. Uncontrolled anthropogenic human activities including burning of fossil

fuels (for transportation, heating and the generation of electrical power), clearing and burning of natural forests are the major causative agents for exponential rise in atmospheric $[\text{CO}_2]$ (Fig. 1.2).

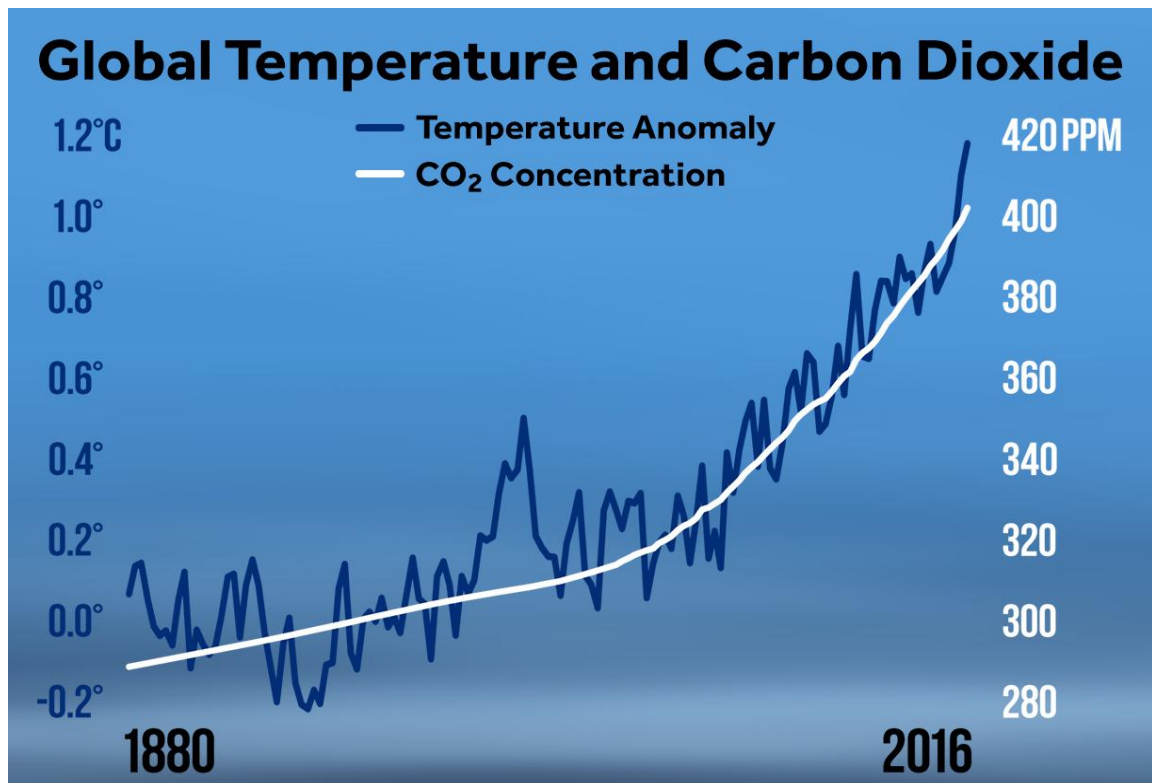


Fig 1.1 Exponential rise in $[\text{CO}_2]$ and temperature in the atmosphere from 18th to 21st century. (From: IPCC, 2013)

Approximately 7 gigatons of CO_2 is released into the atmosphere annually through anthropogenic activities, these emissions are equal to 3% of the total emissions of CO_2 by natural resources and this augmented anthropogenic carbon load far exceeds the offsetting capacity of natural sinks (Dyson, 2005). Substantial increase of $[\text{CO}_2]$ in the atmosphere also raises concerns on usage of non-renewable fossil fuels, which are the most abundant and reliable energy resources available at present. Increased atmospheric $[\text{CO}_2]$ and other GHGs also influence the air temperature, which is predicted to increase

by 2.6°C-4.8°C by the end of 21st century (IPCC, 2013; NASA 2014). Precipitation patterns are reported to be coupled with changes in air temperature, which together results in intermittent warmer as well as drier environments in many areas of the world causing a strong impact on eco-physiological responses of terrestrial plants (Albert et al., 2011a).

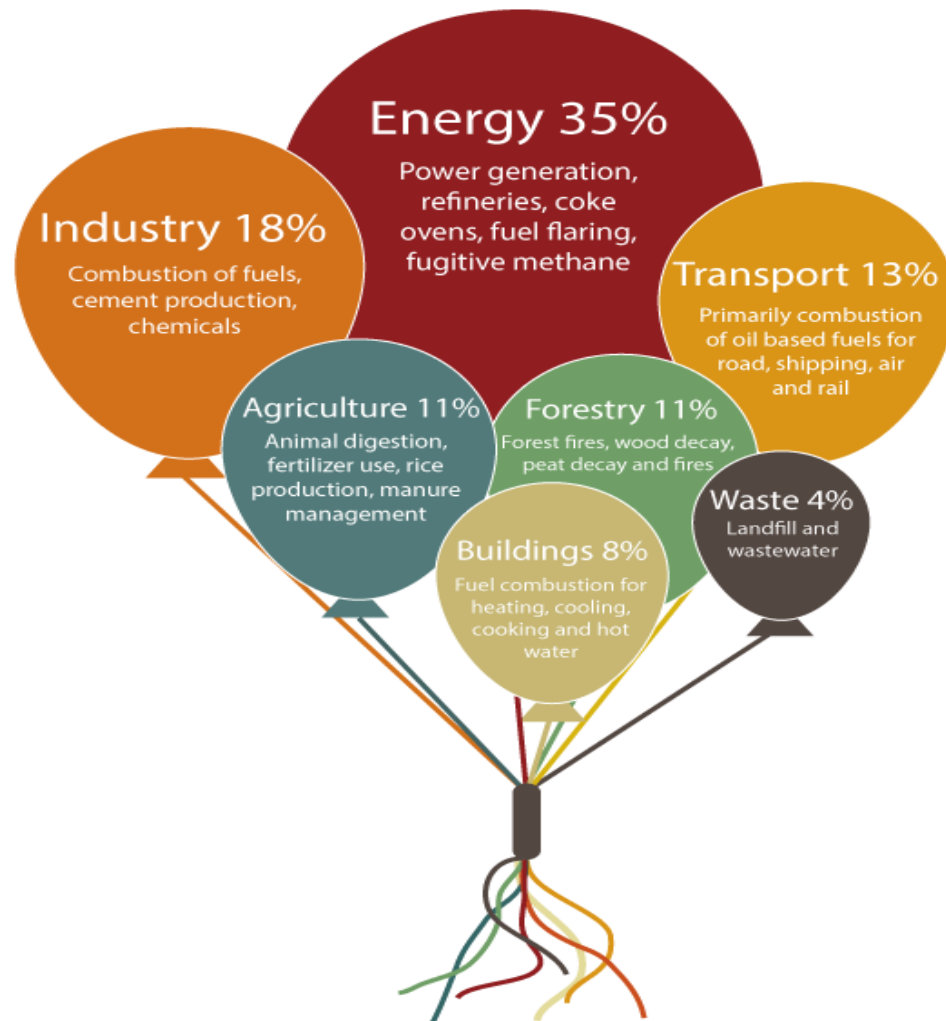


Fig 1.2 Different sources of anthropogenic emission of GHGs in to the atmosphere.
(From: NASA, 2014)

Prolonged intermittent dry environments, which are predicted to prevail under future climate change scenarios, can induce widespread mortality of seedlings as well as mature trees leading to modifications in forest's structure and function. Thus, in order to mitigate such adverse environmental consequences, it is highly crucial to understand mechanisms underlying drought-induced tree mortality under elevated $[\text{CO}_2]$ conditions (Duan et al., 2014). Most of the studies on effect of abiotic factors including elevated $[\text{CO}_2]$, ozone, drought, salinity and temperature on plants have been primarily carried out as an effect of a single factor and reports on interactive effects of more than one factor, on plant growth and physiology are quite rare. However, in nature, environmental changes occur concurrently during plant growth and hence, plants frequently face more than one abiotic stress factors during its life span. For a comprehensive analysis, it is essential to investigate individual effects as well as potential interactions between various stress factors (Xu et al., 2015). Drought is one of the most important abiotic stress factor affecting plant community, which is predicted to prevail in future climate change scenarios, especially with increased atmospheric $[\text{CO}_2]$ (Xu et al., 2015). Thus, studies involving integration of both drought and increased atmospheric $[\text{CO}_2]$ are crucial as the combination of individual factors might provide an evidence for non-additive effects if any (Albert et al., 2011b).

1.2 Effect of elevated atmospheric $[\text{CO}_2]$ on plant growth and photosynthetic physiology

Elevated $[\text{CO}_2]$ stimulates photosynthesis in plants and the magnitude of stimulation varies among species, growth conditions and period of exposure. In brief, increased atmospheric $[\text{CO}_2]$ stimulates light saturated net photosynthetic rates (A_{Sat}) by favoring Rubisco's carboxylation process over photorespiration and by increasing the inter cellular CO_2 concentration (C_i) despite reduced stomatal conductance (g_s) (Ainsworth and Long 2005; Ainsworth and Rogers 2007). Studies have reported that long-term growth under elevated $[\text{CO}_2]$ induces photosynthetic acclimation in some plants (Long et al., 2004) (Fig 1.3). Occurrence of photosynthetic acclimation is the result of an imbalance in source-sink relationship due to reduced foliar nitrogen content

resulting in accumulation of leaf carbohydrates, especially starch (Long et al., 2004). Accumulation of carbohydrates trigger feedback inhibition of photosynthetic capacity through reduction of Rubisco protein and/or activity termed as Ribulose 1, 5- bisphosphate (RuBP) carboxylation (V_{cmax}) limitation (Ainsworth and Long 2004). Apart from V_{cmax} limitations, RuBP regeneration (J_{max}) in terms of maximum electron transport can also limit photosynthesis under high $[\text{CO}_2]$ atmosphere and known to be associated with decreased expression levels as well as activities of certain rate limiting enzymes including chloroplast sedoheptulose-1,7-bisphosphatase (SBPase), fructose-1,6-bisphosphatase (FBP) and phospho ribulose kinase (PRK) (Ellsworth et al., 2004; Nowak et al., 2004). Similarly, reduced photosystem-II (PS-II) efficiency can also induce photosynthetic acclimation in $[\text{CO}_2]$ enriched environment due to diminished synthesis of ATP as well as NADPH, which are the vital components for activation of most enzymes involved in RuBP carboxylation and regeneration (Sekhar et al., 2014). Along with reduced V_{cmax} and J_{max} , photosynthetic acclimation is also associated with reduced light and CO_2 saturated photosynthesis (A_{max}), photosynthetic nitrogen use efficiency (PNUE) and specific leaf area (SLA) with concomitant increase in leaf mass per area (LMA) (Sholtis et al., 2004). However, photosynthetic acclimation in response to elevated $[\text{CO}_2]$ is not a uniform phenomenon and genotypic variations in response to elevated CO_2 in certain herbaceous species have been reported; but, very limited information is available on woody tree species (Liu et al., 2006). Studies on intra-specific variations in woody tree species, in response to climate change, including increased atmospheric $[\text{CO}_2]$ will be highly useful for tree improvement programs for mitigating atmospheric $[\text{CO}_2]$ apart from their social and economic benefits (Wang et al., 2006). Further, plants grown under elevated CO_2 showed reduced transpiration (E) by lowering stomatal conductance (g_s), which in turn is associated with substantial increase in water use efficiency (WUE_i). Mesophytic plants with higher WUE_i were considered as drought tolerant (DT) and can exhibit better photosynthetic performance, even under extended drought environments. Proportionate changes in WUE_i were also linked to their biomass accumulation under CO_2 enriched atmosphere (Broeckx et al., 2014).

1.3 Impact of elevated $[\text{CO}_2]$ -drought interaction on photosynthetic performance and oxidative stress response of plants

In contrast to elevated $[\text{CO}_2]$ responses, drought causes acclimation in g_s and which in turn is associated with reduction in C_i along with A_{Sat} in C_3 plants due to mesophyll conductance (g_m) limitations (Reddy et al., 2004; Lawlor and Tezara 2009).

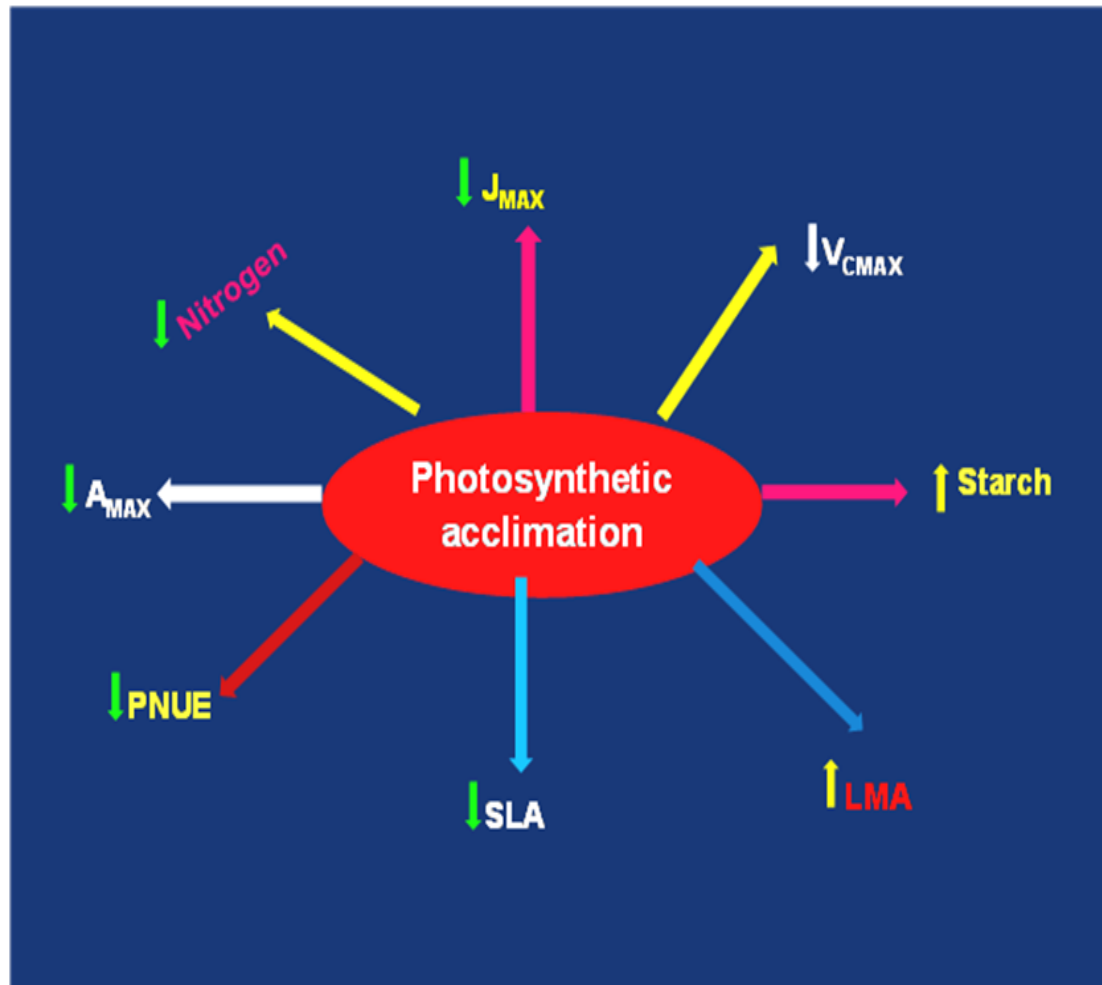


Fig 1.3 Cardinal symptoms of photosynthetic acclimation in plants grown under elevated $[\text{CO}_2]$ environments due to source to sink imbalance under nutrient limiting conditions.

However, plants grown under elevated $[\text{CO}_2]$ atmosphere behave differently during drought periods, and elevated $[\text{CO}_2]$ is reported to ameliorate or delay the drought related symptoms and sustain higher A_{Sat} (Albert et al., 2011b). Further, drought stress impairs the function and structural integrity of cellular organelles having highly oxidizing metabolic activity or with intense rate of electron flow including chloroplasts, mitochondria as well as peroxisomes (Gill and Tuteja 2010). Drought-induced impair in these organelles leads to enhanced leakage of electrons to molecular oxygen resulting in oxidative stress via formation of reactive oxygen species (ROS) such as hydrogen peroxide, superoxide and hydroxyl radicals (Gill and Tuteja 2010). To combat such oxidative stress, plants have developed enzymatic and non-enzymatic antioxidant system to mitigate excessive accumulation of ROS (Tezara et al., 2002; Li et al., 2008; Xu et al., 2015) (Fig 1.4). Certain studies showed that elevated $[\text{CO}_2]$ ameliorates the oxidative stress by reducing the production and accumulation of ROS, which is linked with lower activities and expression levels of ROS scavenging enzymes (Ghasemzadeh et al., 2010; Gillespie et al., 2012; Mishra and Agarwal 2014; Zintha et al., 2014). Some studies also suggested that elevated $[\text{CO}_2]$ had no effect in alleviating the oxidative stress, while others have demonstrated that increased $[\text{CO}_2]$ even exacerbated the effects of oxidative stress (Farfan- Vignolo and Asard 2012). Thus, elevated $[\text{CO}_2]$ mediated ameliorative effects on drought-induced oxidative stress is still a debatable issue and needs further research.

1.4 Correlation of hydraulic conductivity and photosynthetic performance under elevated CO_2 and drought

Terrestrial plants require sufficient water to maintain better photosynthetic performance and growth and water transport from soil to atmosphere via root-shoots-leaves mainly depends on maintenance of water column within the vascular system (Chen et al., 2010; Sengupta and Majumder 2014) (Fig 1.5). Drought stress causes hindrance in water transport or plant hydraulic conductivity, due to increased negative water potential in the soil, which increases the xylem sap flow tension leading to cavitation or embolism within the xylem vessels (Brodersenet al., 2013). Certain studies have demonstrated that

greater negative water potential during extended drought environments stimulate stomatal closure as well as xylem embolism (Brodribb and Cochard 2009). Thus, in order to avoid extensive xylem embolism and drought- induced mortality, plants have to maintain their xylem water status under threshold range (Matorell et al. 2014). Mortality of plants during prolonged drought environments can be explained by two interdependent mechanisms including hydraulic failure hypothesis and carbon starvation hypothesis (Duan et al., 2014). Hydraulic failure hypothesis demonstrates that reduced soil water content and greater evaporative transpiration demand induces extensive embolism in xylem conduits, which constrains water flow leading to plant tissue desiccation and cell death (Brodribb and Cochard 2009; Urli et al., 2013). Carbon starvation hypothesis states that stomatal closure, to avoid hydraulic failure, can reduces $[CO_2]$ uptake and photosynthetic performance considerably, resulting in reduced synthesis as well as increased depletion of stored carbon reserves due to increased respiratory consumption of carbohydrates (Sala et al., 2010). Recent studies have supported the hydraulic failure hypothesis for playing a major role in plant mortality under prolonged water deficit environments (Pou et al., 2013; Nardini et al., 2013; Quirk et al., 2013).

In addition to above, during drought conditions, changes in plant hydraulic conductivity parameters are positively correlated with changes in leaf gas exchange characteristics (Sperry and Pockman 1993, Hubbard et al. 2001, Cochard et al., 2002). Thus, variations in formation of xylem cavitation or embolism is inversely related to plant survivability i.e, plants which are less vulnerable to embolism maintains better water relations and perform superior photosynthesis even under extended water stress (WS) conditions (Costa et al., 2004; Martorell et al., 2014). Contrast to drought responses, studies have demonstrated that increased atmospheric $[CO_2]$ reduces g_s as well as leaf- level water loss in many tree species under WW conditions, which consequently reduce drought induced negative responses (Wullschleger et al., 2002; Ainsworth and Rogers 2007). However, studies on $[CO_2] \times$ drought interactions are not uniform; some studies have demonstrated as elevated $[CO_2]$ ameliorate drought stress (Domec et al., 2010; Lewis et al., 2013), while in some instances, elevated $[CO_2]$ does not alleviate the negative effects of drought (Warren et al., 2011; Duan et al., 2014).

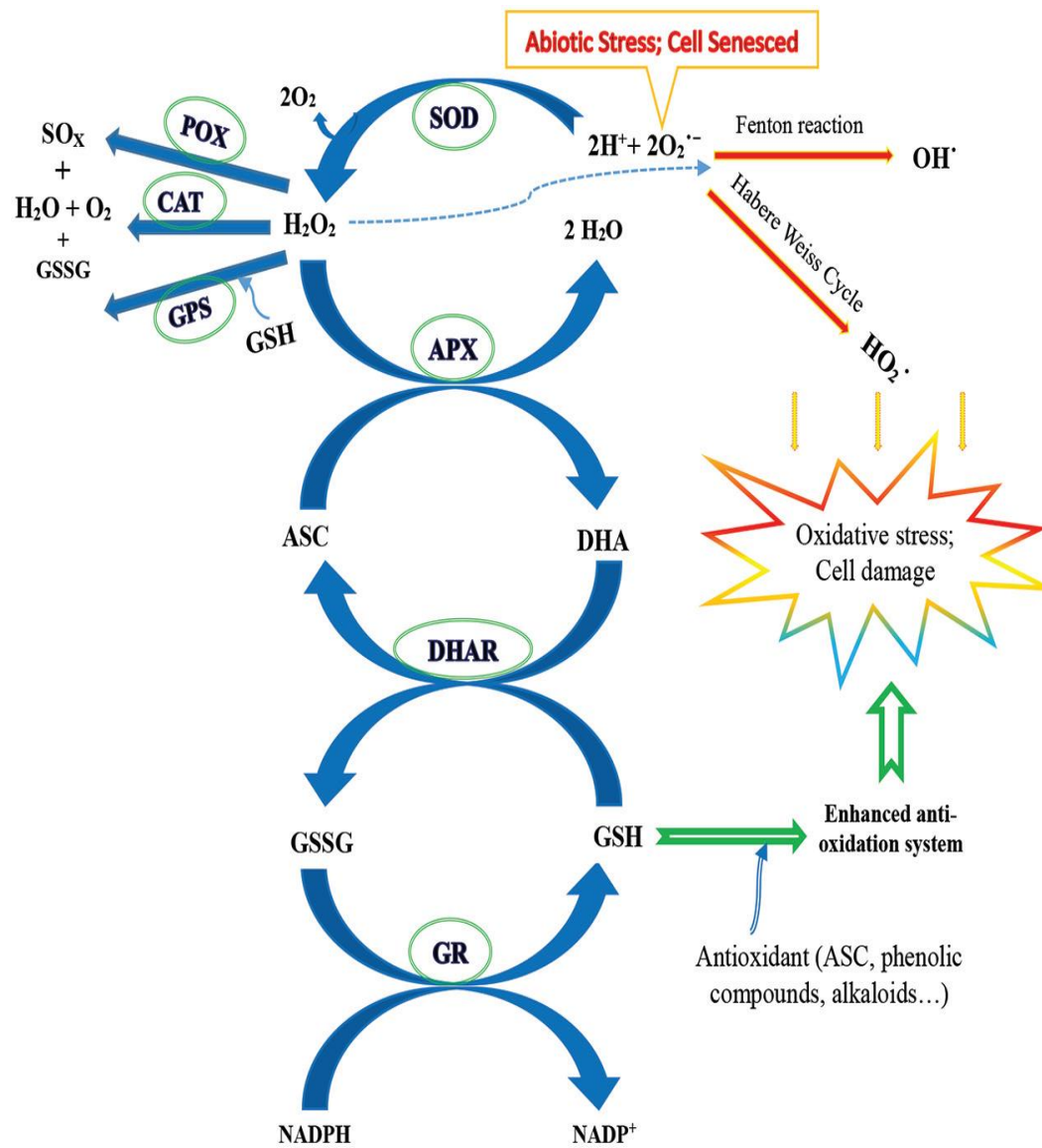


Fig 1.4 Schematic representation of enzymatic and non-enzymatic antioxidant defense mechanism in plants to combat the oxidative stress induced by different types of abiotic stress factors. (From: Xu et al. (2015) Front Plant Sci.)

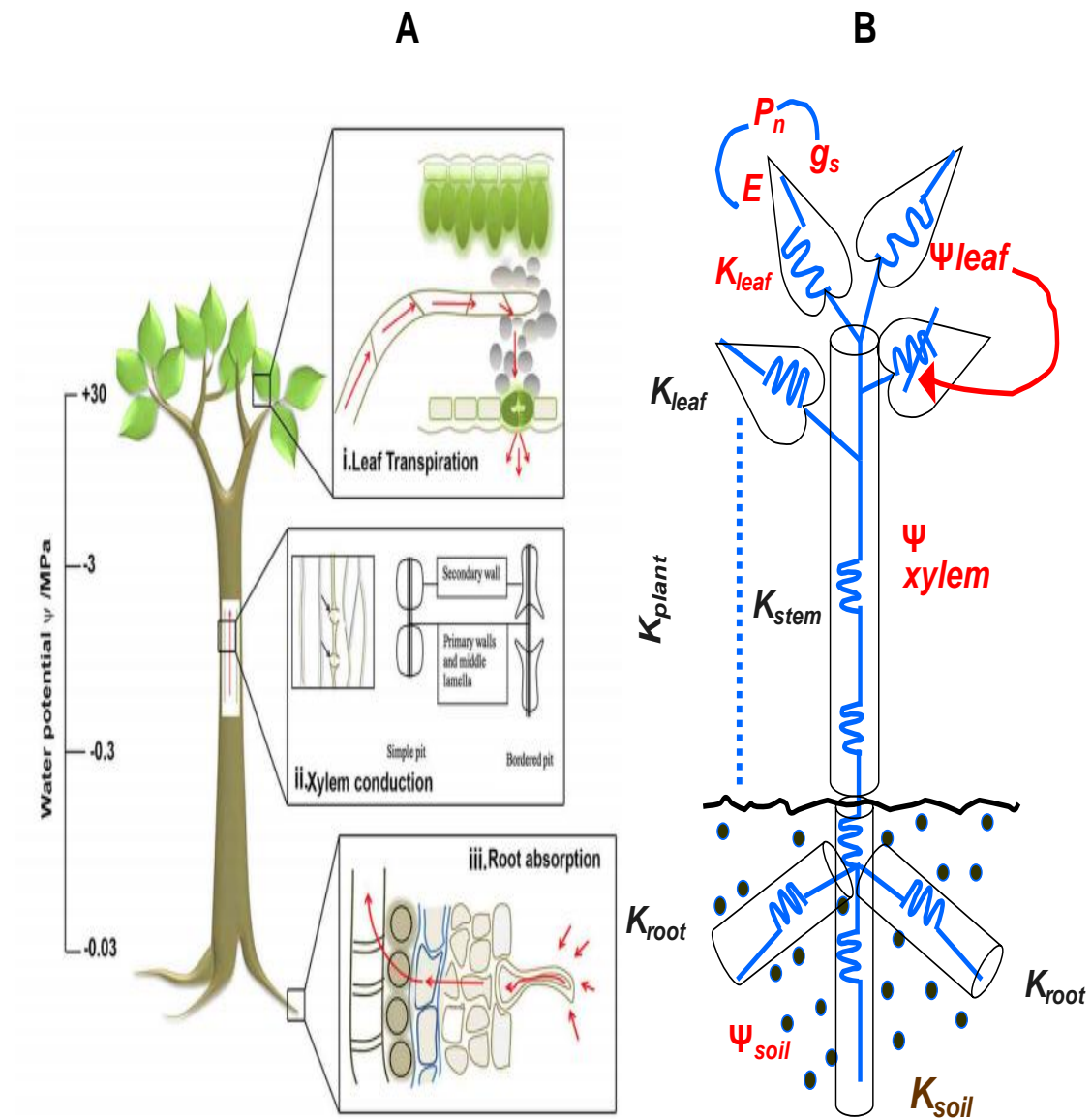


Fig 1.5 (A) Soil-plant-air continuum functioning in maintenance of water transport column, (B) Fine coordination between leaf gas exchange and whole plant hydraulic conductance (K_{plant}). (Modified from: Sengupta and Majumder (2014) Front Plant Sci.)

Moreover, positive effects of elevated [CO₂] on drought disappear when stomata are nearly closed with increasing intensity of WS (Franks et al., 2013; Duan et al., 2014). These results clearly demonstrated that the process of delayed drought- induced plant mortality under increased atmospheric [CO₂] is highly variable between species, functional groups, genotypes and duration of stress imposition time.

1.5 Role of aquaporins (AQPs) in regulating hydraulic conductivity and photosynthesis under elevated [CO₂] and drought conditions

In addition to above, water uptake and its transcellular movement in terrestrial plants are controlled by a family of proteins so called aquaporins (AQPs) or membrane intrinsic proteins (MIPs) (Alexandersson et al., 2005; Kaldenhoff et al., 2008) (Fig 1. 6). Certain studies have demonstrated that variations in AQPs expression can proportionally influence plant hydraulic dynamics as well as photosynthetic performance under various abiotic stress factors especially during drought conditions. Along with cell to cell permeability of water, AQPs also facilitate the movement of certain uncharged solutes like glycerol, urea and boric acid in plants. Based on their sequence homology and distinct sub-cellular localizations, AQPs were subdivided in to five major classes; (1) plasma membrane intrinsic proteins (PIPs), which localize to plasma membrane, (2) tonoplast intrinsic proteins (TIPs), targeted to the vacuolar membrane (tonoplast), (3) NOD26-like intrinsic proteins (NIPs), localizing to the plasma membrane or the endoplasmic reticulum (ER), (4) small intrinsic proteins (SIPs) and (5) uncategorized X intrinsic proteins (XIPs) (Li et al., 2014). However, among the all AQPs, both PIPs and TIPs are reported to be significantly involved in water uptake as well as its transport in both leaves as well as in roots (Olaetxea et al., 2015; Matsumoto et al., 2009; Suga et al., 2004). Further, for efficient water transport, both PIP1 and PIP2 aquaporins combined together as a heterotetramer and form water channels (Fetter et al., 2004). Gene expression studies of AQPs showed inconsistent expression patterns among different plants, showing both up and down regulation under WS (Alexandersson et al., 2005; Kaldenhoff et al., 2008). Some studies have demonstrated that increased expression of AQPs under different abiotic stress factors influence the tolerance characteristics, plant

hydraulic conductivity and recovery rates (Martre et al., 2002; Aharon et al., 2003; Parent et al., 2009; Postaire et al., 2010; Hu et al., 2012; Wang et al., 2014).

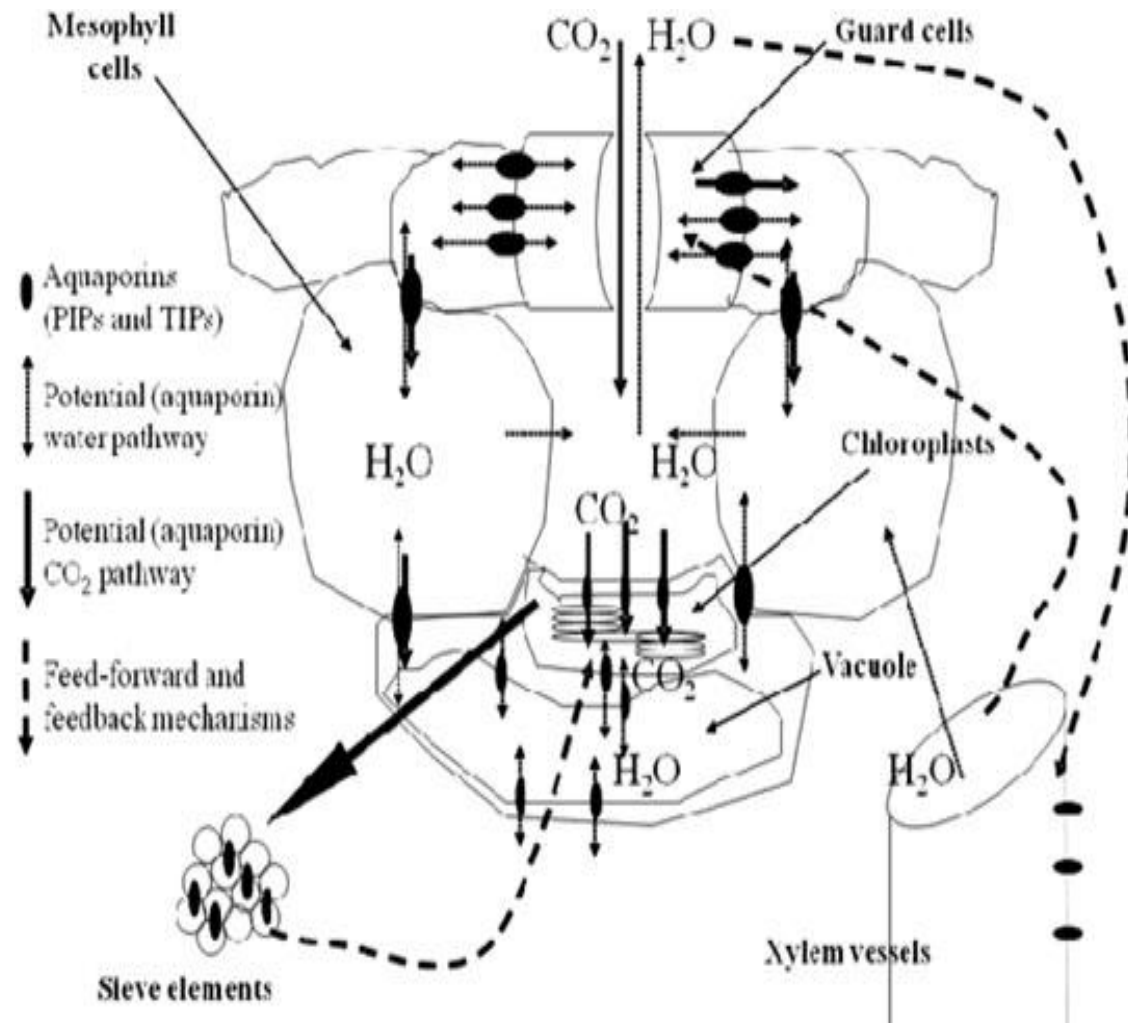


Fig 1.6 Aquaporins (PIPs and TIPs) facilitates the movement of both H₂O and CO₂ in different compartments as well as organelles of plant cells. (From: Kaldenhoff et al. (2008) Plant Cell Environ)

However, in contrast to above, certain transgenic tobacco plants transformed with PIP1 showed faster wilting compared to their wild types under WS (Aharon et al., 2003). These results clearly demonstrated that increased expression of AQPs Vs drought

tolerance mechanism shows dynamic variation among different plant species, between genotypes and functional groups. In addition to above, negative or positive effects of increased atmospheric $[\text{CO}_2]$ on drought may possibly associated with changes in hydraulic dynamics and AQPs gene expression. So far, studies reporting changes in hydraulic characteristics as well as AQPs gene expression during $[\text{CO}_2] \times$ drought interactions on tree species are very scanty. Thus, in the context of the future climate change scenarios, such types of experimental studies are necessary to quantify the main as well as interactive effects of elevated $[\text{CO}_2]$ on drought- induced plant mortality (Duan et al., 2014).

1.6 Importance of woody tree species as bio-energy resources and potential carbon sinks under future climate conditions

There is an urgent need to reduce CO_2 emissions and at the same time have to provide energy sources for the growing energy demand of the world (Lemus and Lal, 2005). None of the competing energy resources including nuclear energy appear to be in a position to fill this gap and fossil fuel based energy consumption need to be substantially reduced. Kyoto protocol came in to the picture in the year 1997 with the aim of reducing CO_2 emissions and stabilization of $[\text{CO}_2]$ in the atmosphere by minimizing extensive usage of fossil fuels and creation of new carbon sinks within a specified time frame (Streck and Scholz, 2006). As CO_2 is continuously exchanged between the atmosphere and terrestrial ecosystems, carbon sequestration through the cultivation of energy crops is the best way to mitigate increased atmospheric $[\text{CO}_2]$ significantly as well as to produce renewable bio-energy to meet the energy demand for ever growing world population (Lemus and Lal 2005). Creation of artificial forests by means of afforestation and reforestation will be highly useful as new sinks to sequester increased atmospheric $[\text{CO}_2]$ and stabilize the climate change (Ellsworth et al., 2004; Reddy et al., 2010). Hence, development of short rotation coppice (SRC) forestry with dense plantation of fast growing tree species having higher photosynthetic rates is essential (Calfapietra et al., 2010). Coppice is a cut back process to generate new sinks in the plants at regular time intervals. SRC plantations can be maintained up to 50- 60 years and usually have a

rotation cycle of less than 10 years (ranging from 3-6 years) (Liberloo et al., 2006; Guha and Reddy 2012). Biomass produced by these tree plantations can be effectively used for the production of renewable bio-energy, along with their traditional uses like pulp, paper, construction wood and fodder (Fig 1.8). Bio-energy can replace fossil fuels to some extent and have additional advantage of being almost CO₂ neutral because the emitted [CO₂] is primarily sequestered by the plants through photosynthesis and generate bio-mass which partly fulfill the commitments of the Kyoto protocol (Calfapietra et al., 2010). Understanding the interactions between management options (coppice and fertilization) and climate change is essential to determine the contribution of biomass plantations to mitigate the rise in atmospheric CO₂ concentration and their ability to substitute fossil fuel carbon indefinitely (Liberloo et al. 2006).

1.7 Important woody tree species for SRC, acting as potential bio-energy sources and carbon sinks

Due to their faster growth rates and greater bio-mass yield, *Populus*, *Salix* and *Eucalyptus* spp. are the most widely used tree species in SRC under different global climate conditions. In certain geographical regions, species of the genera *Robinia*, *Nothofagus*, *Betula* and *Alnus* are also utilized. For several species and hybrids of *Populus* and *Salix*, large number of genotypes have been chosen to allow the distribution of these plantations in different latitudes and climatic conditions (Heilman et al., 1994; Ceulemans and Deraedt, 1999; Mitchell et al., 1999; Karacic et al., 2003). Above ground wood bio-mass yields are highly differ according to the type of clone, climatic variables and nutritional status, but are usually in the range of 8–12 Mg of dry weight ha⁻¹ year⁻¹ though it is possible to achieve productivity of more than 20 Mg of dry bio-mass ha⁻¹ year⁻¹ (Mitchell et al., 1999). At present, SRC forestry crops are gaining greater importance in many countries where surplus agricultural land is available. Perennial character of the tree crops usually allows a reduction in herbicide application compared to traditional agricultural crops. Along with environmentally advantageous attributes, due to their dense rooting system SRC crops also offer a buffering effect on nitrogen leaching, which

allow better nutrient utilization and consequently greater bio-mass yields when compared to agricultural crops (Goor et al., 2000).

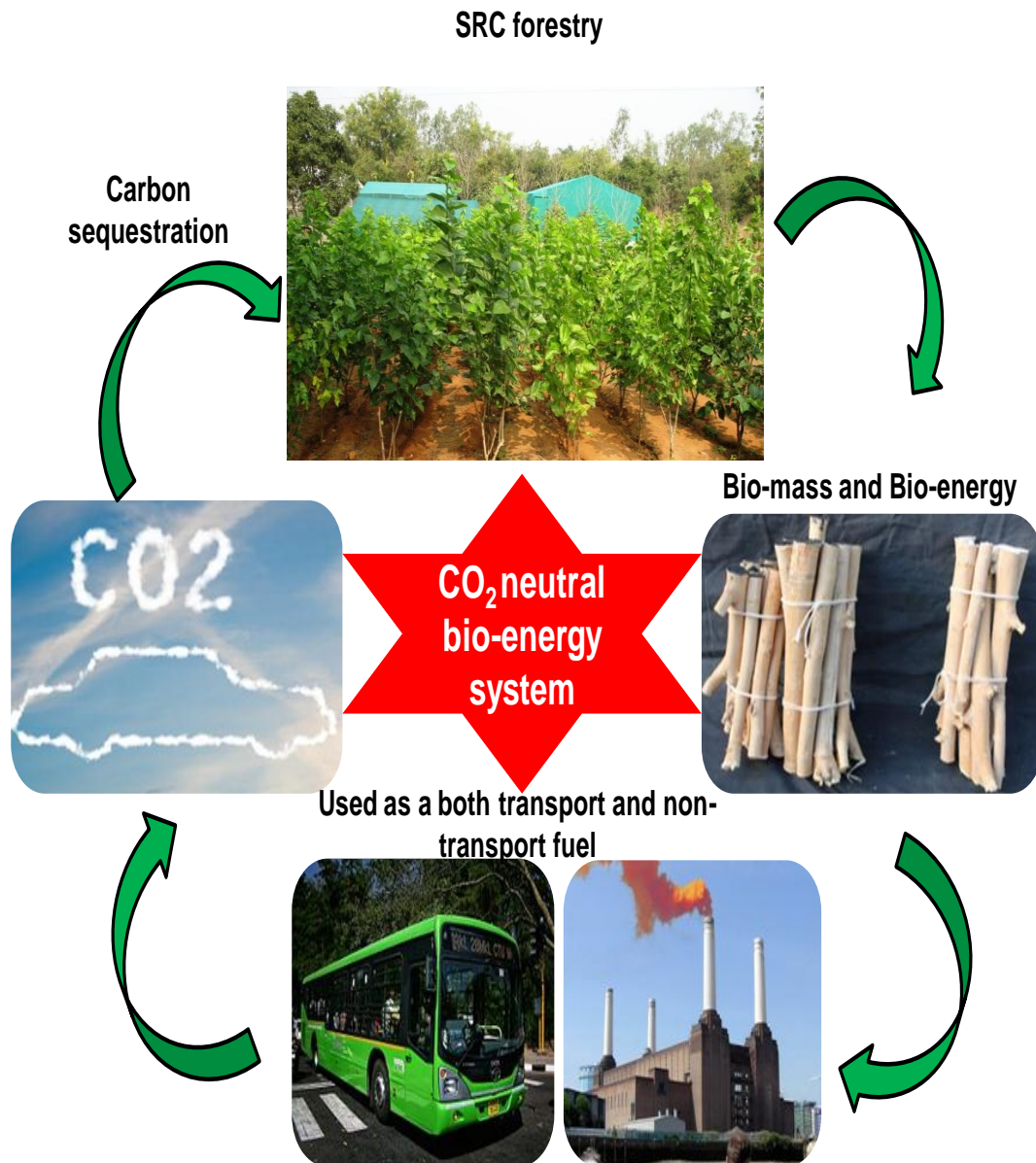


Fig 1.7 Schematic representation of carbon neutral renewable bio-energy production from short rotation coppice (SRC) forestry

Finally, SRC plantations are gaining huge importance for their potential uses in phytoremediation as they uptake large quantities of nutrients and heavy metals from municipal and industrial wastewater (Aronsson and Perttu, 2001). Due to their substantial contribution in the context of climate stabilization, is crucial to understand the responses of SRC cultures under current as well as future climate change scenarios (Weih, 2004). Thus, many manipulative studies have been conducted in different geographical regions on *Populus*, *Salix* and *Eucalyptus* spp. by imposing single or in the combination of multiple stress factors (CO₂, nitrogen, temperature, ozone and water stress) for better understanding of realistic behavior of plants towards future climate change scenarios (Table. 1.1). Differential responses of SRC for *Populus* spp. under elevated CO₂ have been reported in literature. Some reports showed that persistent stimulation of light saturated photosynthetic rates (A_{Sat}) even with long term growth (5-6 years) under elevated CO₂ atmosphere indicating absence of photosynthetic acclimation (Liberloo et al., 2009), while other studies have reported the photosynthetic down regulation by decreasing A_{Sat} during the first year following coppice (Bernacchi et al., 2003). Such varied responses reported on growth of SRC plants under elevated CO₂ concentration makes it imperative to study new candidate fast growing woody tree species which can be easily propagated and cultivated in varied agro- climatic regions, can undergo intensive coppicing treatments to generate new sinks, produce quality fuel wood and offer several other economic and social benefits (Sekhar et al., 2014).

1.8 Mulberry: a potential bio-energy tree species for SRC forestry

Mulberry (*Morus* spp L.) is a fast growing ever green/semi deciduous tree, which is the first commercialized foliage crop in the world and has been cultivated trans-continentially over 50 countries across the world (Chaitanya et al. 2003). There are about 68 species of the genus *Morus*, majority of them occur in Asia, especially in China (24 species) and Japan (19 species). Further, mulberry is also widely distributed in Europe, North America, South America, Latin America and Africa. Earlier, mulberry was predominantly cultivated for sericulture industry to rear the silkworm *Bombyx mori* (Guha et al., 2010).

Table1.1 Studies including global change manipulations on SRC Poulas, salix and Eucalyptus spp.

Location (experiment name)	Facility	Factors examined	Species
Viterbo, Italy (POP-EUROFACE)	FACE	CO ₂ N	<i>Populus alba</i> , <i>Populus nigra</i> , <i>Populus deltoids</i> × <i>Populus nigra</i>
Rhineland, WI, USA (AspenFACE)	FACE	CO ₂ O ₃	<i>Populus tremuloides</i> (different clones)
Oracle, AZ, USA (Biosphere 2)	Mesocosms	CO ₂ Temperature	<i>Populus deltoides</i>
Rapolano, Italy	mini-FACE	CO ₂	<i>Populus deltoids</i> × <i>Populus nigra</i> , <i>Populus deltoides</i>
Antwerp, Belgium	OTCs	CO ₂	<i>Populus deltoids</i> × <i>Populus nigra</i> <i>Populus trichocarpa</i> × <i>Populus</i> <i>deltoides</i>
Alberta, MI, USA	OTCs	CO ₂ O ₃	<i>Populus tremuloides</i> (different clones)
Gunnarsholt, Iceland	Closed-top chambers	CO ₂ N	<i>Populus trichocarpa</i>
Headley, UK	OTCs	CO ₂ O ₃	<i>Populus trichocarpa</i> × <i>Populus</i> <i>deltoides</i>
Pellston, MI, USA Gainesville, FL, USA	Cooling boxes Tunnels	Temperature N CO ₂ Water stress	<i>Populus tremuloides</i> <i>Populus trichocarpa</i> × <i>Populus</i> <i>deltoides</i> , <i>Salix sagitta</i>
Mekrijärvi, Finland	Closed-top chambers	CO ₂ Temperature	<i>Salix myrsinifolia</i>
Melbourne, Australia	Glasshouse	CO ₂ Water stress	<i>Eucalyptus cladocalix</i>
Darwin, Australia	Chambers	CO ₂	<i>Eucalyptus tetradonta</i>
Edinburgh, UK	OTCs	O ₃	<i>Eucalyptus grandis</i> , <i>E. urophylla</i> , <i>E.</i> <i>camaldulensis</i> , <i>E. torelliana</i> , <i>E.</i> <i>phaeotrica</i>
Canberra, Australia	Growth chambers	CO ₂ Temperature Water stress	<i>Eucalyptus macrorhyncha</i> , <i>Eucalyptus</i> <i>rossii</i>

Nevertheless, studies from the last two decades have revealed several other potential benefits of mulberry. In many Asian countries including China and India, mulberry leaves are used as medicinal herb and leafy vegetable. Moreover, as the leaves are highly rich in protein, antioxidants and minerals without any toxic elements mulberry is gaining popularity in many countries (Mediterranean areas of Europe, India, Cambodia, Tanzania, Turkey, China, etc.) as forage for livestock feeding (Papanastasis et al. 2008; Guha et al. 2010). Several reports have emphasized the prospect of mulberry foliage as a feed for both ruminants and non-ruminant animals. The “SILK-N-MILK” scheme is gaining huge popularity in India in which farmers are exploiting mulberry foliage for both silkworm rearing as well as for dairy milk production (Papanastasis et al., 2008). Mulberry plantation is maintained as low to high bush and it produces very large amounts of renewable biomass in the form of branches, shoots, leaves and fruits. In tropics and sub-tropics, mulberry tree is mainly propagated by cuttings wherein some of the pruned branches are used for preparation of cuttings and the remaining are used as fuel-wood (Lu et al. 2009). One hectare of mulberry plantation can give yield of 12.1 MT of mulberry sticks from which the energy generated/ha (50% moisture loss) will be almost 27830 Kcal as = i.e, equivalent to 4600 calories/kg of mulberry wood (Guha and Reddy 2013). Therefore, mulberry can be exploited as a “energy plantation” in wasteland/cultivable/low lying areas/road side/canal bund /fringe areas of the forest etc. under various afforestation, watershed development and soil conservation programmes. Thus, mulberry is considered as a multipurpose tree crop, which can fulfill a number of roles in small-holder agricultural production (Machii et al. 2000). Many species of *Morus* are found in India, of which *M. alba*, *M. indica*, *M. serrata* and *M. laevigata* grow wild in the Himalayas and several other cultivars are also introduced recently belonging to *M. sinensis*, *M. multicaulis*, *M.nigra* and *M. phillippinensis* (Karaba et al., 2008). Most of the Indian mulberry cultivars are belongs to *M. indica* and some belong to *M. alba* (Dandin et al., 2003). Although mulberry cultivation is practiced in various climatic conditions, 90% of the cultivated area is in the tropical zone covering Andhra Pradesh, Karnataka and Tamil Nadu states. In the subtropical zone, Himachal Pradesh, West Bengal and north-eastern states have major areas under mulberry cultivation. Total mulberry

cultivated land in India is around 282,244 ha and mulberry growth and productivity are remarkably influenced by the climatic variations (Dandin et al., 2003).

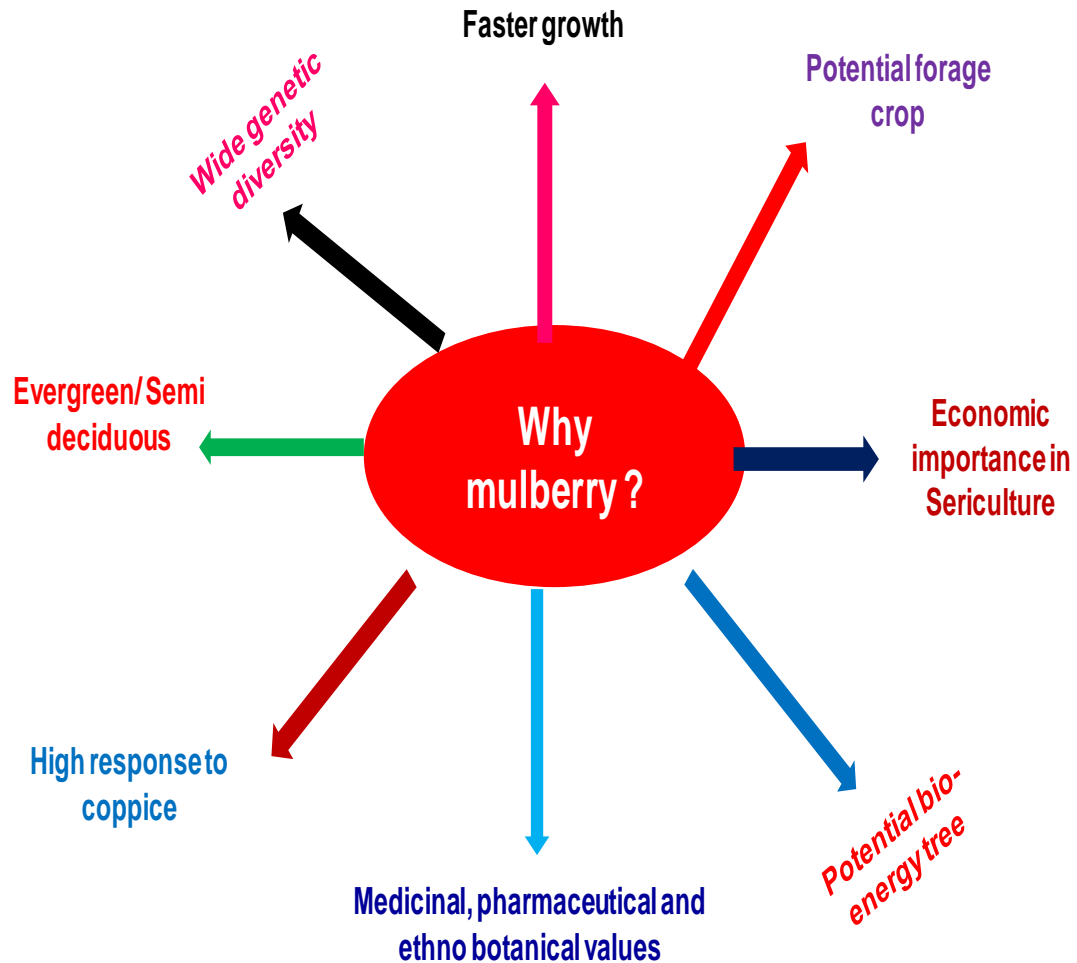


Fig 1.8 Rationale for selecting the mulberry as the model plant for the present study

Among all the climate variables, water availability is one of the most important determinants and which can significantly affects the bio-mass yield in mulberry (Chaitanya et al., 2003). To produce one kilogram of fresh leaf mulberry needs 500 to

700 liters of water, high yielding mulberry cultivars use more water due to their faster growth rates, large cumulative leaf area and canopy size (Karaba et al., 2008). Thus, water deficient environment can arrest the growth and bio-mass yield performance of elite mulberry cultivars due to down regulation of photosynthesis (Karba et al., 2008). Studies have demonstrated that relationship between water stress severity and yield loss can differ significantly among the mulberry genotypes leading to divide them in to drought tolerant (DT) and drought susceptible (DS) mulberry genotypes. From agro-economical viewpoint, DT mulberry genotypes exhibited stable photosynthetic performance as well as better yield compared to DS genotypes when exposed to extended water deficit environments. Their faster growth, quick response to coppice treatment, wider agro climatic adaptability and high responsiveness to agronomic inputs make mulberry plantations suitable for horticulture, agro-forestry and landscaping (Sekhar et al. 2015). Several morphological, physiological and biochemical mechanisms including photosynthetic capacity, water use efficiency, light use efficiency, rooting vigour, osmotic adjustment, antioxidative protection etc. are mostly associated with improved performance and yield under variable climatic conditions. Thus, prior knowledge of this candidate crop towards anticipated climatic conditions, especially elevated [CO₂], drought, salt and temperature, is highly essential before designing mulberry crop improvement programmes. So far, we have very limited information on the responses of mulberry genotypes towards different abiotic stress factors including drought, salt as well as temperature and these studies are provide expected information on changes in morpho-physiological, photosynthetic characteristics, biochemical and bio-mass yields (Ramanjulu et al. 1998; Chaitanya et al. 2003). Drought is the most predominant abiotic stress factor affecting the photosynthetic performance as well as bio-mass yields in mulberry and incidences of drought occurrences will be more under future climatic changes, especially with increased atmospheric [CO₂]. Hence, the present study was aimed to understand the responses of mulberry, a potential bio-energy tree species, to elevated [CO₂] and drought as well as their interactive influence on growth, and photosynthetic productivity of mulberry.

1.9 Objectives for the current study

- 1. Variations in photosynthesis, growth and bio-mass yield responses of two contrasting drought tolerant mulberry genotypes under elevated [CO₂] atmosphere.**
- 2. Establishing the long term carbon sequestration potential of mulberry with coppice management practices under [CO₂] enriched environment.**
- 3. Exploring the dynamic changes of antioxidant systems in short rotation coppice (SRC) mulberry in response to elevated [CO₂] and drought individually as well as in their combination.**
- 4. Investigating the coordinate changes of hydraulic conductance and photosynthesis with particular reference to expression profiles of certain AQPs in short rotation coppice mulberry.**



Chapter 2

Materials and Methods

2.1 Experimental facility

For [CO₂] enrichment studies, open top chambers (OTCs) (Neo Genesis Engineering, Mumbai, India), having 4×4m dimension and octagonal shape, were installed in the botanical garden of University of Hyderabad, India located between 17.3°10" N and 78°23" E at an altitude of 542 m above mean sea level. OTCs were equipped with temperature, rainfall and humidity sensors for regular monitoring and recording the climate change variations. Series of CO₂ gas cylinders were used to pump 100% commercial grade CO₂ gas into the chambers through manifold fitted with solenoid valve to regulate the gas supply. Equipment for monitoring and controlling the [CO₂] in the OTCs was fully automated and required [CO₂] was maintained with the help of non dispersion infra-red (NDIR) CO₂ gas analyzer and thermal mass flow meter. Two OTCs were used for CO₂ enrichment (550 µmol mol⁻¹ CO₂) and remaining two OTCs were maintained with ambient [CO₂].

2.2 Plant material and Experimental Layout

Based on earlier studies from our laboratory, two mulberry genotypes including Selection-13 (S13) and Kanva-2 (K2) were selected for the present study from a wide range of mulberry germplasm. Genotype S13 is considered as a drought tolerant (DT); while, K2 is drought susceptible (DS). Six- month - old healthy rooted plant saplings of S13 and K2 were selected and three representative plants of each genotype were transferred into individual OTCs. We observed DT S13 exhibited better photosynthetic performance, growth and biomass yields with respect to DS K2 cultivar. Further, long term effects of elevated [CO₂] as well as interactive studies with drought experiments were continued with DT S13 mulberry cultivar. Three representative plants were transferred into each of four OTCs; two were used for CO₂ enrichment (550 µmol mol⁻¹ [CO₂]) and the remaining two chambers were considered as controls. The mean [CO₂] in the control OTCs ranged from 390 to 410 µmol mol⁻¹ depending on weather conditions, whereas the mean [CO₂] in elevated CO₂ OTCs was maintained at 550 µmol mol⁻¹ (±20). Once these plants were established under both elevated and ambient CO₂ environments, plants were cut manually at the stump height of 30cm above the soil surface to create a

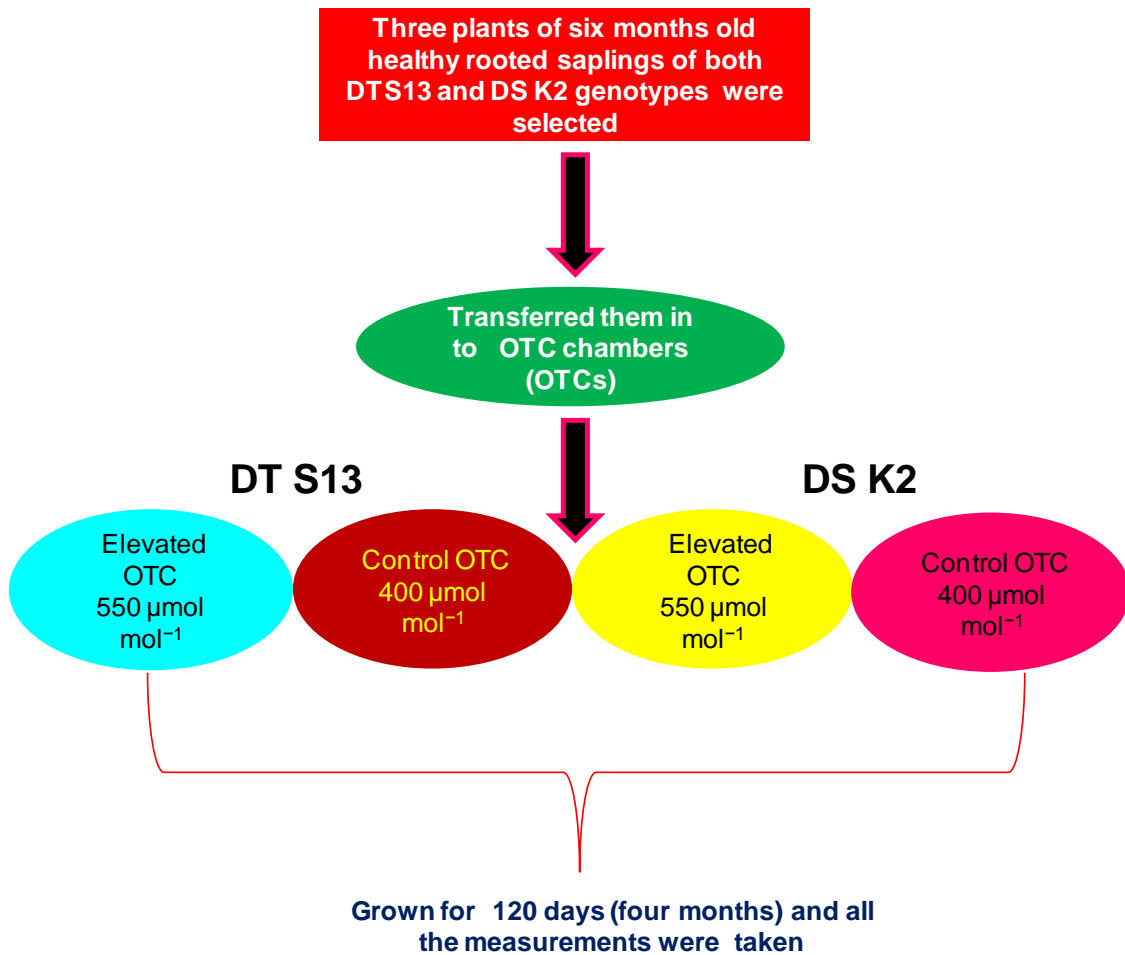
coppice culture system. Later, plantation was coppiced for every 120 days (4 months) which constitute one short rotation cycle. Shoots, resprouted from the remaining stumps, were grown for the next four months for the subsequent harvests. After 365 days, plants growing in two OTCs (one ambient and one elevated) were subjected to water withholding, stopped being watered completely, for 30 days.



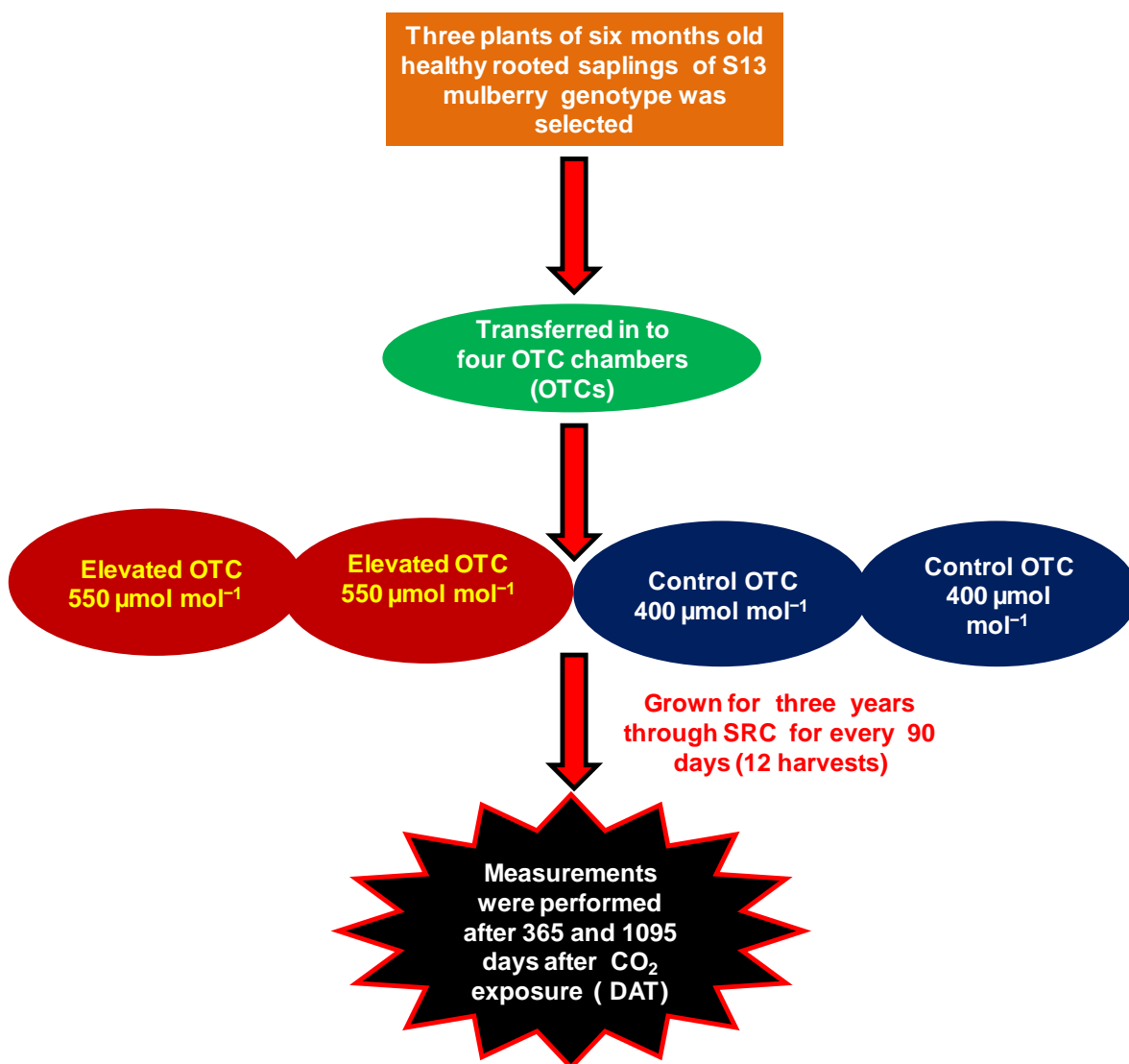
Fig 2.1 Experimental facility: OTCs established in the botanical garden of University of Hyderabad for [CO₂] enrichment studies.

Experimental layout to investigate the formulated objectives of the present study:

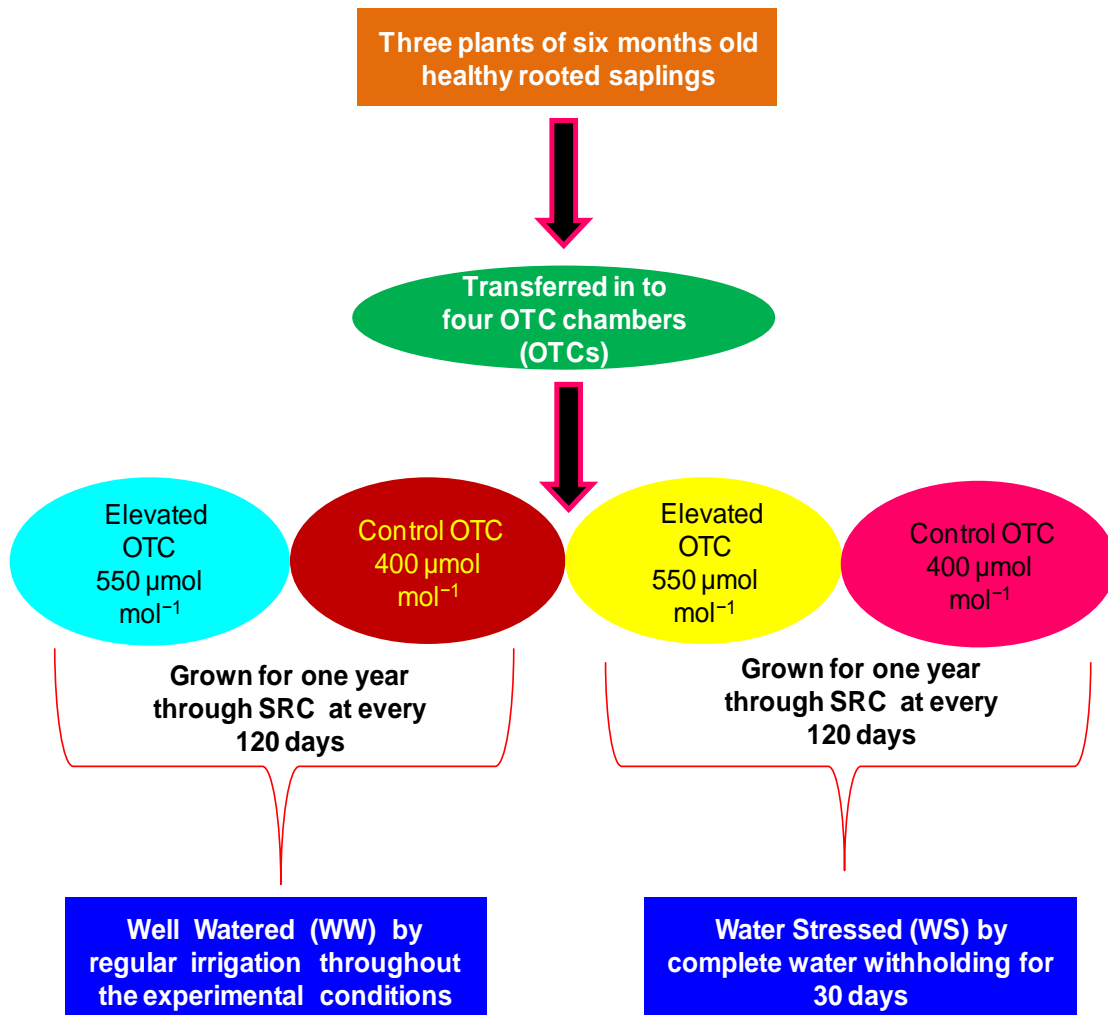
1. Experimental design to investigate short term responses of mulberry genotypes (S13 and K2) under elevated $[\text{CO}_2]$ atmosphere:



2. Experimental plan to examine the long term carbon sequestration potential in mulberry with altered coppice management practice



3. Experimental design to investigate the interactive effects of elevated $[\text{CO}_2]$ and drought in mulberry:



2.3 Photosynthetic leaf gas exchange physiology

All the photosynthetic measurements were performed *in-situ* on young, well-expanded and light-exposed 2nd or 3rd leaves which were randomly chosen from the upper half of the plant canopy between 10:00-11:00h by using a portable infrared CO₂/H₂O gas analyzer (IRGA) (LC Pro+, ADC Bioscientific Ltd. U.K.), equipped with a broad leaf chamber (Fig 2.2 A). Throughout the measurements, the following conditions were maintained: a saturating photosynthetically active radiation (PAR) of 1600 $\mu\text{mol m}^{-2} \text{s}^{-1}$ supplied by a LED light source (LCpro Lamp 32070 - Broad, ADC Bioscientific Ltd. U.K.) attached to leaf chamber, air temperature of 25-26°C and relative humidity of 55-60%. Instantaneous photosynthetic leaf gas exchange measurements were taken at growth [CO₂] of 550 and 400 $\mu\text{mol mol}^{-1}$ for elevated and ambient [CO₂] grown plants respectively. Once a leaf was enclosed in the chamber, an incubation time of 2 min was given to the leaf to re-adjust to its new microclimate and the measurements on light saturated net photosynthetic rates (A_{Sat} ; $\mu\text{mol m}^{-2}\text{s}^{-1}$), stomatal conductance (g_s ; $\text{mol m}^{-2}\text{s}^{-1}$), intercellular [CO₂] (C_i ; μmol) and transpiration rates (E ; $\text{mmol m}^{-2}\text{s}^{-1}$) were recorded. The instant water use efficiency (WUE_i) was also calculated from the above data ($WUE_i = A/E$; $\text{mmol CO}_2 \text{mol}^{-1} \text{H}_2\text{O}$).

2.4 Photosynthetic response (A) to increased photosynthetic photon flux density (PPFD or Q) and intercellular CO₂ concentration (C_i)

Modulation of photosynthetic response with increasing light intensity and [CO₂] was analyzed by determining the A/Q and A/C_i curves respectively using the same leaves, which were taken for the measurement of photosynthetic leaf gas exchange. A/Q studies were performed on elevated (550 μmolmol^{-1}) and ambient (400 μmolmol^{-1}) [CO₂] grown plants with an automated program of eight steps of gradually increasing light intensities (0, 250, 500, 750, 1,000, 1250, 1500 and 2,000 $\mu\text{mol m}^{-2}\text{s}^{-1}$ photosynthetic photon flux density, PPFD) and each step duration was 3 minutes. A/C_i studies were determined with a range of CO₂ concentrations (50–1500 $\mu\text{mol mol}^{-1}$) at a saturating light intensity of 1600 $\mu\text{mol m}^{-2} \text{s}^{-1}$ with an automated program of 10 steps, each step

constitutes 3 minutes was used for elevated (550, 400, 200, 100, 50, 550, 750, 1000, 1250 and 1500 $\mu\text{mol mol}^{-1}$) and ambient (400, 200, 100, 50, 400, 550, 750, 1000, 1250, 1500 and 2000 $\mu\text{mol mol}^{-1}$) CO₂ grown mulberry plants.



Fig 2.2 Infra red gas analyzer (IRGA) used for the measurements of photosynthetic leaf gas exchange physiology (A) and Handy PEA used for measuring PS-II efficiency (B) in mulberry.

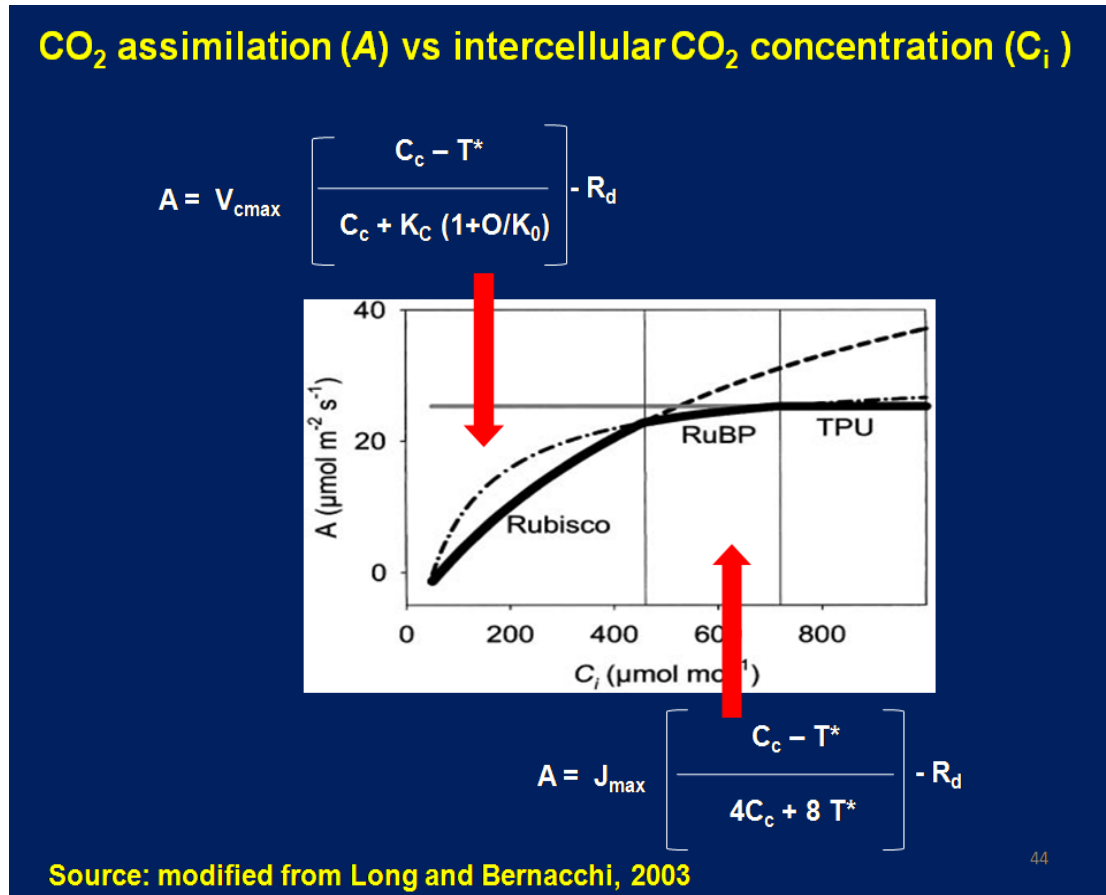


Fig. 2.3 An ideal A/C_i curves showing changes of *in vivo* RuBP carboxylation (V_{cmax}) and its regeneration (J_{max})

Both A/Q and A/C_i curves were fitted with curve-fitting software (Sigma Plot for Windows 11.0; Systat Software) by three component exponential function equation $A = [a(1 - e^{-bx}) + c]$, where A = photosynthetic rate and $x = \text{PPFD} / C_i$ and a, b and c were parameters estimated by the nonlinear regression. From these curves, parameters like light-saturated photosynthetic rate (A_{sat}), calculated as a + c, and the apparent quantum efficiency (AQE) as the initial slope at A = 0 [calculated as b (a + c)] were deduced. Light compensation point (LCP) was determined by solving this equation for PPFD at A of 0 μmol m⁻²s⁻¹ (Watling et al., 2000). From A/C_i curves, parameters including maximum *in vivo* RuBP carboxylation (V_{cmax}), maximum RuBP regeneration (J_{max}) and

light and CO₂ saturated maximum photosynthetic rates (A_{\max}) were calculated (Long and Bernacchi 2003 ; Sharkey et al., 2007).

2.5 Chlorophyll a fluorescence measurements

Chlorophyll a (Chl a) fluorescence measurements were taken on the same leaves used for the photosynthetic leaf gas exchange measurements by using MINI- PAM (HeinzWalz GmbH, Effeltrich, Germany) on the adaxial side of the leaves with saturated light flashes. Maximal photochemical efficiency of photosystem-II, $(F_M - F_0)/F_M = F_V/F_M$, was calculated on the leaves which were pre-dark adapted for 30 minutes, where as the effective quantum yield of photosystem-II, $(F_M' - F)/F_M' = \Delta F/F_M'$, under natural light conditions were determined by illuminating saturated light flashes. From the above parameters, non photochemical quenching ($NPQ = (F_M - F_M')/F_M'$) was also calculated (Maxwell and Jhonson 2000).

In addition to above, chlorophyll *a* fluorescence measurements were also taken using portable Handy-PEA chl fluorometer (Handy-Plant Efficiency Analyser-2126, Hansatech Instruments, King's Lynn, UK) for detailed analysis of changes in PS-II efficiency under both elevated [CO₂] and drought environments. Before these measurements, leaves were pre dark-adapted for 30 min by fixing leaf clips (Hansatech, UK) to make sure that all PSII reaction centers (RCs) were open (Guha et al., 2013). Then chl *a* fluorescence transients were recorded by illuminating the leaves with a beam of saturating light ($3000 \mu\text{mol m}^{-2} \text{s}^{-1}$) of 650 nm peak wavelength obtained from three light-emitting diodes focused on the leaf surface through the leaf clips on a spot of 5 mm diameter circle. Fast fluorescence kinetics were recorded from 10 μs to 1s and the fluorometer was set using the following program: the initial fluorescence (F_0) was set as O (50 μs), L (150 μs), K (300 μs), J (2 ms) and I (30 ms) are the intermediates and P (500 ms-1s) as the maximum fluorescence (F_M). Raw (without normalization) OJIP chl *a* fluorescence transient (F_t) curves were transferred with WINPEA 32 and analyzed with Biolyzer P3. For subsequent detailed analysis of the whole digitized fluorescence kinetics, different normalizations, calculation of kinetic differences or ratios as well as time derivatives were undertaken. The original OJIP transients were double normalized

between the two fluorescence extreme O (F_O) and P (F_M) phases and the variable fluorescence between OP expressed as V_{OP} was determined. In addition to above, chl *a* fluorescence transients were double normalized between F_O (30 μ s) and F_K (300 μ s) expressed as V_{OK} [$V_{OK} = (F_t - F_O) / (F_K - F_O)$] to reveal the possibility of fluorescence rise at an early step at about 300 μ s. Subsequently, for each sampling date the difference in transients (ΔV_{OK}) with respect to a reference was calculated to reveal the L-band. Further, the chl *a* fluorescence transients were double normalized between F_O and F_J expressed as V_{OJ} [$V_{OJ} = (F_t - F_O) / (F_J - F_O)$] and the difference between transients expressed as ΔV_{OJ} was determined periodically for each sampling dates to visualize and assess the K-band. From OJIP chlorophyll *a* fluorescence transients, several phenomenological and biophysical expressions were deduced, known as JIP test parameters, which provide structural and functional information of PSII (Table.1).

2.6 Scanning Electron Microscopy (SEM)

Leaf samples of 3×3 and 3×1 mm sizes were fixed overnight in 2.5% glutaraldehyde solution prepared in phosphate buffer (pH 7.2). After 24hrs, samples were processed for dehydration in graded series of ethyl alcohol (30, 50, 70, 90 and 100 %). Samples were then dried in critical point drier (EMS850) and mounted on to copper stubs using double stick cellophane tape. The mounted samples were coated with gold in sputter coater (FC-1100, Jeol) and observed under Scanning electron microscope (Philips XL 30 ESEM). The behavioural changes in stomata were observed and stomatal density in the leaf samples were determined using a photomicroscope system (MPS 60, Leica, Wetzlar, Germany). Stomatal size was defined as the length in micrometers (μ m) between the junctions of guard cells at each end of the stomata which indicates the maximum potential opening of stomatal pore (Teng et al., 2006).

2.7 Specific leaf area (SLA) and leaf biochemistry

Same leaves used for photosynthetic leaf gas exchange and chlorophyll *a* fluorescence measurements were used for these measurements. Leaf discs were collected with 1.53cm² leaf borer and were completely dried by keeping in incubator at 72⁰C. Dry

weights were measured and used for calculation of SLA by using leaf area/leaf dry weight and values were expressed as $\text{cm}^2\text{g}^{-1}\text{dw}$. Leaf samples of 10 mg were used for the estimation of both starch and total sugars. For estimating starch, samples were extracted in 10 ml of 80 % ethanol using a water bath at 80°C. After drying the residue over water bath, 0.5 ml of H_2O and 0.65 ml of perchloric acid was added. The homogenate was centrifuged at maximum speed for 20 min to collect the supernatant and made up to 10 ml with double distilled H_2O . For estimating total sugars, samples were extracted in 5 ml of 2.5 N HCL for 3 hours on hot water bath. After hydrolysis, the extracts were neutralized with Na_2CO_3 and made up to 10 ml with double distilled H_2O and supernatants were collected by centrifugation. These supernatants were used for the quantitative estimation of both starch and total carbohydrates. In addition to above, chlorophyll pigments were also estimated by the methodology of Isrealstam (1979), these samples were used to calculate Chl *a*, chl *b* and total chl contents (Arnon 1949) and the final values were expressed as $\text{mg g}^{-1}\text{fw}$. Foliar nitrogen concentrations were estimated by Dumas method.

2.8 Antioxidant enzyme activities and gene expression

Same leaves which were used for photosynthetic leaf gas exchange parameters as well as for chlorophyll a fluorescence measurements were collected between 10:00-11:00h and were used for both antioxidant enzyme activities and gene expression studies. Antioxidant enzymes including ascorbate peroxidase (APX), monodehydroascorbate reductase (MDHAR), glutathione reductase (GR), superoxide dismutase (SOD) and catalase (CAT) activities were measured. Leaf extracts were prepared from 0.5 g of frozen tissue in 2.5mL of 50 mM potassium phosphate buffer (pH 6.0) containing 0.04 M KCl, 1 mM ascorbate (ASC), 1mM PMSF and 8% PVPP. Enzymes of ascorbate-glutathione cycle (ASC-GSH) like APX, GPX, MDHAR and GR activities were determined according to Murshed et al. (2008) with minor modifications. The homogenate was centrifuged at 14,000g for 10 min at 4°C and the supernatant was immediately used for the enzyme activities.

Table.2.1

Selected chlorophyll a fluorescence JIP-test parameters

Formulae	Description of the individual JIP-test parameter
F_O	Minimum fluorescence value after the onset of actinic illumination at 50 μ s
F_L	Fluorescence value at 150 μ s
F_K	Fluorescence value at 300 μ s
F_J	Fluorescence value at 2 ms
F_I	Fluorescence value at 30 ms
$F_P=F_M$	Maximum fluorescence intensity under saturating illumination at P-step
F_V	Variable chlorophyll fluorescence
K_N	Non-photochemical de-excitation rate constant
K_P	Photochemical de-excitation rate constant
$\phi_{P_0} = TR_O/ABS = F_V/F_M = [1 - (F_O/F_M)]$	Maximum quantum yield of primary photochemistry
$\psi_0 = ET_O/TR_O = (1 - V_J)$	Possibility that a trapped exciton moves an electron into the electron transport chain beyond QA
$\phi_{E_0} = ET_O/ABS = [1 - (F_O/F_M)] \psi_0$	Quantum yield of electron transport (at t = 0)
$DI_O/RC = (ABS/RC) - (TR_O/RC)$	Dissipated energy flux per RC
$RC/CS_m = \psi_0 (V_J/M_O) (ABS/CS_m)$	Density of active reaction centers per cross-section (CS)
$ABS/CS_m = F_M$	Absorption flux per excited CS
$TR_O/CS_m = \phi_{P_0} (ABS/CS_m)$	Trapped energy flux per excited CS
$ET_O/CS_m = \phi_{E_0} (ABS/CS_m)$	Electron transport flux per excited CS
$DI_O/CS_m = (ABS/CS_m) - (TR_O/CS_m)$	Dissipated energy flux per excited CS
$PI_{(ABS)} = (RC/ABS) (\phi_{P_0} / (1 - \phi_{P_0})) \times (\psi_0 / (1 - \psi_0))$	Performance index on absorption basis
$PI_{(CS_m)} = (RC/CS_m) (\phi_{P_0} / (1 - \phi_{P_0})) \times (\psi_0 / (1 - \psi_0))$	Performance index on cross section basis

For APX activity assay, 1 ml reaction buffer consisting of 50 mM potassium phosphate buffer (pH 7.0) and 10 mM ascorbic acid (ASA). Then 25 μ l of sample supernatant or extraction buffer was added to reaction buffer, total solution was mixed with gentle shaking for 5 s and the absorbance of the reaction was measured at 290 nm for 3 min at 25° C to determine nonspecific ascorbate degradation. Further, 200 mM H₂O₂ was added to the 1 ml of reaction mixture and measured the decrease in the reaction rate/absorption at 290 nm for 3 min. Specific activity was calculated from the 2.8 mM⁻¹ cm⁻¹ extinction coefficient. A correction was carried out for the nonspecific oxidation of ascorbate in the sample (first reading) and by H₂O₂ in the absence of the enzyme sample (blank). To measure the activity of MDHAR, reaction was started by adding of 0.4 units of ascorbate oxidase to the 1 ml reaction buffer containing 50mM phosphate buffer, 10mM ASA, 10 mM NADH, 25 μ l of sample supernatant or extraction buffer to generate monodehydroascorbate radical. MDHAR activity was determined by measuring the decrease in the reaction rate/absorption at 340 nm for 3 min. Specific activity was calculated using the 6.22 mM⁻¹ cm⁻¹extinction coefficient. Rate of nonspecific NADH oxidase activity was subtracted.

Glutathione reductase (GR) activity was estimated spectrophotometrically by measuring the NADPH oxidation at 340 nm in the presence of 10 mM NADPH. The GR reaction was started by the addition of 20 mM GSSG to the 1 ml reaction mixture consist of 50mM phosphate buffer, 10mM EDTA and 25 μ l of sample supernatant or extraction buffer. The specific activity was calculated from the 6.22 mM⁻¹cm⁻¹ extinction coefficient. Nonspecific NADPH oxidation was determined before adding GSSG and subtracted from the GR specific activity. In order to define activity as micromole of substrate consumed or product formed per minute per milligram of protein, the protein concentration was quantified by Bradford (1976) method.

Glutathione peroxidase (GPx) activity was measured according to the procedure given by Paglia and Valentine (1967). Reaction buffer (1 ml) contains 50mM phosphate buffer, 10mM NADPH, 10mM EDTA, 50mM reduced GSH, 200mM H₂O₂, 5U of GR enzyme and 25 μ l of sample supernatant or extraction buffer. Decrease in absorbance at 340 nm was

measured for 3 min and enzyme activity was calculated from the $6.22 \text{ mM}^{-1}\text{cm}^{-1}$ extinction coefficient.

Similarly, SOD activity was determined according to Dhindsa et al. (1981) by measuring the inhibition of P- nitro blue tetrazolium chloride (NBT) reduction at 560 nm. The 3 ml reaction mixture contained 50 mM phosphate buffer (pH 7.8), 13 mM methionine, 75 μM NBT, 2 μM riboflavin, 0.1 mM EDTA and 50 μl of enzyme extract. Riboflavin was added last and the tubes were shaken and placed 30 cm below a light bank consisting of two 15 W fluorescent lamps for 10 min. The absorbance by the reaction mixture was read at 560 nm. Catalase activity was assayed according to Aebi (1984) by monitoring the H_2O_2 decomposition rate. To measure the catalase activity, 1 ml reaction buffer consist of 50 mM phosphate buffer (PH 7.0), 200 mM H_2O_2 and 25 μl of plant extract.

Based on existing draft genome sequence of mulberry, *Morus notabilis*, gene specific primers were designed for antioxidant enzymes and given in Table 1 (He et al. 2013). These primers were checked for their amplification by PCR (Fig.), confirmed through their sequence analysis and the same were used to perform quantitative real time-PCR (qRT-PCR) to check their gene expression in mulberry under both elevated $[\text{CO}_2]$ as well as drought conditions with their respective controls. Total RNA was isolated using plant spectrum RNA isolation kit (Sigma-Aldrich, USA) and cDNA synthesis was performed by using Revert AidTM first strand synthesis kit (Fermentas Life Sciences, Germany) and qRT-PCR was performed using Eppendorf Realplex Master Cyclor (Eppendorf, Germany) with the KAPA SYBR FAST (Mastermix (2X) Universal) (KAPA Bio systems, USA) real time PCR kit following manufacturer's protocol. Expression levels of the target genes were calculated by comparing the cycle threshold value (Ct) to the reference gene actin, since its expression was stable under all experimental conditions. The relative quantification (comparative method) was done using the $2^{-\Delta\Delta\text{Ct}}$ method (Livak and Schmittgen 2011).

Table 2.2 Gene specific primers designed for antioxidant enzymes (Cyt- cytosolic, Chl- chloroplastic, Mit- Mitochondrial) and aquaporins (AQPs).

Gen Bank ID	Target description	Forward	Reverse
EXC01121	GPX-1	CAGGCCAAAGGGAGCCG	CATCAATATCCTTTACAGTGAAGTC
EXB68679	GPX-2	GGAATGATGCGAGTCTAAGTG	CCTAGTGCATACAACCTCCTG
EXB39342	GPX-4	CTCGTCGTTAACGTCGCTTC	CAGCTTTGTATCTAGTGCATGC
EXB37365	GPX-6	CCAATCCAGCAAAGGCTCTG	CTGTTTCATTGGTCCCTGGC
EXB37363	GPX-8	AGGAGGAACCTGGAAGTAATG	GTCAACGACTTTCCCGTCC
EXC21081	Chl Fe SOD	CCAAGTTTGAGCTAAAGCCTC	CCAAACTTGTGCTGCATTGTTG
EXB96397	Fe SOD	GCTATACTATGGATGAACTTGT C	CAGAGCCAAATAGAGTTAGTGC
EXB67662	Cyt Cu-Zn SOD	CTTAAGCCCGGGCTTCATG	CAGCACGGCCGATGATGG
EXC19545	Mit Mn SOD	CTGCCGGACCTTCCGTAC	GTTAACAGGAGCGAGATTCTTC
EXB96516	Chl Mn SOD	GTACGACTATGGCGCTCTG	CCACCTCCTTCACTGATAGG
EXB37740	MDHAR-1	GGGAAAACTCTTATAAGCGCA G	GACCAATATATCCTCCTCCAAC
EXB37705	MDHAR-2	GTTTCCGCCGGTTACGCG	CGGACTATTTCCGTGTTGAGG
EXB37294	MDHAR-3	GCAGATGCTGATGCACTAATA TC	CTCTGGGCAAGTGAAGGAGT
EXC20301	MDHAR-4	GGAGGTGGCTATATAGGAATG	CATCTCTAAGAATAACAGCTGTG
EXB87094	GTR-1	GCGGGATGGGTGCTACTG	CGGTGGCAAACAATACAACATC
EXB26575	GTR-2	CGGTGGATACATTGCCTTGG	AATGATCCATCGGCAACTTTAAT G
EXC35333	APX-3.1	GTCATCCAGATGCCAAACAAG	GGGAAGTTTCAATAGCCCTTTTG
EXC35330	APX-3.2	GTCTATCTGACAAGGAAATTG TG	GTATAGCTCAACGTAGCTACG
EXC33221	APX-3.3	GTACCCAGAGGAGCTCGC	CAGAACCCTTGGTAGCATCAG
EXB60099	APX-T	GAAGTTTGAGGTTTGAGATTG AG	TCTCCCTTCTTCTGGGCAC
EXB37691	APX-2	GACCGCTCTGGATTTGAAGG	CCAAGCTCCGATAACTTCAAATG
EXC51646	CAT	GTGGTGTCAAGTCTCTGTTG	CTGCAAAGAAGTTATCAATGTTG
gi 703093878	PIP 1.1	GGTCATGGGCGTCGTCAAG	GAACACTGCCCTAGTTAACGAC
gi 703115256	PIP 2.1	CGGTGGCGTTGGGATTCTC	CAAACCTCTGGGCCACTATGTAC
gi 703141596	PIP 2.2	GTCGGCATTGTTGGGAATTGCC	CACAGATGGCCCCCAAGC
gi 703142030	PIP 2.7	GCCTCCTCGGCATCGCC	CACGAGCCCAACCCCGC
gi 703099448	TIP 1.3	GGGGCATCGACCCCTTCG	CGGATCCCAAAAGCTGTGCG
gi 703104858	TIP 2.1	GCGCCAACATCTCCGGTG	CAATGGCACCAACTCCGGC
gi 703131479	TIP2.3	CATTGCCGCCAACATCTCAG	CCCAACCCCGCGGCTAG
gi 703069838	TIP 4.1	GTGGCCATCTTAACCCGGCCTC	CTTGGAAGTGTCTACC

2.9 Estimation of oxidative stress parameters, osmolytes and molecular antioxidants

Lipid peroxidation was determined by quantifying malondialdehyde (MDA) according to Fu and Huang (2001). Fresh leaf samples (0.5 g) were taken and homogenized in 5 ml of 0.1% (w/v) trichloroacetic acid (TCA) at 4°C and the homogenate was centrifuged at 5,000g for 10 min at 4°C. The reaction mixture contained 0.5 ml of the supernatant and 4 ml of 0.5% (w/v) thiobarbituric acid (TBA) in 20% (w/v) TCA, incubated at 95°C in a shaking water bath for 30 min and the reaction was stopped by quickly cooling the tubes in an ice water bath. The samples were centrifuged at 5,000g for 15 min and the absorbance of the supernatant read at 532, 600 and 440 nm. MDA concentration was calculated using an extinction coefficient of $155 \text{ mM}^{-1} \text{ cm}^{-1}$.

Proline content in leaf tissues of mulberry from all the treatments was determined according to Bates et al. (1973). Fresh leaf samples (0.5 g) were homogenized in 10 ml of 3% sulphosalicylic acid and were centrifuged at 9,000g for 15 min at room temperature. The reaction mixture containing 1 ml leaf extract, 2 ml acid ninhydrin and 2 ml glacial acetic acid was incubated for 1 h in boiling water bath. After incubation, 4 ml of toluene was added to the reaction mixture and mixed vigorously by vortexing for 15–20 s. The upper reddish pink color toluene layer was separated and the absorbance was read at 520 nm, proline content was determined from the standard curve and was expressed as mg g^{-1} fw.

Ascorbic acid (ASA) was estimated according to Omaye et al. (1979), fresh leaf tissue (0.5 g) was homogenized with 5 ml of 10% (w/v) trichloroacetic acid (TCA). The extract was centrifuged at 10,000 g for 20 min at room temperature. The pellet was re-extracted twice; supernatants were combined and used for assay. To 0.5 ml of extract, 1 ml of 2% DNTPH (2, 4-dinitrophenyl hydrazine in 0.5 N H_2SO_4), a drop of 10% thiourea (in 70% ethanol) were added and incubated at 37°C for 3 h. After incubation, 1.75 ml of ice-cold 65% H_2SO_4 was added, allowed to stand at 30°C for 30 min and the absorbance of the resulting color was detected at 520 nm. The ASA content was determined from the standard curve and was expressed in mg g^{-1} fw.

Total glutathione content in mulberry leaves was determined according to Griffith and Meister (1979). Fresh leaf tissue (0.2 g) was homogenized with 0.8 ml of 10%

sulphosalicylic acid and centrifuged at 15,000g for 5 min at 4°C. The supernatant was neutralized by adding 0.6 ml of 10% sodium citrate. 1 ml reaction mixture was prepared by adding 0.1ml extract, 0.2ml double distilled water (ddw), 0.7ml of 0.3 mM NADPH in potassium phosphate buffer (20 mM, pH 7.5) and 6 mM 5'-dithio-bis (2-nitrobenzoic acid) (DNTB). The reaction mixture was stabilized at 25°C for 3–4 min, then 10 µl glutathione reductase (GR) was added to the reaction mixture and the absorbance of the resulting color was read at 412nm and concentrations were expressed in µmol g⁻¹ fw.

Total phenolic content was determined according to Stankovic (2011). The reaction mixture was prepared by mixing 0.5 ml of methanolic solution of extract (1mg/ml), 2.5 ml of 10% Folin-Ciocalteu's reagent dissolved in water and 2.5 ml 7.5% NaHCO₃. Blank was concomitantly prepared, containing 0.5 ml methanol, 2.5 ml 10% Folin-Ciocalteu's reagent dissolved in water and 2.5 ml of 7.5% of NaHCO₃ and incubated at 45°C for 45 min. The absorbance was determined at 765 nm and content of total phenolics (TPC) in extracts were expressed in terms of gallic acid equivalents as mg of GA/g fw.

2.10 Measurements of leaf relative water content (RWC), plant hydraulic conductivity parameters and aquaporins (AQPs) gene expression

To check the RWC, fresh leaf discs (1.5 cm²) were weighed immediately, then re-hydrated by immersing them in distilled water for 24 h at 4°C in darkness and subsequently oven-dried for 24 h at 105°C. The RWC was determined as $[(fw-dw)/(tw-dw)] \times 100$, where fw is the fresh weight of leaf discs, tw is the turgid weight after re-hydrating the discs for 24 h, and dw is the oven-dried weight of discs. Along with RWC, we also measured stem xylem water potential (Ψ_x ; MPa) by using a commercially available psychrometer (PSY; ICT International, Australia) (Dixon and Downey 2013). PSY was installed on to the stem at 100cm above from the ground to record stem xylem water potential. Leaf water potential (predawn, Ψ_{pd} and midday Ψ_{md} ; MPa) was measured with PSY on fully matured and young leaves.

In addition to above, we obtained xylem sap flow rate (F; kg/hr) by heat ratio method by using commercially available sap flow meter (Model: SFM; ICT International, Australia).

SFM was installed at 150cm height and maintained constantly during all the experimental conditions. Stem hydraulic conductivity was calculated as: $K_S = [F \times L / (\Psi_{in} - \Psi_{out})]$ ($\text{kg m}^{-1} \text{sec}^{-1} \text{MPa}^{-1}$), where F is sap flow rate (kg/sec), L is distance between two PSY (m), Ψ_{in} is water potential at inlet (MPa) and Ψ_{out} is water potential at outlet (MPa). Leaf hydraulic conductance (K_L) was also determined by using transpiration rates measured with leaf gas analyzer and the water potential differences of leaf and xylem. K_L was calculated according to Ohm's Law as: $K_L = [E / (\Psi_X - \Psi_{md})]$ ($\text{mmol m}^{-2} \text{s}^{-1} \text{MPa}^{-1}$), where E is transpiration rate ($\text{mmol m}^{-2} \text{s}^{-1}$), Ψ_{md} is midday leaf water potential (MPa), Ψ_X is xylem water potential (MPa). We also checked gene expression patterns of membrane intrinsic proteins (MIPs) or aquaporins (AQPs), gene specific primers were designed based on existing draft genome sequence and these primers were given in Table 2.

2.11 Changes in morphological characteristics, plant growth, destructive biomass yield and carbon sequestration potential

At 30 days after stress (30DAS), plants grown under both elevated and ambient $[\text{CO}_2]$ environments were photographed to visualize the drought effects. Further, these pictures were analyzed by ImageJ software to quantify their morphological changes such as amount of greenery leaves as well as senescence leaves and expressed their values in integrated density/ m^2 area/plant. In addition to above, we also measured individual leaf density by choosing leaves randomly on images from all over the plant and expressed values in terms of integrated density/ mm^2 area/ leaf. Plant height (Ht) from the ground to the canopy top was measured using measuring tapes. The shoots of all the representative plants were coppiced using a sharp secateur (a type of pruner), and the aboveground components (leaves, branches and stems) were separated and immediately fresh weight was taken in the field to get total leaf fresh weight (TLFW) and total stem fresh weight (TSFW) (primary + axillary branches). After taking fresh weights, subsamples (200mg) from leaves and stems were chipped and mixed in order to evenly distribute wood of different densities and oven-dried at 80°C for several days until constant weight was achieved.

Measurement of stem hydraulic conductance



Stem hydraulic conductance

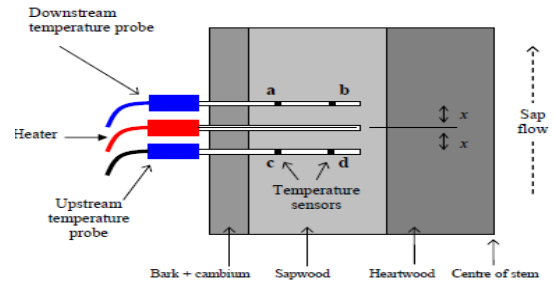
$$(K_{\text{stem}}) = [F \cdot L / (\psi_{\text{in}} - \psi_{\text{out}})]; \text{ kg m}^{-1} \text{ sec}^{-1} \text{ Mpa}^{-1}$$

Where **F** is sap flow per time (**kg/sec**),

ψ_{in} is water potential at inlet (**Mpa**)

ψ_{out} is water potential at outlet (**Mpa**)

L is distance between two Psy (**m**)



Measurement of leaf hydraulic conductance



Leaf hydraulic conductance

$$(K_L) = E / (\psi_L - \psi_x); \text{ mmol m}^{-2} \text{ s}^{-1} \text{ Mpa}^{-1}$$

where **E** is transpiration rate (**mmol m⁻² s⁻¹**)

ψ_L is leaf water potential (**Mpa**)

ψ_x is xylem water potential (**Mpa**)

Fig 2.5 Measurements of *in situ* stem and leaf hydraulic conductance by hydraulic conductivity meter (HCM) in mulberry

This weight was used to calculate total dry weights of respective samples for individual plant. Dry weights as well as fresh weights of leaf and stem were used to calculate total above ground fresh weight (TAGFW) and total above ground dry weight (TAGDW) per plant. After three years, roots were collected from an area of 1m×1m×1m volume around the plant base. The roots were brought to the laboratory, fresh weights (RFW) were taken and were then oven dried to obtain dry weights (RDW). This carbon content in DW was multiplied with constant value of 3.66 to get the total CO₂ sequestered in the respective plants per year. After three years, both dry weights as well as its carbon sequestration potential of mulberry plants were calculated per hectare and these values were expressed as Mg/hectare/3 years.

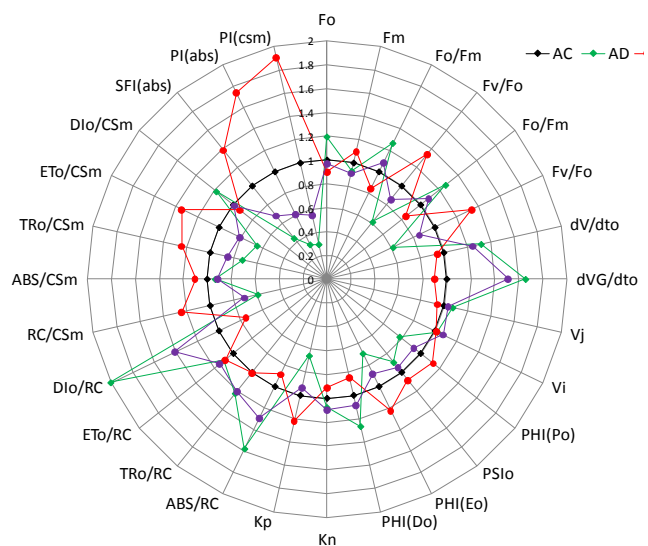
2.12 Statistical analysis

Data on leaf gas exchange characteristics, chlorophyll *a* fluorescence, changes in antioxidant enzyme activities, oxidative stress parameters, molecular antioxidants and bio-mass yield in mulberry grown under elevated and ambient CO₂ atmosphere under WW and WS conditions, were given as mean ± SD of 3 plants (n = 3). Analysis of variance (ANOVA) was performed to check the statistical significance between the treatments (elevated [CO₂], drought, and time) by using statistical package Sigma Plot 11.0. Relationship between leaf gas exchange and plant hydraulic variables were plotted using statistical package excel 2007. Correlations between parameters were evaluated by calculating simple linear correlation coefficient of determinations (r^2).



Chapter 3

Results



3.1 Objective 1- Variations in photosynthesis, growth and bio-mass yield responses of two contrasting drought tolerant (DT) mulberry cultivars under elevated [CO₂] atmosphere

3.1.1 Photosynthetic leaf gas exchange physiology

Elevated [CO₂] atmosphere induced significant changes in photosynthetic leaf gas exchange parameters between the two genotypes and treatments (Table 3.1). [CO₂] enrichment increased light saturated net photosynthetic rates (A_{Sat}) by 35% in both the genotypes compared to their respective controls. However, elevated [CO₂] grown S13 (ES13) showed 13% ($22 \mu\text{mol m}^{-2}\text{s}^{-1}$) more A_{Sat} than EK2 ($18 \mu\text{mol m}^{-2}\text{s}^{-1}$). Decreased stomatal conductance (g_s) and transpiration rates (E) in both genotypes of mulberry grown under elevated [CO₂] were recorded. g_s decreased from 0.35 to 0.24 $\text{mol m}^{-2}\text{s}^{-1}$ (31%) in S13 whereas in K2 it reduced from 0.42 to 0.30 $\text{mol m}^{-2}\text{s}^{-1}$ (28%). In consistent with g_s , both mulberry genotypes grown in high [CO₂] showed reduction in E by an average of 30%. Because of lower E , both ES13 and EK2 showed an average increase in WUE_i by 55% than their respective controls. However, ES13 showed further improvement in WUE_i (33%) than EK2 due to additional reduction in E .

Intercellular [CO₂] (C_i) was more in K2 than S13 under both ambient and elevated [CO₂], but plants which were grown under elevated [CO₂] had comparatively higher C_i of 34% and 32% in S13 and K2 respectively than their corresponding ambient CO₂ grown plants. Changes in instantaneous photosynthetic rates (A) with increasing photosynthetic photon flux density (PPFD), known as A/Q curves, between the treatments and genotypes were given in Fig 3.1 and parameter deduced from A/Q curves including apparent quantum efficiency (AQE) was significantly enhanced in the [CO₂] enriched plants with concomitant decrease in light compensation point (LCP) as shown in Table 3.1.

The AQE in control S13 increased from 0.031 to 0.042 (23%) during [CO₂] enrichment, where as in K2 it increased from 0.027 to 0.037 (27%). In contrast to above, LCP was decreased by 65% and 50% in ES13 and EK2 genotypes respectively than their ambient (A) controls.

Table 3.1 Changes in photosynthetic leaf gas exchange characteristics and foliar biochemistry of two mulberry genotypes (S13 and K2) grown under elevated and ambient CO₂ atmosphere. The measurements were taken on randomly selected young fully expanded 3rd or 4th leaf from the apex in the upper canopy region. Values are means \pm SD (n=3)

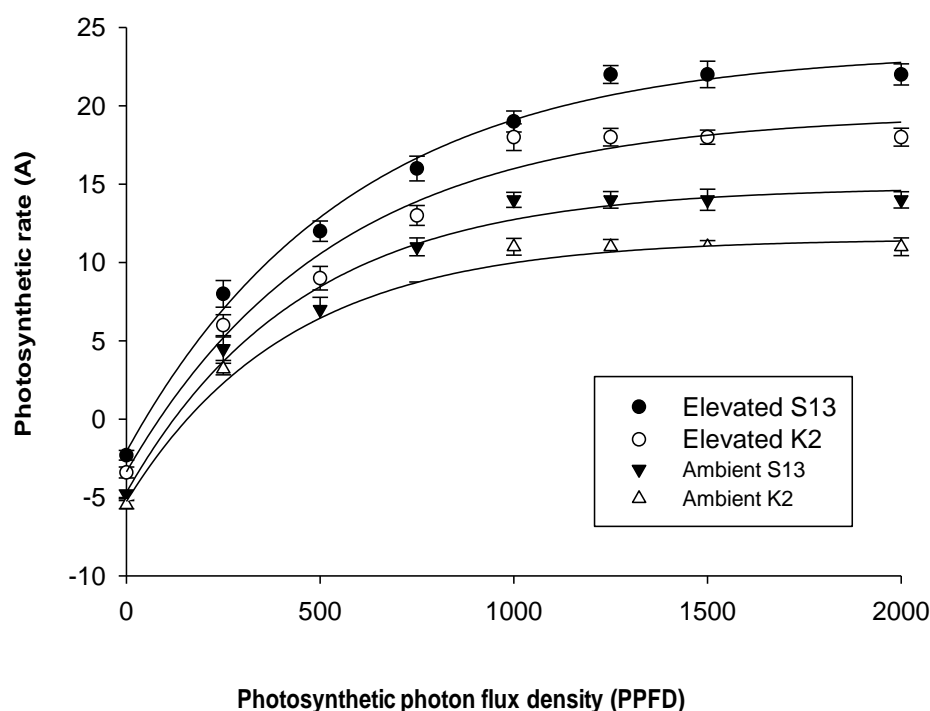


Fig 3.1 Photosynthetic rates in relation to photosynthetic photon flux density (PPFD) in S-13 and K-2 mulberry genotypes grown in ambient and elevated [CO₂]. These measurements were recorded using fully mature leaves randomly taken from upper shoot apex. Values are mean \pm SD (n=3).

3.1.2 Chlorophyll *a* fluorescence measurements

Significant variations in chlorophyll *a* fluorescence were observed between the two mulberry genotypes under elevated [CO₂] atmosphere as depicted in the radar plot (Fig 3.2 and Table 3.2). The data on fluorescence JIP-test parameters were normalized with

proprietary control S13 by giving a numeric value of 1. Parameters like minimal (F_0) and maximal fluorescence (F_M) were significantly higher in K2 when compared to S13 genotype under both ambient and elevated $[\text{CO}_2]$ conditions. However, $[\text{CO}_2]$ enrichment resulted in lower F_0 and higher F_M than control plants. In EK2, F_0 and F_M were increased by 9% and 10% respectively than ES13. The F_0/F_M significantly increased by 9% and 12% in AK2 and AS13 genotypes respectively, compared to their $[\text{CO}_2]$ enriched counterparts. In parallel with above parameters, there was significant rise in dissipation energy flux per absorption flux (DI/ABS), dissipation energy flux per PS-II reaction centers (DI/RCs), dissipation energy flux per PS-II cross section of the leaf (DI/CSm) and the sum of non-photochemical de-excitation rate constant (K_n) in both genotypes grown under ambient $[\text{CO}_2]$. Similar trend was recorded for ABS/RC and ABS/CSm in both ambient $[\text{CO}_2]$ grown mulberry genotypes. Though there was a decrease in the above parameters in elevated $[\text{CO}_2]$, ES13 showed comparatively higher reduction by 9%, 8% and 14% in DI/RCs, DI/CSm and K_n respectively than EK2.

The F_v/F_0 (efficiency of water splitting complex) was significantly increased by 32% and 30% in EK2 and ES13 respectively than their ambient counterparts. There was also a significant increase in F_v/F_M , ψ_o , ΦE_0 , ET/RCs, ET/CSm, RC/CSm, K_p , and $PI_{(ABS)}$ in $[\text{CO}_2]$ enriched mulberry genotypes compared to ambient $[\text{CO}_2]$ plants. However, greater enhancement in these parameters was observed in ES13 by 3%, 7%, 14%, 13%, 17%, 5%, 14%, 22% and 13% respectively compared to EK2.

3.1.3 Leaf biochemistry and specific leaf area (SLA)

Significant changes in leaf biochemistry and SLA between the treatment and genotypes were given in Table 3.1. Leaves harvested from elevated $[\text{CO}_2]$ grown mulberry plants accumulated more non structural (total soluble sugars and starch) carbohydrates than their controls. However, K2 showed more accumulation of sugars than S13 in both ambient and elevated $[\text{CO}_2]$ atmosphere. Total soluble sugars in AS13 was 315mg g^{-1} DW and increased to 410 mg g^{-1} DW in ES13, where as in K2 the sugars increased from 380 to 470 mg g^{-1} DW under $[\text{CO}_2]$ enrichment with an average increase of 23% and 19%

in ES13 and EK2 respectively. Similarly, starch content increased by 30% and 35% in ES13 and EK2 respectively than their ambient counterparts. However, EK2 had more total soluble sugars (12%) and starch (25%) than in ES13. In contrast to non structural carbohydrates, [CO₂] enriched leaves had lower chlorophyll content by 27% and 25% in ES13 and EK2 respectively than their respective controls. Specific leaf area (SLA) showed inverse relationship with leaf thickness which was reduced in both genotypes of mulberry grown under elevated [CO₂].

3.1.4 Growth and bio-mass yields

After four months, both genotypes of mulberry grown under elevated and ambient [CO₂] were harvested for growth and biomass yield measurements. Morphological changes of plants grown under elevated as well as ambient [CO₂] atmosphere within and between the S13 and K2 genotypes were shown in Fig 3.3. High CO₂ grown mulberry plants showed increased plant height, number of leaves and branches cumulatively leading to greater fresh and dry biomass than their ambient [CO₂] counter parts. However, S13 showed more bio-mass accumulation than K2 in both elevated and ambient [CO₂] grown plants. Leaf fresh biomass (LFBM) was 0.95kg in AS13 which increased to 1.45 kg (34%) in ES13, whereas the same was 0.8 kg in AK2 which increased to 1.24 kg (35%) in EK2 (Fig 3. 4 A). Similar trend in stem fresh biomass (SFBM) was observed in both genotypes which were grown under [CO₂] enriched environment. An average increase of SFBM by 32% and 42% in ES13 and EK2 respectively compared to ambient [CO₂] grown plants was observed (Fig 3. 4 C). Similar enhancement was observed in leaf dry biomass (LDBM) and stem dry biomass (SDBM) and an average increase of 38% and 40% respectively in both the genotypes grown under elevated [CO₂] conditions (Fig 3. 4 B & D). There was a substantial increase in root fresh (RFBM) and dry weights (RDBM) in both genotypes grown under increased [CO₂] (Fig 3. 4E & F). Significant increase in fresh and dry biomass of above (leaf + stems) and below ground (root) components leading to an increase in total fresh (TFBM) and dry bio-mass (TDBM) in both the mulberry genotypes grown under elevated [CO₂] atmosphere compared to their respective

controls. An average increase in TFBM and TDBM by 34% and 39% respectively was observed in ES13, where as 36% and 44% increase was observed in EK2 when compared to their ambient counterparts (Fig 3.4 G & H). Nevertheless, ES13 showed more biomass accumulation of 14% and 17% in terms of TFBM and TDBM respectively when compared to EK2.

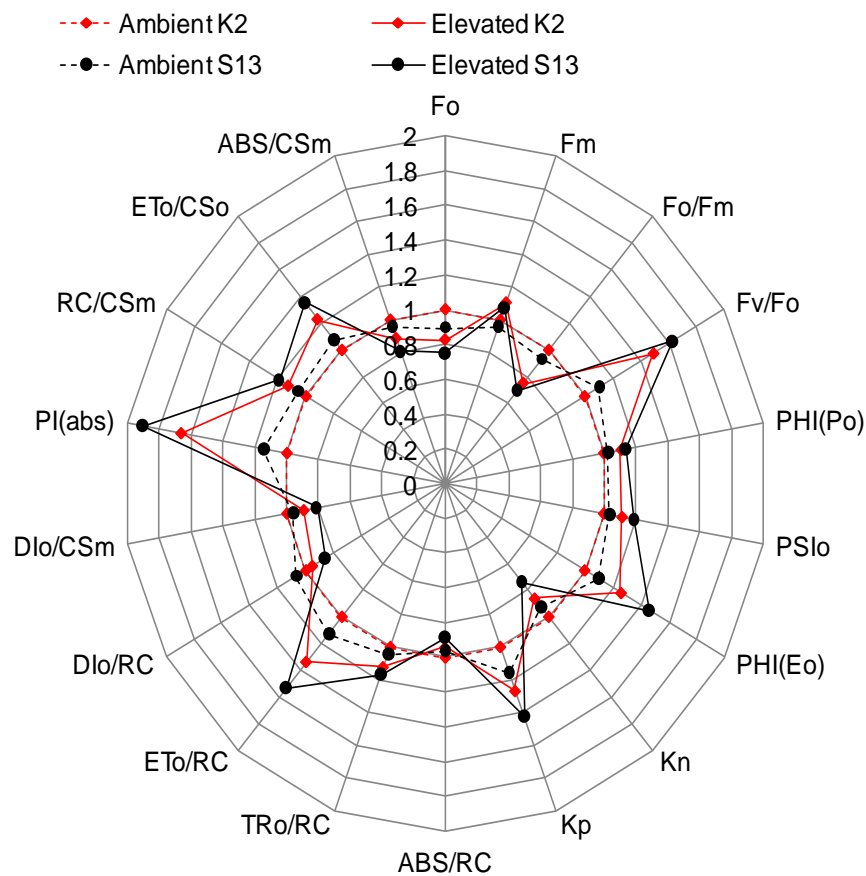


Fig 3.2 Radar plot showing mean changes of chlorophyll *a* fluorescence JIP-test parameters in S-13 and K-2 grown under elevated and ambient [CO₂] atmosphere. The measurements were taken on randomly chosen fully mature leaves at 3rd or 4th position from the apex in upper canopy region during 11:00-11:30 h. Data are mean \pm SD (n = 3).

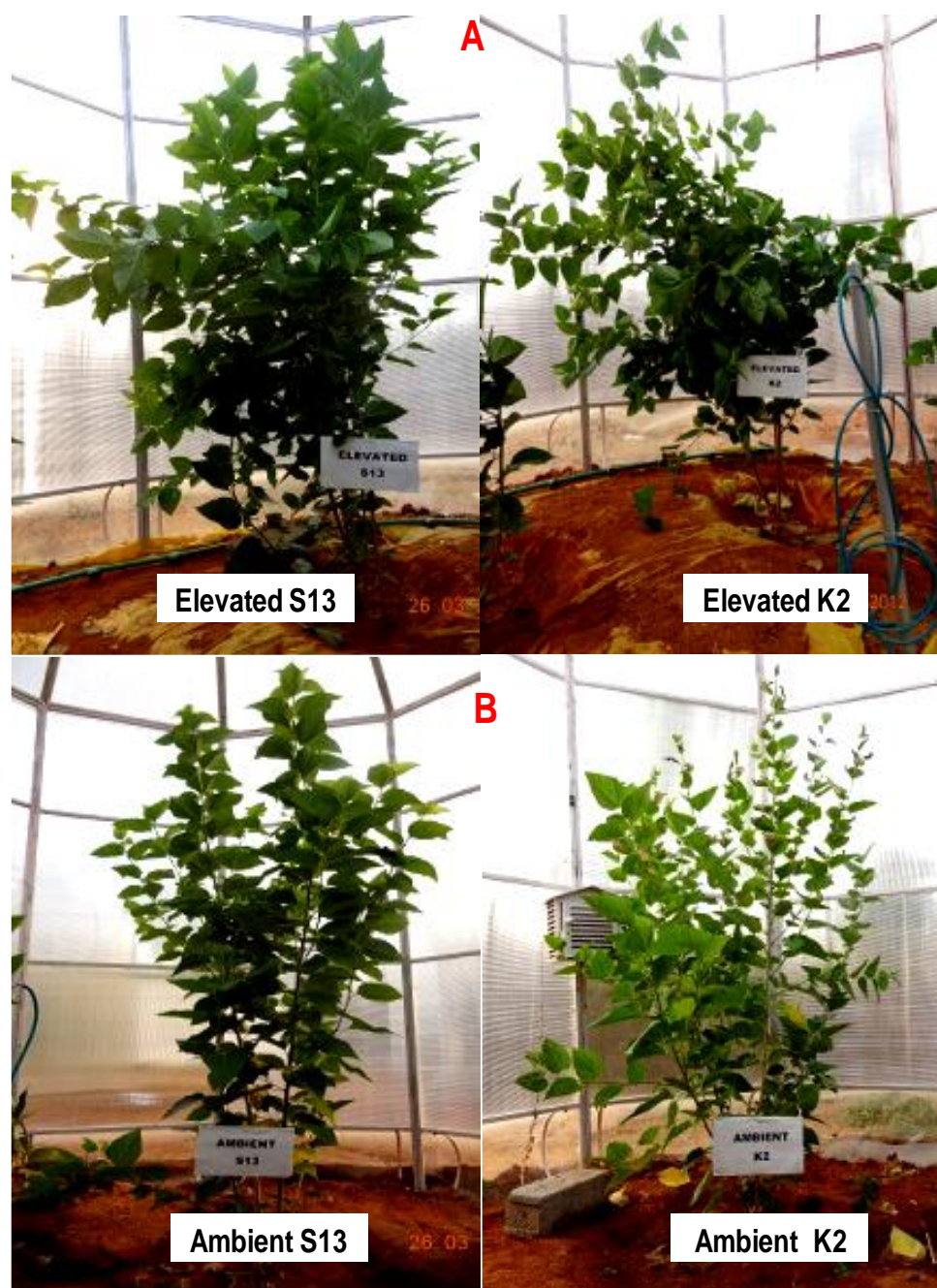


Fig 3.3 Morphology and phenology of S-13 and K-2 mulberry genotypes grown under elevated (A) and ambient (B) [CO₂] atmosphere.

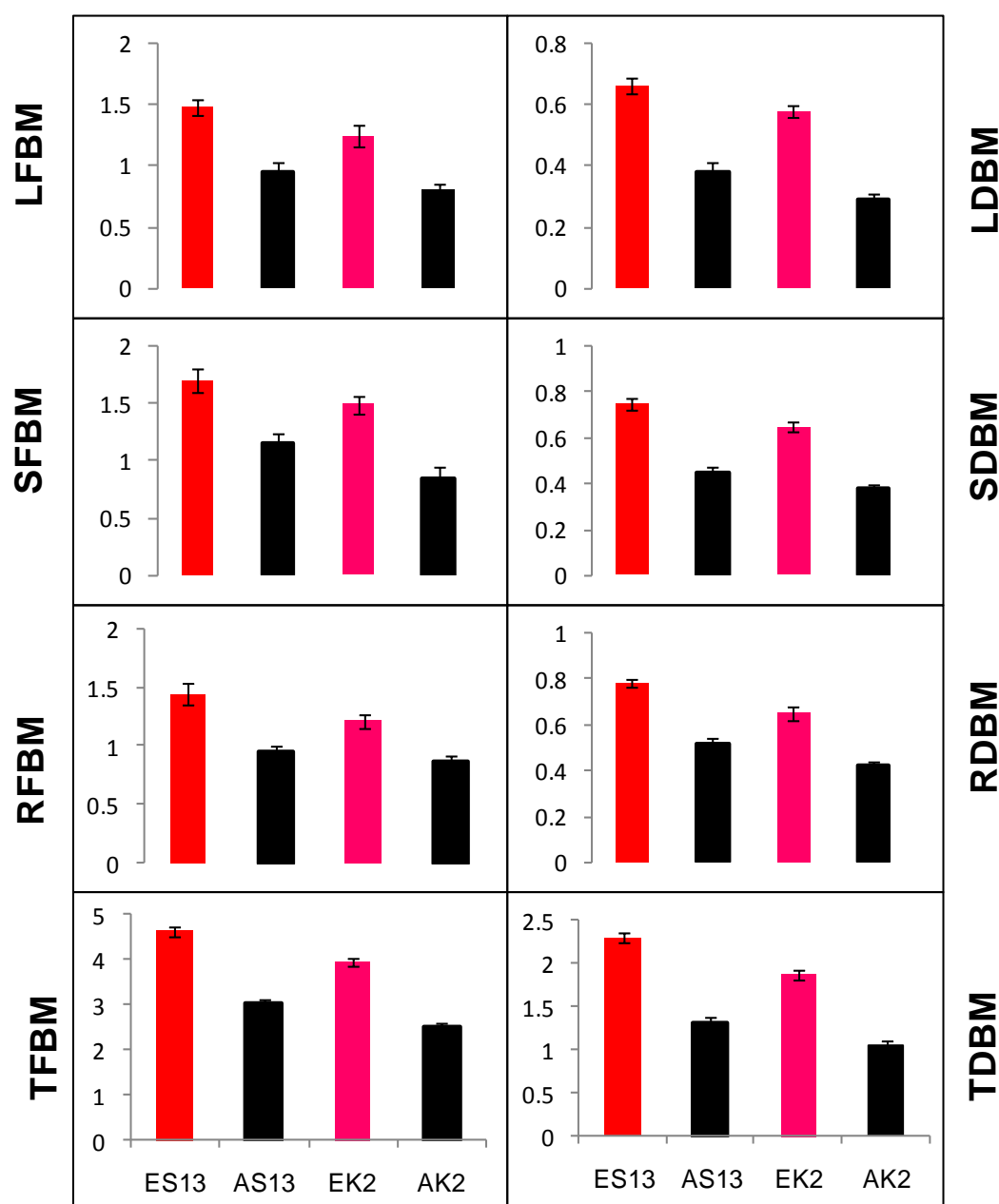


Fig 3.4 Changes in biomass accumulation patterns in the two mulberry genotypes (S13 and K2) grown under ambient and elevated $[CO_2]$ concentrations. (A) Total leaf fresh biomass (TLFB), (B) Total leaf dry biomass (TLDB), (C) Total stem fresh biomass (TSFB), (D) Total stem dry biomass (TSDB), (E) Root fresh biomass (RFBM), (F) Root dry biomass (RDBM), (G) Total (above and below ground) fresh biomass (TFBM), (H) Total dry biomass (TDBM). Values represented are the mean \pm standard deviation ($n=3$).

Table 3.2

Changes in photosynthetic leaf gas exchange characteristics, foliar biochemistry, destructive biomass and JIP test parameters between the treatments and genotypes. Values are \pm SD of three plants (n=3) with statistical significance of * (P<0.05), ** (P<0.01) and *** (P<0.001). E- Elevated, A- Ambient.

	Parameter	Genotype	CO ₂		CO ₂ x genotype
			S13	K2	
Photosynthetic physiology	A_{Sat}	***	***	***	***
	g_s	*	***	***	*
	E	**	**	***	**
	C_i	*	***	***	*
	WUE _i	***	***	***	***
	AQE	*	***	***	*
Foliar biochemistry	LCP	*	***	***	*
	Starch	**	***	***	**
	Total sugars	***	***	***	***
	Total Chl	***	***	***	***
Destructive biomass	SLA	**	***	***	*
	LFBM	**	***	***	*
	LDBM	**	***	***	*
	SFBM	**	***	***	*
	SDBM	**	***	***	*
	RFBM	*	***	***	*
	RDBM	*	***	***	*
	TFBM	**	***	***	*
	TDBM	**	***	***	*
	F_0	**	***	***	**
Chlorophyll a fluorescence JIP test parameters	F_M	*	***	***	*
	F_V/F_0	**	***	***	**
	Φ_{Po}	ns	***	***	ns
	Ψ_o	*	***	***	**
	Φ_{Eo}	*	***	***	**
	K _n	*	***	***	*
	K _p	*	***	***	**
	ABS/RC	*	*	*	*
	TRo/RC	***	***	***	***
	ETo/RC	**	***	***	**
	DIo/RC	*	***	***	*
	DIo/CSm	*	***	***	*
	RC/ CSm	*	***	***	*
	ET/CSm	*	***	***	*
	ABS/CSm	*	***	***	*
	PI(abs)	**	***	***	**

3.2 Objective 2- Establishing the long term carbon sequestration potential of mulberry with coppice management practices under [CO₂] enriched environment

Our results from long term [CO₂] enrichment studies clearly demonstrated that mulberry plants showed significant variations between short-term responses and long term responses under elevated [CO₂], wherein plants grown under elevated [CO₂] environments showed reduced photosynthetic performance with increasing [CO₂] exposure time compared to their ambient [CO₂] counterparts.

3.2.1 Photosynthetic leaf gas exchange physiology

[CO₂] enrichment induced significant changes in photosynthetic leaf gas exchange characteristics in mulberry throughout the experimental period compared to ambient [CO₂] grown plants (Table 3.2). In the present study, both [CO₂] and time showed significant effects on photosynthetic leaf gas exchange characteristics (A_{Sat} , g_s , E , C_i and WUE_i) in SRC mulberry plants grown under both elevated and ambient [CO₂] conditions. Recorded A_{Sat} was 22 $\mu\text{mol m}^{-2}\text{s}^{-1}$ and 14 $\mu\text{mol m}^{-2}\text{s}^{-1}$ at 365 DAT and which were reduced to 18 $\mu\text{mol m}^{-2}\text{s}^{-1}$ and 10 $\mu\text{mol m}^{-2}\text{s}^{-1}$ at 1095 DAT for elevated and ambient [CO₂] grown plants respectively. Thus, SRC mulberry plants grown under elevated [CO₂] environments displayed higher A_{Sat} by 50% at 1080 DAT compared to their current [CO₂] grown plants.

In contrast to A_{Sat} , g_s , and E were reduced considerably in [CO₂] enriched mulberry plants by 35% and 40% respectively at 1080 DAT than their control counterparts. Substantial reduction in E should be linked with greater WUE_i throughout the experimental period in elevated [CO₂] grown plants and a 70% increase in WUE_i was observed at 1095 DAT in [CO₂] enriched SRC mulberry plants. Similarly, plants grown under high [CO₂] conditions showed increased C_i throughout the experimental period in spite of reduced g_s compared to their ambient [CO₂] counterparts.

SRC mulberry plants grown under elevated [CO₂] atmosphere showed significant variations in A/C_i and A/Q curves at 365 as well as 1095 DAT compared to their ambient

[CO₂] counter parts (Fig 3. 4 and 6). In addition to above, we also observed significant variations in parameters including V_{cmax} , J_{max} and A_{max} , which were deduced from A/C_i curves, between elevated and ambient [CO₂] grown SRC mulberry plants throughout experimental conditions (Fig 3.5). At 365 DAT, high [CO₂] grown plants showed reduced V_{cmax} , J_{max} and A_{max} by 10%, 9% and 11% respectively with respect to current [CO₂] grown plants. With increasing [CO₂] exposure time, both elevated as well as ambient [CO₂] grown plants showed further decrease in V_{cmax} , J_{max} and A_{max} relatively. But, at 1095 DAT, elevated [CO₂] grown plants showed greater reduction in V_{cmax} , J_{max} as well as A_{max} compared to the ambient [CO₂] grown SRC mulberry plants. Parameters deduced from A/Q curves including AQE progressively decreased with an increase in [CO₂] exposure time along with simultaneous increase in LCP in both elevated and ambient [CO₂] grown plants (Fig 3.6). However, elevated [CO₂] grown plants showed higher values of AQE (44%) and reduced LCP (-52%) even at 1095 DAT when compared to current [CO₂] grown plants. Further, changes in V_{cmax} , J_{max} and A_{max} in SRC mulberry plants grown under both elevated and ambient [CO₂] environments showed positive correlation with the changes in foliar nitrogen content. In addition to above, we also observed that changes in V_{cmax} proportionally influence the J_{max} in both elevate and ambient [CO₂] grown mulberry plants (Fig 3.8).

3.2.2 Chlorophyll *a* fluorescence measurements

In addition to above photosynthetic leaf gas exchange physiology, elevated [CO₂] significantly influenced the PS-II efficiency in SRC mulberry compared to their ambient [CO₂] counterparts (Table 3.2). Plants grown under [CO₂] enriched environment showed significant increase in F_v/F_M (5%) and $\Delta F/F_m'$ (8%) with concomitant decrease in NPQ (-38%) compared to their ambient [CO₂] counterparts. Both elevated and ambient [CO₂] grown plants showed significant decrease in efficiency of PS-II as manifested by reduced F_v/F_M and $\Delta F/F_m'$ with concomitant increase in NPQ at 1095 compared to 365 DAT.

Table 3.3 Changes in photosynthetic leaf gas exchange characteristics, chlorophyll a fluorescence parameters and foliar biochemistry in SRC mulberry grown under elevated and ambient [CO₂] atmosphere at 365 DAT and 1095 DAT. The measurements were taken on randomly selected young fully expanded 3rd or 4th leaf from the apex in the upper canopy. Values are means \pm SD (n=6)

Parameters	365 DAT (1 year)		1095 DAT (3 years)	
	E	A	E	A
A_{Sat}	22 (\pm 0.85)*	14 (\pm 0.69)	18 (\pm 0.45)*	11 (\pm 0.76)
C_i	410 (\pm 25)*	290 (\pm 15)	395 (\pm 15)*	280 (\pm 13)
g_s	0.32 (\pm 0.035)*	0.48 (\pm 0.028)	0.29 (\pm 0.018)*	0.44 (\pm 0.012)
E	4.5 (\pm 0.85)*	6.7 (\pm 0.6)	3.5 (\pm 0.15)*	5.8 (\pm 0.35)
WUE_i	4 (\pm 0.34*)	1.79 (\pm 0.14)	4.46 (\pm 0.18)*	1.37 (\pm 0.25)
F_v/F_M	0.785 (\pm 0.032) *	0.754 (\pm 0.025)	0.715 (\pm 0.028)*	0.745 (\pm 0.035)
ΔF/F_m'	0.765 (\pm 0.032)*	0.714 (\pm 0.025)	0.735 (\pm 0.028)*	0.685 (\pm 0.035)
NPQ	1.42 (\pm 0.14)*	2.27 (\pm 0.17)	2.84(\pm 0.12)*	2.45(\pm 0.15)
Total Chl mg/g FW	1.8 (\pm 0.19)*	2.4 (\pm 0.24)	1.43(\pm 0.22)*	2.12 (\pm 0.26)
Total Sugars mg/g DW	320 (\pm 15)*	216 (\pm 18)	430 (\pm 22)*	325 (\pm 14)
Starch mg/g DW	184 (\pm 12)*	134 (\pm 8)	256 (\pm 18)*	188 (\pm 16)
Nitrogen mg/g DW	56 (\pm 2.4)*	68 (\pm 2.7)	41 (\pm 2.8)*	54 (\pm 3.5)

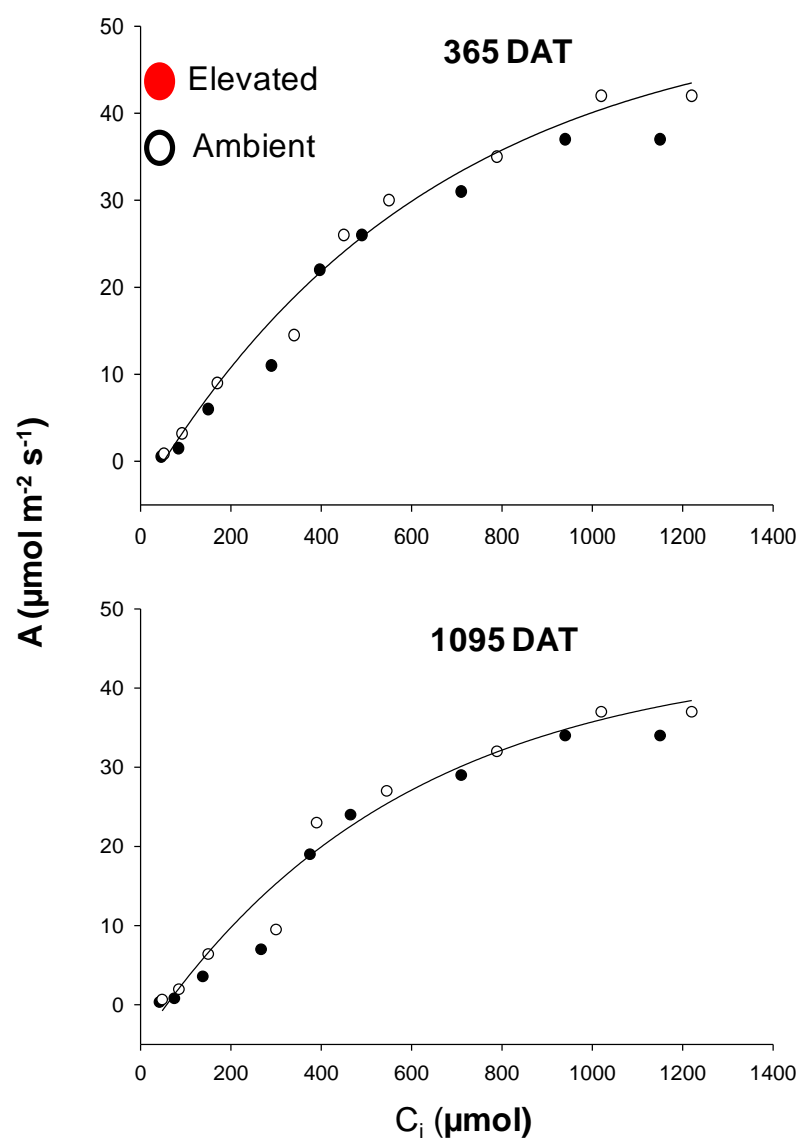


Fig 3.4 Changes in A/C_i curves in SRC mulberry grown under elevated and ambient $[\text{CO}_2]$ environments.

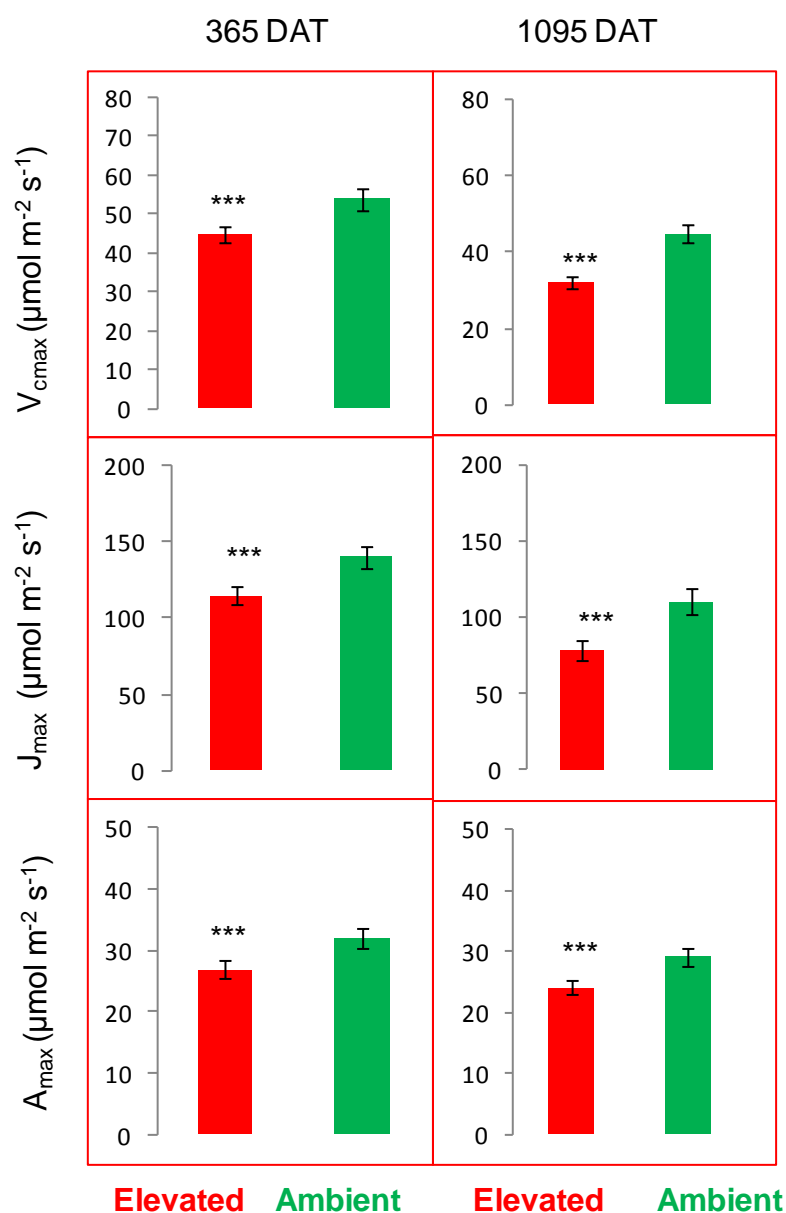


Fig 3.5 Variations in parameters (V_{cmax} , J_{max} and A_{max}) deduced from A/C_i curves in mulberry grown under elevated and ambient $[\text{CO}_2]$ environments. Values represent mean \pm SD (n=6). Results shown in the figures are an average of time points and values are \pm SD of six plants (n = 6) with statistical significance of *(P < 0.05),**(P < 0.01),*** (P < 0.001) and ns- not significant.

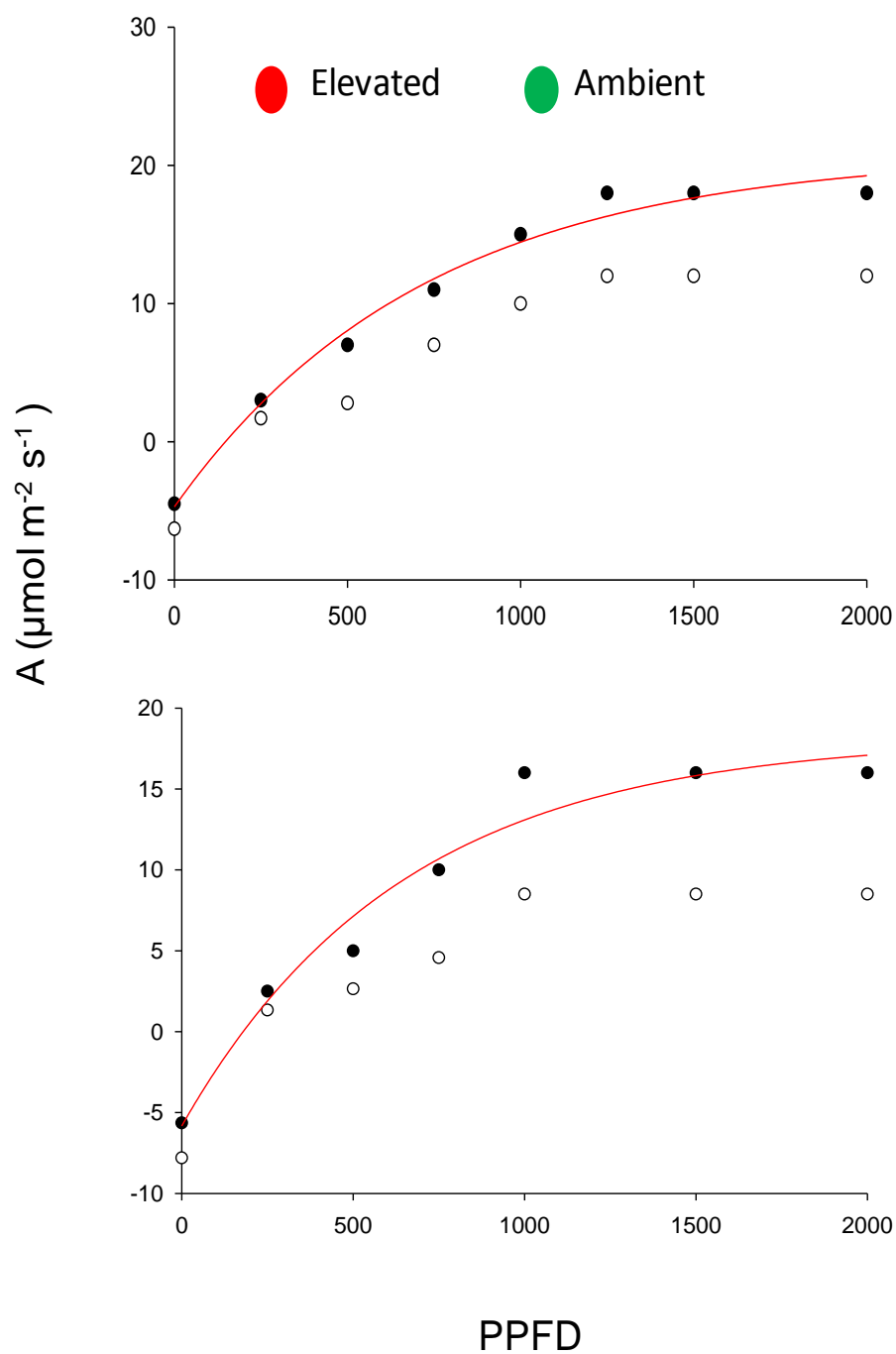


Fig 3.6 Changes in A/Q curves in SRC mulberry grown under elevated and ambient $[\text{CO}_2]$ environments.

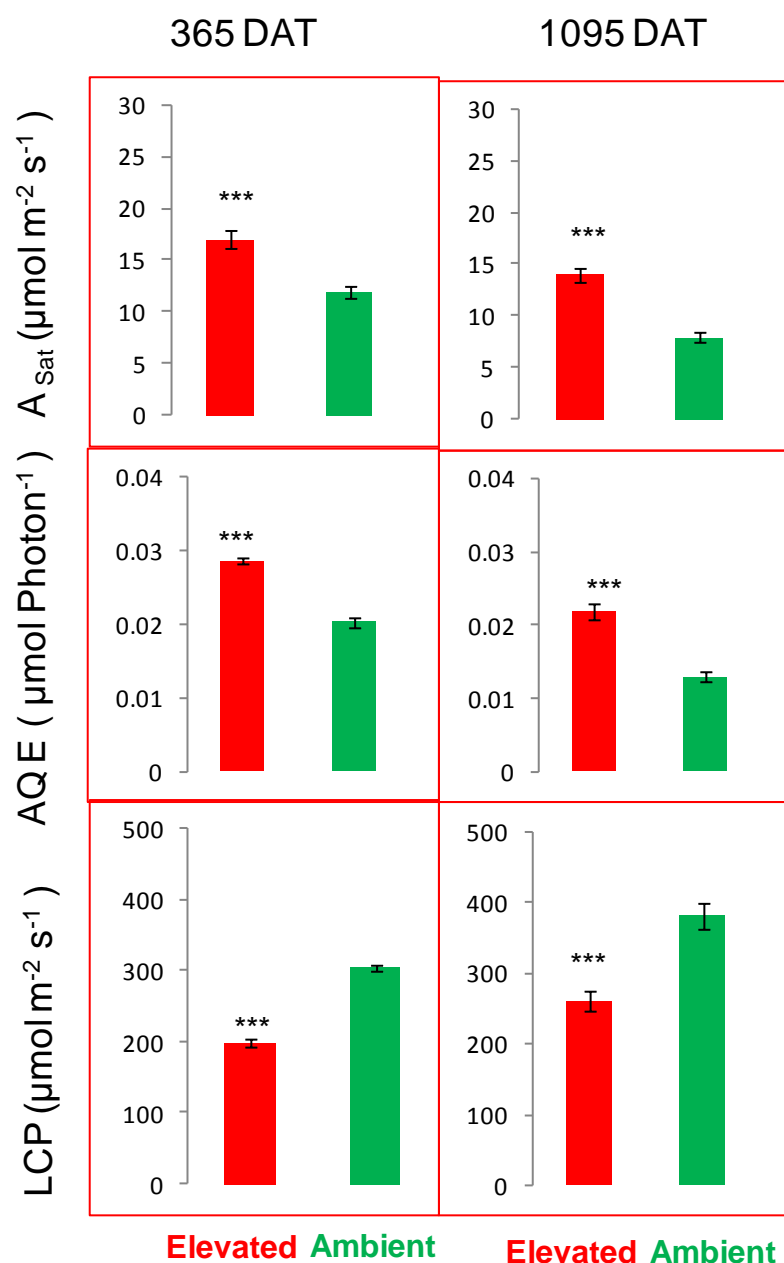


Fig 3.7 Variations in parameters (A_{Sat}, AQE and LCP) deduced from A/Q curves in mulberry grown under elevated and ambient [CO₂] environments. Values represent mean ±SD (n=6). Results shown in the figures are an average of time points and values are ± SD of six plants (n = 6) with statistical significance of *(P < 0.05),**(P < 0.01), *** (P < 0.001) and ns- not significant.

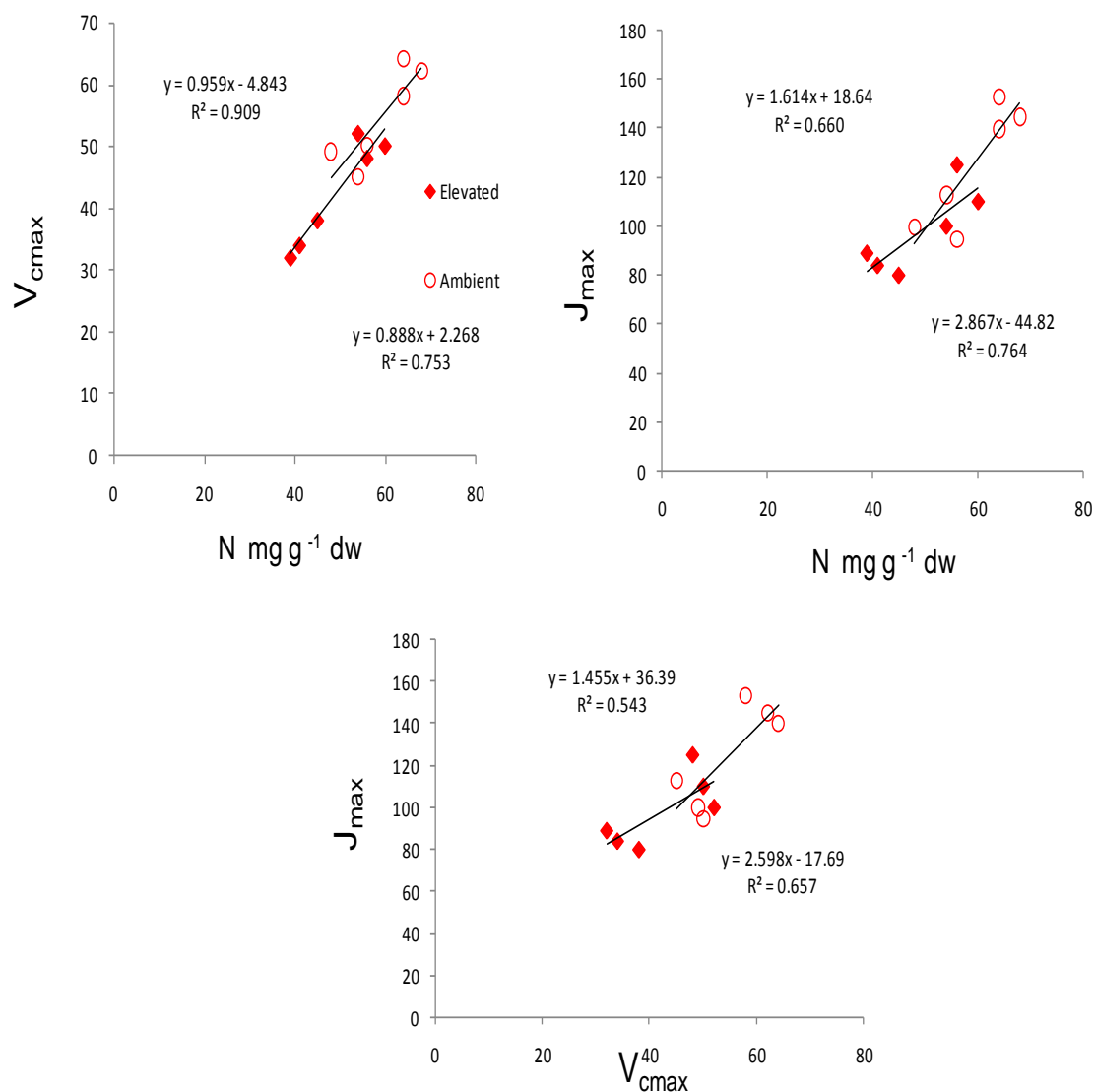


Fig 3.8 Correlation between foliar nitrogen Vs V_{cmax} and J_{max} and V_{cmax} Vs J_{max} in mulberry grown under elevated and ambient $[CO_2]$ environments.

However, plants grown under high [CO₂] environments showed more reduction, except $\Delta F/F_m'$, in F_v/F_m (-4%) along with parallel increase in NPQ (13%) compared to ambient [CO₂] grown plants.

3.2.3 Leaf bio-chemistry

Both CO₂ and time showed significant effect on foliar bio-chemistry in SRC mulberry plants (Table). Throughout the experimental period, plants grown under [CO₂] enriched environment showed significant increase in foliar carbohydrates with simultaneous reduction in chlorophyll as well as nitrogen content compared to their ambient [CO₂] counterparts. At 365 DAT, recorded total sugars and starch contents in elevated [CO₂] atmosphere were 320 and 184 mg/g DW respectively, where as it was 216 and 134 mg/g DW in ambient [CO₂] grown plants. Though, both elevated and ambient [CO₂] grown plants showed augmented accumulation of carbohydrates with time, elevated [CO₂] grown plants showed comparatively greater accumulation compared to their ambient [CO₂] counterparts. In contrast to above, mulberry plants grown under elevated [CO₂] showed reduced foliar total chlorophylls as well as nitrogen content throughout the experimental period compared to the ambient [CO₂] grown plants. But, the reduction was more prominent at 1095 DAT by 35% and 24% in chlorophyll and nitrogen content respectively compared to their ambient [CO₂] counterparts.

3.2.4 SEM analysis for understanding the stomatal behavior under high [CO₂]

Pictorial images of stomata by SEM on the abaxial side of the leaves grown under both ambient and elevated [CO₂] were taken at 120 DAT (four months) to elucidate stomatal behavior (Fig 3.9). Elevated [CO₂] grown plants showed 25% reduction in stomatal density (SD) compared to their ambient [CO₂] grown plants. In addition to above, we also observed that most of the stomata were partially opened and stomatal aperture was reduced significantly in elevated [CO₂] when compared to ambient [CO₂] grown plants.

3.2.5 Bio-mass yields and carbon sequestration potential

Elevated $[\text{CO}_2]$ significantly enhanced the growth, bio-mass yield and carbon sequestration potential in SRC coppice mulberry throughout the experimental conditions compared to their ambient $[\text{CO}_2]$ counterparts (Fig 3.11- 14). Mulberry plants grown under $[\text{CO}_2]$ enriched environments exhibited greater above ground fresh bio-mass including leaves and stems (AGFBM) as well as belowground root fresh bio-mass (BGFBM) at 365 DAT (one year) and 1095 DAT (three years) compared to their control plants. Increased fresh bio-mass could be linked with the greater above ground dry bio-mass (AGDBM) and below ground dry bio-mass (BGDBM) in SRC mulberry plant grown under increased $[\text{CO}_2]$ environment with respect to current $[\text{CO}_2]$ grown SRC mulberry plants. Thus, plants grown under elevated $[\text{CO}_2]$ conditions exhibited greater total fresh bio-mass ($\text{TFBM} = \text{AGFBM} + \text{BGFBM}$) as well as total dry bio-mass ($\text{TDBM} = \text{AGDBM} + \text{BGDBM}$) than their ambient $[\text{CO}_2]$ counterparts. Recorded cumulative TDBM in SRC mulberry grown under ambient CO_2 environment at 365 DAT was 15 kg plant^{-1} (Fig 3.11) and which was increased to 42 kg plant^{-1} at 1095 DAT (Fig 3.14) ; while, TDBM in $[\text{CO}_2]$ enriched SRC mulberry plants were 25 kg plant^{-1} and 90 kg plant^{-1} at 365 DAT and at 1080 DAT respectively (Fig 3. 11 and 14). Hence, high $[\text{CO}_2]$ grown plants showed higher bio-mass yields by 40% and 53% at 365 DAT and 1095 DAT respectively compared to ambient $[\text{CO}_2]$ grown plants. Further, we calculated TDBM yield of SRC mulberry plants grown under both elevated and ambient $[\text{CO}_2]$ environments on hectare basis and recorded TDBM were $60 \text{ Mg hectare}^{-1}$ and $35 \text{ Mg hectare}^{-1}$ at 365 DAT and $180 \text{ Mg hectare}^{-1}$ and $95 \text{ Mg hectare}^{-1}$ at 1095 DAT respectively (Fig 3. 11 and 14). We also calculated the amount of $[\text{CO}_2]$ sequestered, carbon sequestration potential, by the SRC mulberry plants based on their TDBM yields and elevated $[\text{CO}_2]$ grown plants showed greater carbon sequestration potential compared to ambient $[\text{CO}_2]$ counterparts. Amount of $[\text{CO}_2]$ sequestered by elevated $[\text{CO}_2]$ grown SRC mulberry plants was 45 kg plant^{-1} and $115 \text{ Mg hectare}^{-1}$, whereas in ambient $[\text{CO}_2]$ grown plants it was 24 kg plant^{-1} and $58 \text{ Mg hectare}^{-1}$ at 365 DAT. Both elevated and ambient $[\text{CO}_2]$ grown plants showed significantly greater carbon sequestration potential

at 1080 with respect to 365 DAT. However, at 1080 DAT, $[\text{CO}_2]$ enriched plants displayed greater $[\text{CO}_2]$ sequestration of $190 \text{ kg plant}^{-1}$ and $395 \text{ Mg hectare}^{-1}$ compared to their control counterparts (85 kg plant^{-1} and $200 \text{ Mg hectare}^{-1}$). Thus, these results clearly demonstrated that elevated $[\text{CO}_2]$ grown plants showed augmented bio-mass yields and carbon sequestration potential by $\sim 45\%$ to $\sim 55\%$ throughout the experimental period compared to their ambient $[\text{CO}_2]$ counterparts.

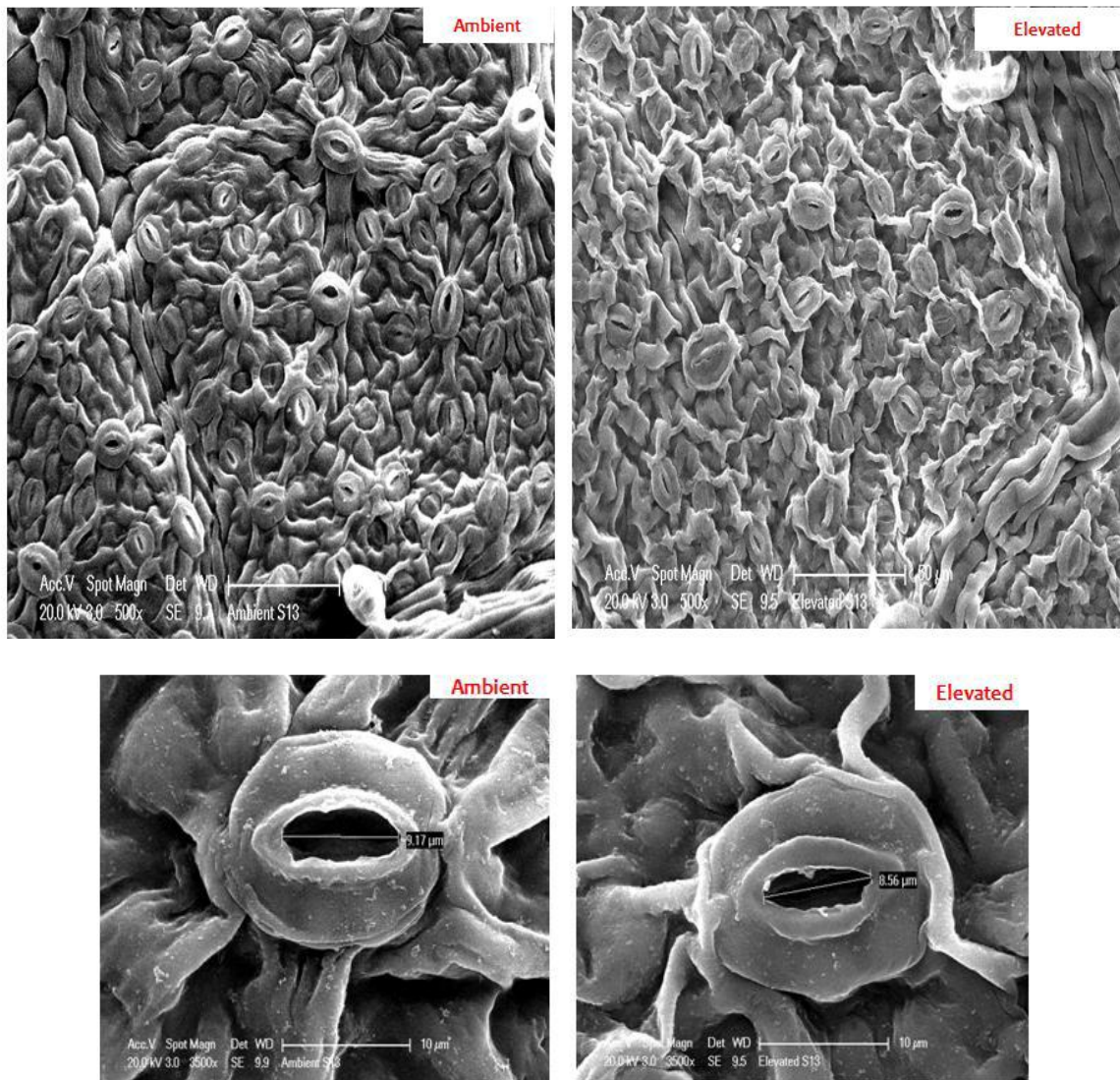


Fig 3.9 SEM images of an abaxial surface of mulberry leaves grown under ambient and elevated $[\text{CO}_2]$ grown plants to represent stomatal density and aperture ($n=6$).

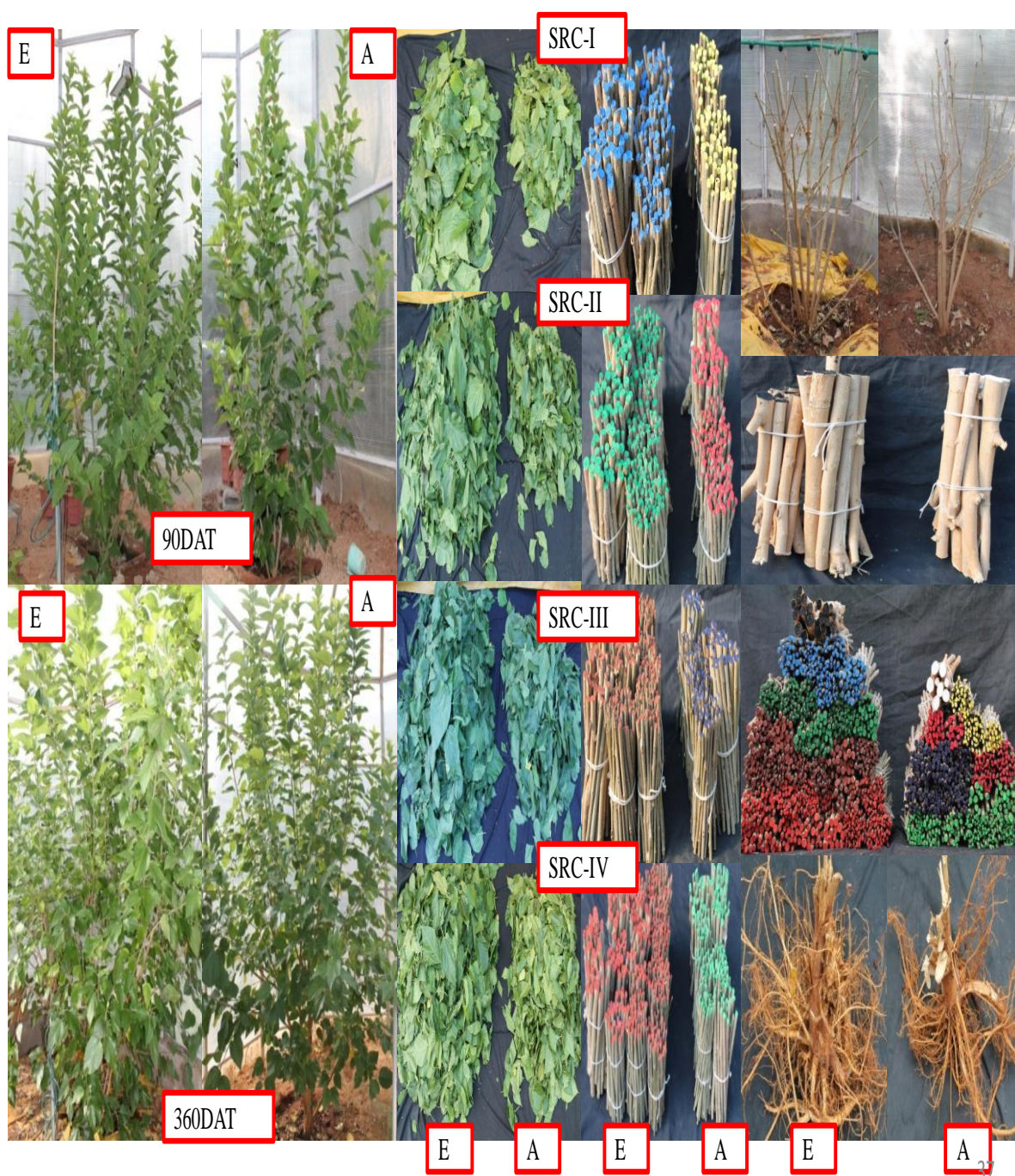


Fig 3.10 Morphological changes and destructive biomass yields from SRC-I to SRC-IV in both ambient and elevated $[CO_2]$ grown mulberry plants ($n= 6$). E- elevated, A- Ambient.

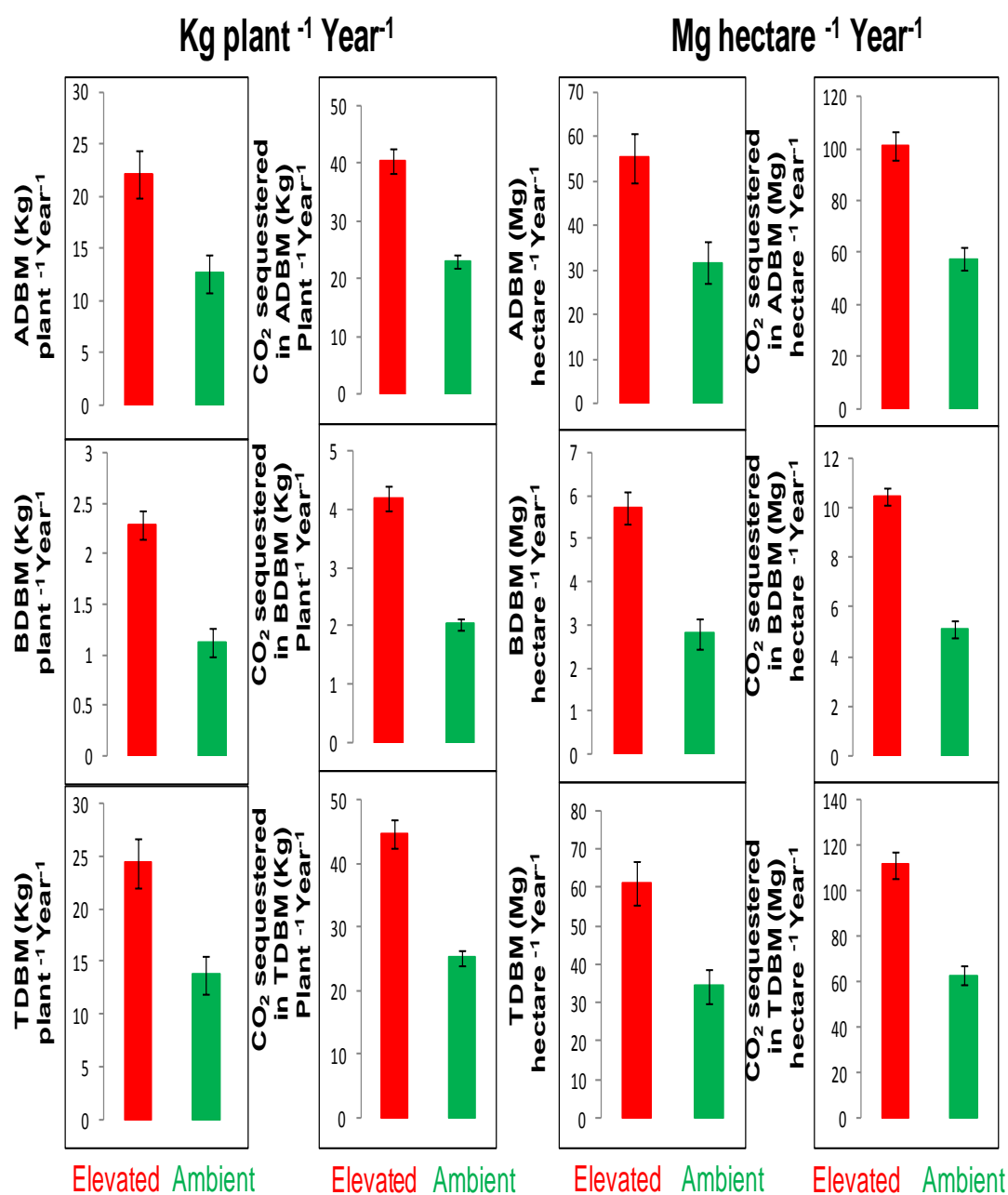


Fig 3.11 Biomass yields and carbon sequestration in SRC mulberry plants grown under both ambient and elevated [CO₂] atmosphere after one year of [CO₂] exposure. Results shown in the figures are an average of time points and values are \pm SD of six plants (n = 6).



Fig 3.12 Morphological changes between elevated and ambient [CO₂] grown SRC mulberry plants (harvested for every 90 days) after 3 years of [CO₂] exposure.

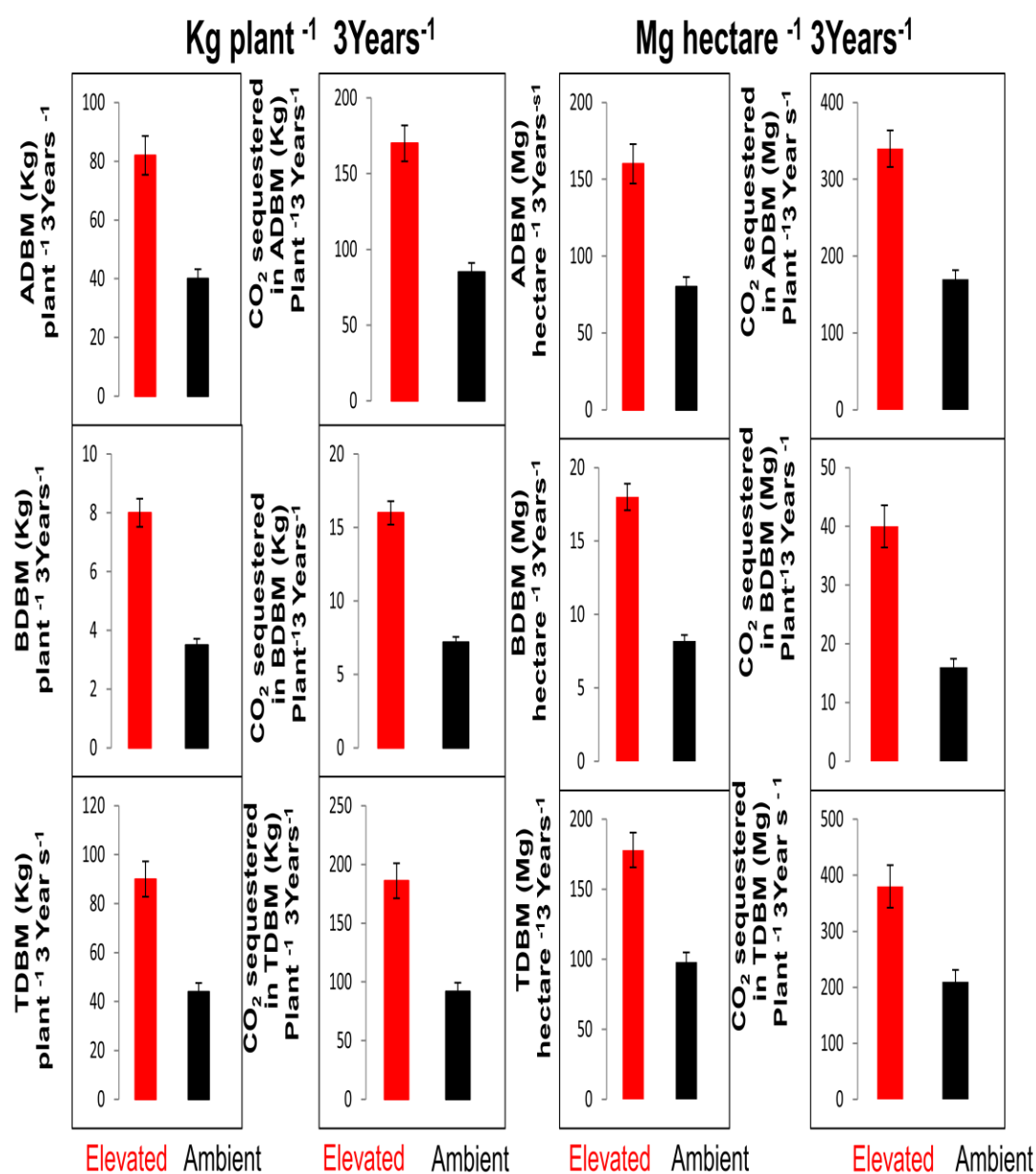


Fig 3.13 Cumulative biomass yields and the amount of carbon sequestered after three years of [CO₂] exposure in mulberry under both ambient and elevated [CO₂] atmosphere. Results shown in the figures are an average of time points and values are \pm SD of six plants (n = 6).

3.3 Objective 3- Exploring the dynamic changes of antioxidant systems in short rotation coppice (SRC) mulberry in response to elevated [CO₂] and drought individually as well as in their combination

3.3.1 Changes in morphological characteristics, chlorophyll content and destructive biomass yield under water stress (WS)

Elevated [CO₂] delayed the drought induced senescence and/or severe stress symptoms like discoloration, wilting and dehydration in mulberry even 30 days after stress (DAS) compared to their ambient counterparts (Fig. 3.14). These visual stress symptoms were further quantified by ImageJ software in terms of leaf greenery, senescent area and individual leaf densities (Fig. 3.15 A, B and C). Plants grown under elevated [CO₂] had greenery leaves (58%) and individual leaf densities (60%) with less leaf senescence (78%) compared to ambient controls. There was a significant decrease in total chlorophyll content (45%) in ambient [CO₂] grown plants compared to high [CO₂] grown plants (Fig 3.15D). In addition to above changes, plants grown under [CO₂] enriched environment showed greater AGFBM (92%) and AGDBM (83%) compared to their ambient counter parts even at 30 DAS (Fig 3.15 E and F).

3.3.2 Photosynthetic leaf gas exchange physiology, chlorophyll *a* fluorescence measurements and leaf relative water content (RWC)

In addition to above morphological changes, mulberry plants showed significant variations in photosynthetic leaf gas exchange physiology, chlorophyll *a* fluorescence characteristics and RWC under WW and during WS conditions between elevated and ambient [CO₂] grown plants (Fig 3.16). Parameters like A_{Sat} (45%), C_i (32%) and WUE_i (60%) were significantly increased with concomitant reduction in g_s (27%) and E (29%) in elevated [CO₂] grown mulberry plants compared to controls (Fig 3.16A, C and E). Our results from interactive studies with drought infer that increased atmospheric [CO₂] offset the drought induced symptoms in mulberry which in turn were linked with higher A_{Sat} (70%) even after 30DAS than their ambient [CO₂] grown plants (Fig 3.16A). In contrast

to A_{Sat} , both g_s and E were reduced proportionally in $[CO_2]$ enriched plants with the progression of drought treatment and showed maximum decrease at 30 DAS by 60% and 58% respectively than ambient plants (Fig 3.16 B and D).



Fig 3.14 Morphological changes in mulberry plants grown under both elevated and ambient $[CO_2]$ atmosphere at 30 days after stress (30DAS).

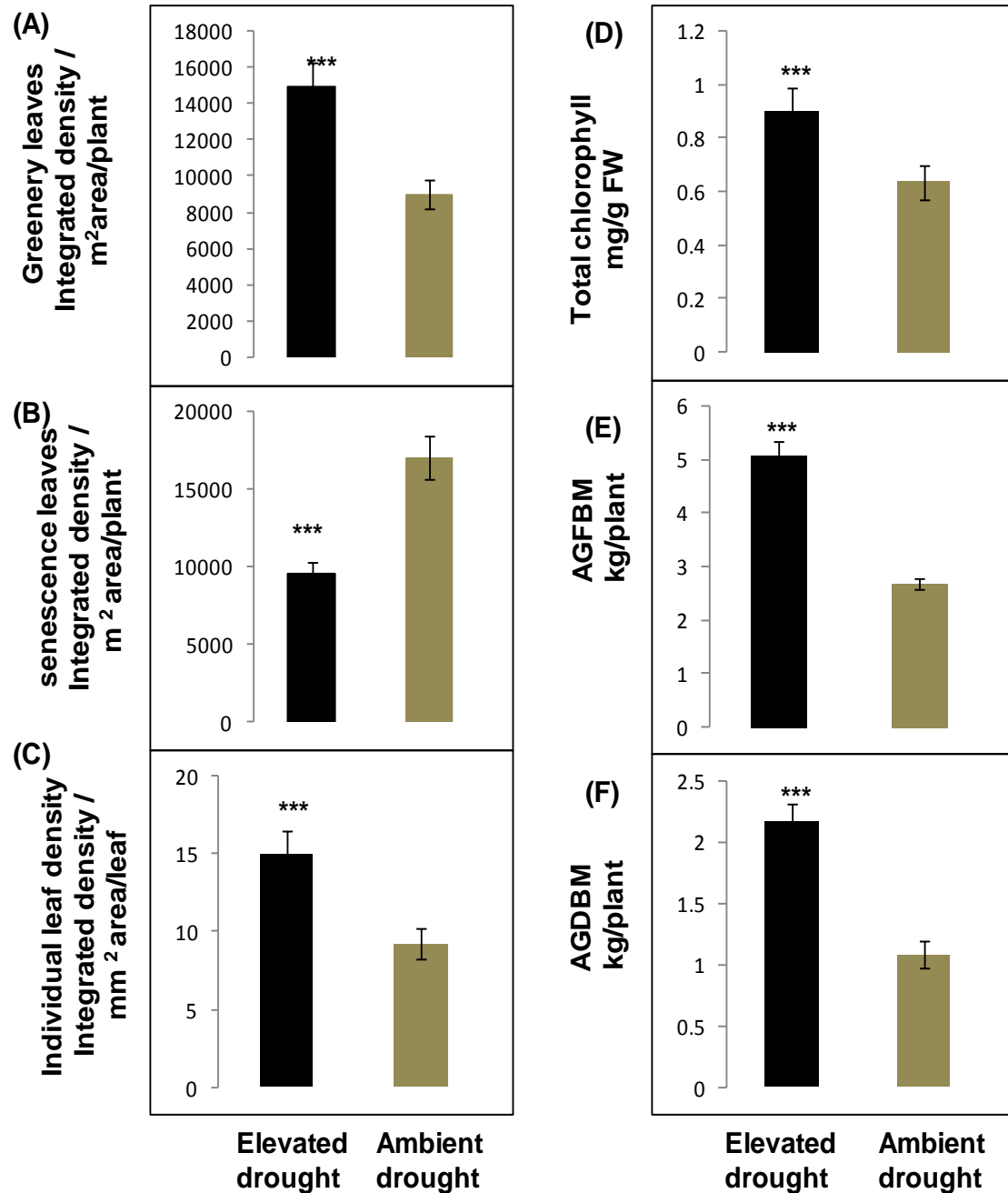


Fig 3.15 ImageJ analysis showing changes in plant phenological characteristics, total chlorophyll content and above ground biomass yields at 30DAS in both elevated and ambient CO_2 grown mulberry. Results shown in the figures are an average of time points and values are \pm SD of three plants ($n = 3$) with statistical significance of * ($P < 0.05$), ** ($P < 0.01$), *** ($P < 0.001$) and ns- not significant.

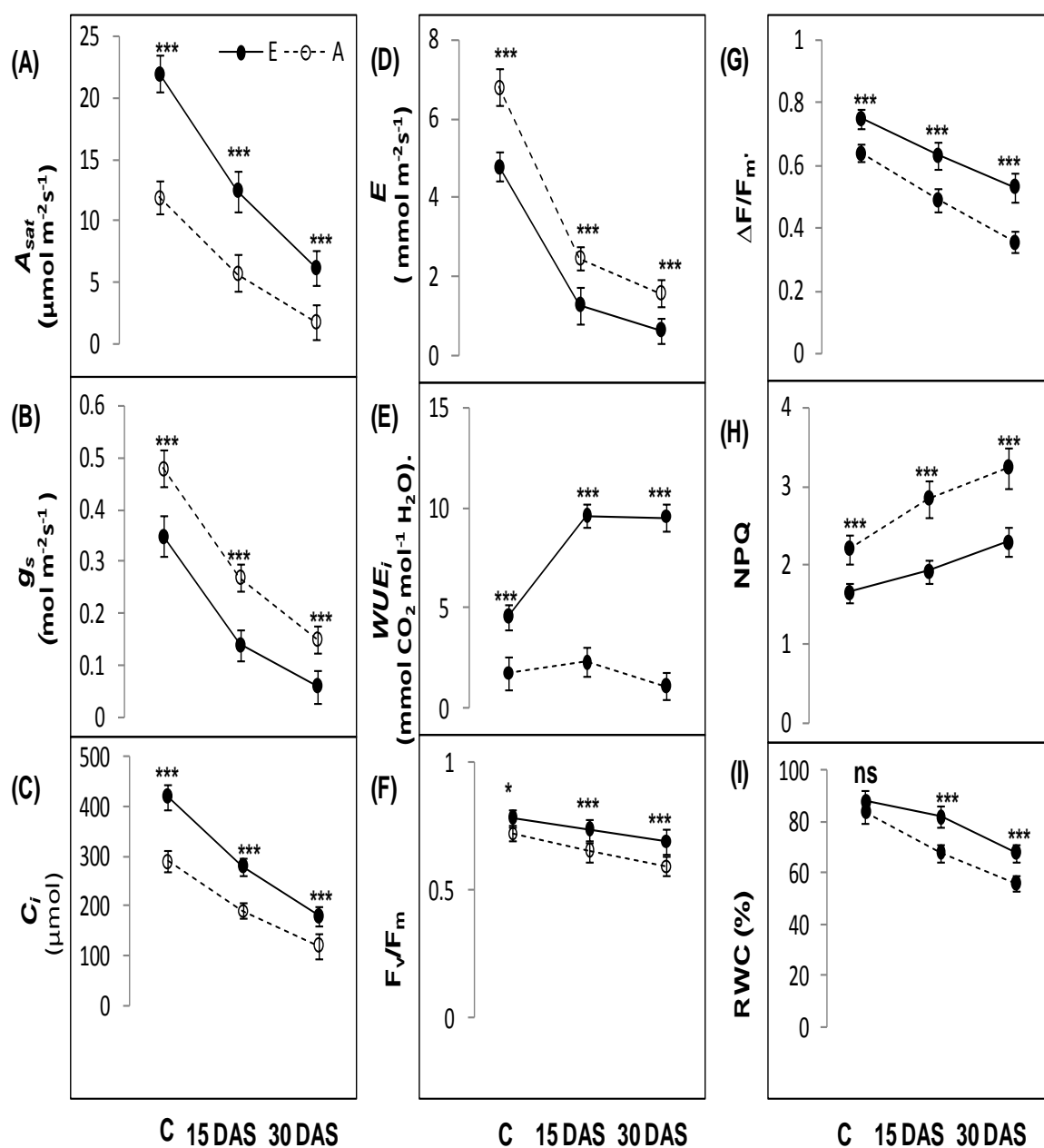


Fig 3.16 Variations in photosynthetic leaf gas exchange physiology, chlorophyll a fluorescence characteristics and leaf relative water content (RWC). These measurements were taken on randomly chosen fully mature leaves at 3rd or 4th position from the upper canopy during 10:00-11:30 h. E- elevated, A- ambient, C- well watered and DAS- days after stress. Results shown in the figures are an average of representative time points and values are \pm SD of three plants (n = 3) with statistical significance of * (P < 0.05), ** (P < 0.01), *** (P < 0.001) and ns- not significant.

Lower E was in turn associated with reduced water loss which resulted in substantial increase of WUE_i by 90% at 30 DAS (Fig 3.16 E) in elevated $[CO_2]$ grown plants. Drought imposition significantly affected C_i in both elevated as well as ambient $[CO_2]$ grown plants, however, elevated $[CO_2]$ grown plants maintained greater C_i throughout the experimental drought period despite their reduced g_s (Fig 3.16 C). Results from chlorophyll a fluorescence measurements demonstrated that photosystem-II (PS-II) efficiency was improved under $[CO_2]$ enriched environment and which was manifested as a significant rise in F_v/F_m (8%) and $\Delta F/F_m'$ (15%) with simultaneous reduction in NPQ (25%). Nevertheless, drought diminished the PS-II efficiency in both elevated as well as ambient $[CO_2]$ grown plants. Ambient plants showed greater reduction in F_v/F_m (13%), $\Delta F/F_m'$ (33%) and with concomitant increase in NPQ (29%) than elevated $[CO_2]$ grown plants at 30 DAS (Fig 3. 16 F, G and H). Further, there was no significant difference in RWC under WW conditions between elevated and ambient $[CO_2]$ grown plants. However, irrespective of $[CO_2]$ treatment, drought imposition caused reduction in RWC. The $[CO_2]$ enriched plants maintained more RWC (68%) than their ambient counterparts (56%) after 30 DAS (Fig. 3.16 I).

3.3.3 Changes in antioxidant enzyme activities and their gene expression

Elevated $[CO_2]$ significantly influenced the enzyme activities and transcript abundance of antioxidant systems under WW as well as during WS than their control plants. The activities of antioxidant enzymes including SOD (40%), CAT (48%), APX (43%), GPX (35%) MDHAR (57%) and GR (59%) were decreased under WW conditions in elevated $[CO_2]$ grown mulberry plants with respect to ambient controls (Fig 3.17). Drought imposition caused further increase in the activities of antioxidant enzymes in both elevated and ambient $[CO_2]$ grown plants. But, control plants showed higher activities of SOD, CAT, APX, GPX, MDHAR and GR by 30%, 47%, 29%, 18%, 39% 41%, respectively at 15DAS. However, with increasing stress severity, ambient $[CO_2]$ grown plants showed down regulation of the protective systems at 30DAS manifested as significant reduction in the activities of above mentioned enzymes compared to CO_2

enriched plants.

Direct primers targeting 200-300 bp regions from genes encoding some of the important antioxidant enzymes were designed and the corresponding target genes were PCR-amplified (Fig 3.18). Amplified products were confirmed through sequence analysis and the same were used to perform quantitative real time-PCR (qRT-PCR) to check their gene expression in mulberry under both elevated [CO₂] as well as drought conditions with their respective controls. Our results from gene expression studies demonstrated that changes in transcript abundance of different antioxidant enzymes were tightly correlated with their enzyme activities (Fig 3.19). Under WW conditions, ambient [CO₂] grown plants showed up regulation (>1.5 fold change) of most of the isoforms of antioxidant enzymes compared to their elevated [CO₂] counterparts other than GPX4, chloroplast Mn-SOD, MDHAR2, MDHAR3, APX3 (Fig. 3.19 A). In consistent with above, at 15DAS, ambient [CO₂] grown plants showed greater transcript abundance of antioxidant enzymes than their elevated [CO₂] counterparts (Fig 3.19 B). However, in contrast to above, with increasing drought severity (30DAS) transcript levels of most of the antioxidant enzymes were reduced in ambient [CO₂] grown plants. In other words, elevated [CO₂] grown plants maintained higher transcripts of antioxidant enzymes even after 30DAS other than GPX2, GPX6, APX3.2 and APX3.3 (Fig 3.19 C).

3.3.4 Oxidative stress indicators, osmolytes and molecular antioxidants

Molecular antioxidants like ASA and TPC were more abundant in elevated [CO₂] grown mulberry plants under WW conditions by 15% and 26% respectively compared to their ambient controls. Drought imposition induced additional increase in ASA and TPC contents in both elevated and ambient [CO₂] grown plants; however, [CO₂] enriched plants had greater ASA and TPC (Fig 3.20 A and B). Further, there was no change in proline content between ambient and elevated [CO₂] grown mulberry plants under WW conditions. Drought induced substantial increase in proline levels in both ambient and elevated [CO₂] grown plants; but, ambient [CO₂] grown plants had 24% more proline content at 30 DAS than the elevated [CO₂] plants (Fig 3. 20C). Oxidative stress indicators

including H_2O_2 and MDA contents were more abundant in ambient $[\text{CO}_2]$ grown plants under WW conditions, which further increased with drought stress compared to those grown in the elevated $[\text{CO}_2]$ (Fig 3.20 D and E). Similar trend was observed for glutathione (GSH) as elevated $[\text{CO}_2]$ grown plants showed reduced GSH levels in WW and WS (Fig 3.20 F).

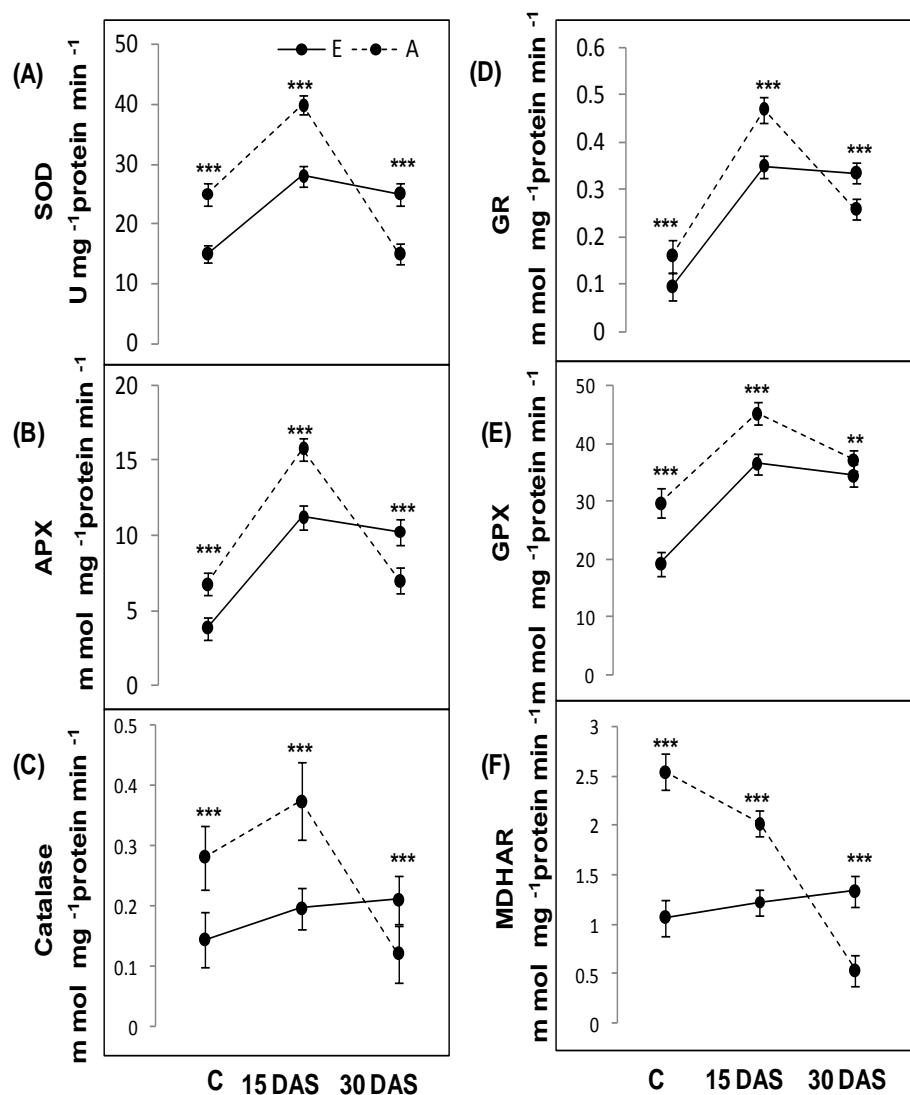


Fig 3.17 Changes in antioxidant enzyme activities in mulberry. E- elevated, A- ambient, C- well watered and DAS- days after stress. Results shown in the figures are an average of time points and values are \pm SD of three plants ($n = 3$) with statistical significance of * ($P < 0.05$), ** ($P < 0.01$), *** ($P < 0.001$) and ns- not significant.

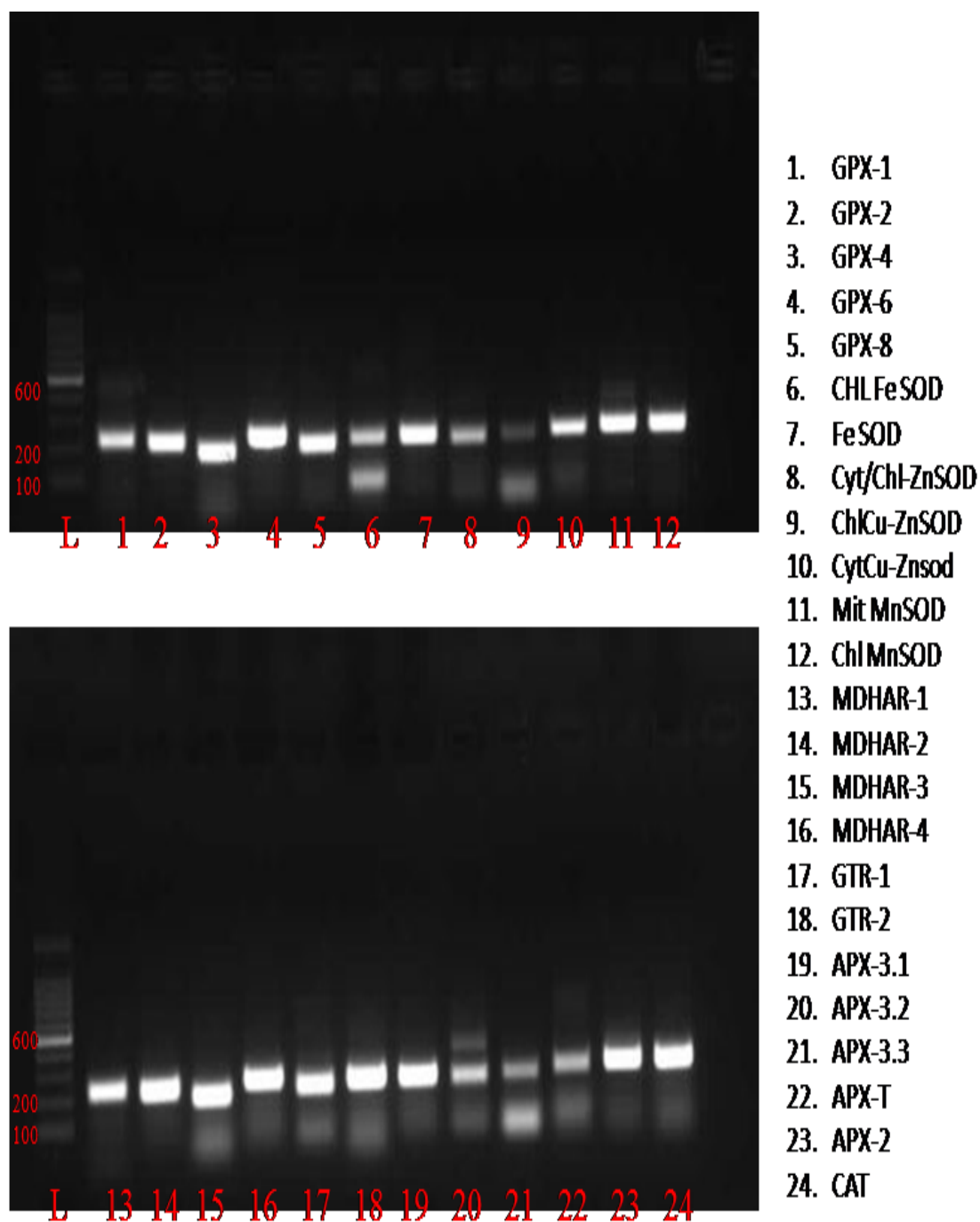


Fig 3.18 Amplification of specific regions (200-300bp) from genes encoding key antioxidant enzymes using gene specific primers.

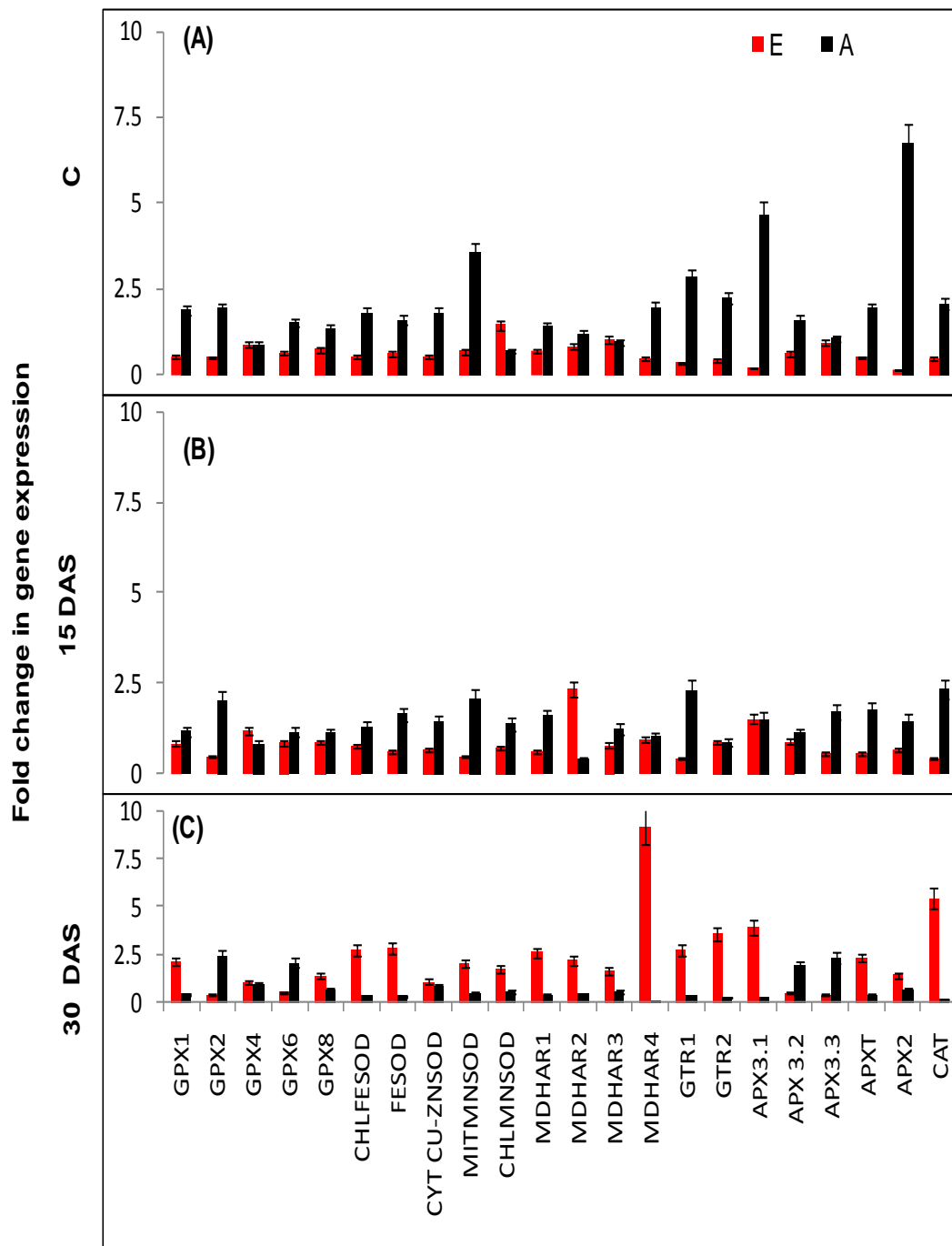


Fig 3.19 changes in transcript abundance of different antioxidant isoforms in mulberry. E- elevated, A- ambient, C- well watered and DAS- days after stress. Results shown in the figures are an average of representative time points and values are \pm SD of three plants (n = 3).

Table 3.4 P- values representing significant changes in photosynthetic leaf gas exchange characteristics, chlorophyll *a* fluorescence, antioxidant enzyme activities, oxidative stress parameters and antioxidants in mulberry grown under both elevated, ambient [CO₂] atmosphere under well watered and WS conditions. Time has a significant effect for these parameters during drought in both elevated and ambient [CO₂] conditions. Values are \pm SD of three plants (n = 3). D- drought, CO₂- elevated CO₂, T-time.

Parameters	CO ₂	D	D×T	CO ₂ ×D	D×T×CO ₂
A _{Sat}	<0.001	<0.001	<0.001	<0.001	<0.001
g _s	<0.001	<0.001	<0.001	<0.001	<0.001
E	<0.001	<0.001	<0.001	<0.001	<0.001
Ci	<0.001	<0.001	<0.001	<0.001	<0.001
WUE _i	<0.001	<0.001	<0.001	<0.001	Ns
F _v /F _M	<0.01	<0.001	<0.001	<0.001	<0.001
ΔF/F _{M'}	<0.001	<0.001	<0.001	<0.001	<0.001
NPQ	<0.001	<0.001	<0.001	<0.001	<0.001
SOD	<0.001	<0.001	<0.001	<0.001	Ns
CAT	<0.001	<0.001	<0.001	<0.001	Ns
GPX	<0.001	<0.001	<0.001	<0.001	Ns
APX	<0.001	<0.001	<0.001	<0.001	Ns
MDHAR	<0.001	<0.001	<0.001	<0.001	Ns
GR	<0.001	<0.001	<0.001	<0.001	Ns
Proline	Ns	<0.001	<0.001	<0.001	<0.001
MDA	<0.001	<0.001	<0.001	<0.001	<0.001
H ₂ O ₂	<0.001	<0.001	<0.001	<0.001	Ns
ASA	<0.05	<0.01	Ns	<0.001	Ns
TPC	<0.05	<0.01	Ns	<0.001	Ns
GSH	<0.001	<0.01	Ns	<0.001	Ns

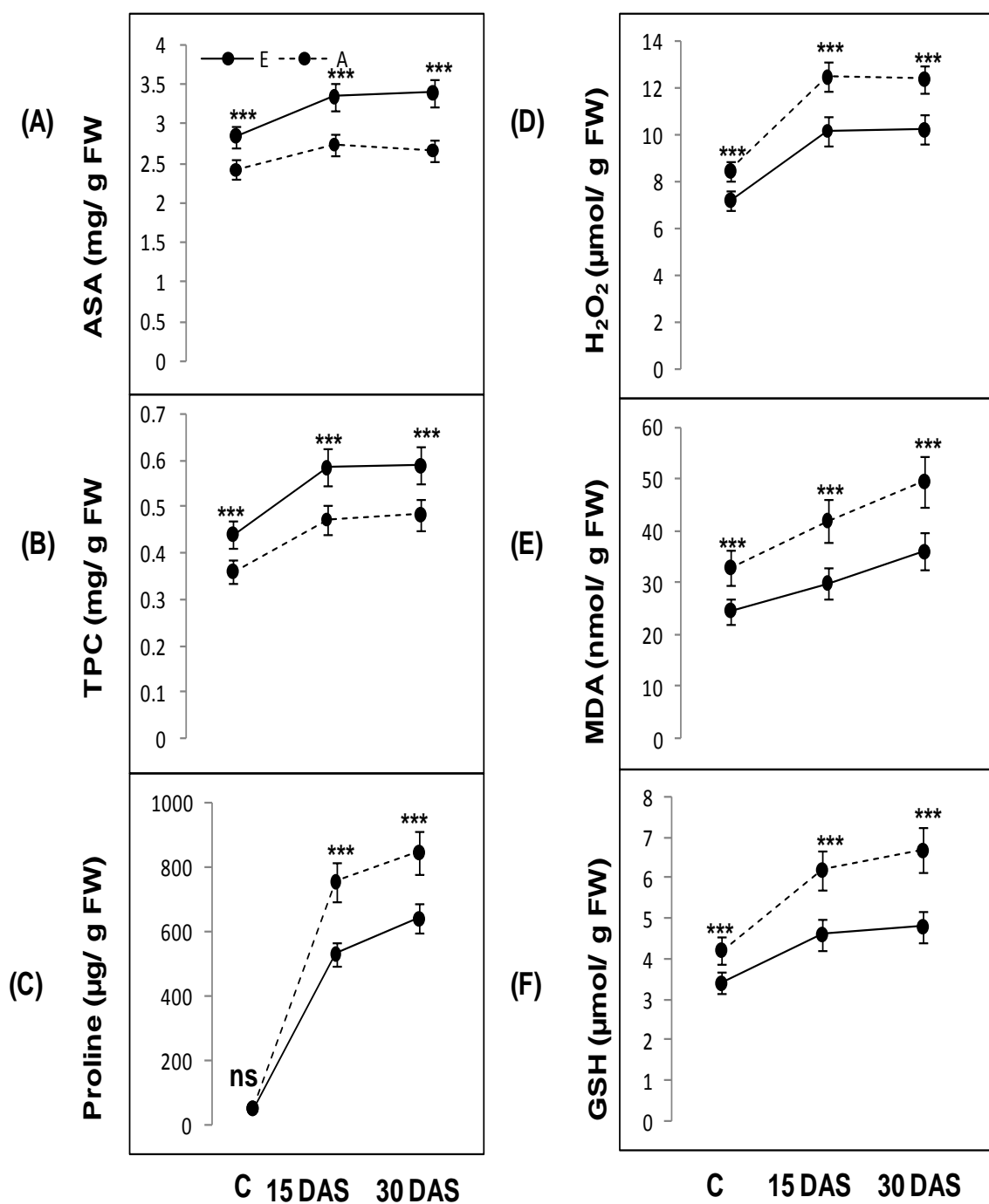


Fig 3.20 Changes in oxidative stress characteristics, osmolyte content and molecular antioxidants in mulberry. Results shown in the figures are an average of time points and values are \pm SD of three plants ($n = 3$) with statistical significance of *($P < 0.05$), **($P < 0.01$), ***($P < 0.001$) and ns- not significant.

3.3.5 Leaf water potential (ψ_L), photosynthetic light response curves ($A/PPFD$) and reciprocal light saturated instantaneous photosynthetic measurements

Leaf water status generally represented as changes in ψ_L and there was no significant variation in ψ_L under WW conditions between elevated as well as ambient $[CO_2]$ grown plants (Fig 3.21 C). However, drought imposition caused significant reduction in ψ_L in both elevated and ambient $[CO_2]$ grown plants indicating that WS negatively affects the leaf water status (Fig. 3.21 C). After 30 days of WS, ψ_L was reduced from -1.25 to -1.85MPa in high CO_2 grown plants whereas in control plants it was reduced from -1.29 to -2.67MPa. Therefore, leaves of plants grown under $[CO_2]$ enriched environment were more turgid (30%, $P \leq 0.001$) than their ambient counterparts even after 30 days of WS. Changes in instantaneous photosynthetic rates (A) with increasing photosynthetic photon flux density (PPFD) under WW as well as after 30 days of WS inferred that plants grown under increased atmospheric $[CO_2]$ were saturated at higher light intensities than their control counterparts (Fig 3.21 A and B). Plants grown under elevated $[CO_2]$ atmosphere showed greater A_{Sat} (45%, $P \leq 0.001$) and AQE (30%, $P \leq 0.001$) with concomitant decrease in LCP (-46%, $P \leq 0.001$) than plants grown at ambient $[CO_2]$. Further, WS showed negative impact in both elevated as well as ambient $[CO_2]$ grown plants, which is manifested as marked reduction in A_{Sat} and AQE compared to their WW counterparts. However, plants grown under $[CO_2]$ enriched atmosphere showed better A_{Sat} (70%, $P \leq 0.001$) and AQE (35%, $P \leq 0.001$) than their ambient counterparts indicating that increased atmospheric $[CO_2]$ ameliorates the drought induced negative effects in mulberry. In contrast to above, our results from the reciprocal instantaneous photosynthetic measurements clearly demonstrated that SRC mulberry plants grown under elevated CO_2 atmosphere showed reduced P_n when measured at common $[CO_2]$ concentration (400 or 550 μmol). Mulberry plants grown under ambient $[CO_2]$ show an increase in P_n by 51% ($P \leq 0.001$) and 76% ($P \leq 0.001$) in WW as well as WS plants respectively when $[CO_2]$ was increased from 400 to 550 μmol (Fig. 3.22 A). There was significant decrease in P_n by - 58% ($P \leq 0.001$) and -80% ($P \leq 0.001$) in WW as well as WS plants correspondingly when $[CO_2]$ was decreased from growth $[CO_2]$ of 550 μmol

to 400 μmol (Fig. 3.22 A). Similarly, mulberry plants exhibited lower stomatal conductance in CO_2 enriched environment than plants grown under current $[\text{CO}_2]$ in WW and during WS environments when measured at either 400 μmol $[\text{CO}_2]$ (-15%, $P \leq 0.001$ and -46%, $P \leq 0.001$ respectively) or 550 μmol $[\text{CO}_2]$ (-22%, $P \leq 0.001$ and -45%, $P \leq 0.001$ respectively) could infer that there was a stomatal acclimation (Fig 3. 22 B). Reduced g_s were intern linked with lower E in elevated $[\text{CO}_2]$ grown plants by -21% ($P \leq 0.001$) when measured at 550 μmol $[\text{CO}_2]$ and -26% ($P \leq 0.001$) at 400 μmol $[\text{CO}_2]$ in WW conditions (Fig 3.22 C). However, drought imposition induced further reduction in g_s in $[\text{CO}_2]$ enriched mulberry plants may possibly associated with substantial decrease in E by 46% and 48% at 550 and 400 μmol $[\text{CO}_2]$ respectively than their ambient counterparts. In spite of reduced P_n , high CO_2 grown plants exhibited tremendous increment in WUE_i especially under water with holding environments by 34% and 21% at 550 and 400 μmol $[\text{CO}_2]$ respectively (Fig 3. 22 D). In addition to above, stomatal acclimation should limits the mesophyll diffusion to $[\text{CO}_2]$ in elevated $[\text{CO}_2]$ grown plants may possibly associated with reduced C_i ($P \leq 0.05$) under WW by 7% and 10% at 550 and 400 μmol $[\text{CO}_2]$ respectively and after 30 days of WS by 18% and 20% at 550 and 400 μmol $[\text{CO}_2]$ compared to their control counterparts (Fig 3. 22 E).

3.3.6 Changes in OJIP chlorophyll *a* fluorescence transients and JIP test parameters

SRC coppice mulberry plants showed significant variations in the shape of the OJIP chlorophyll *a* fluorescence transients and comparison made among the raw OJIP transients between elevated and ambient $[\text{CO}_2]$ grown plants in all the experimental conditions (given in Fig 3.23 A). Dark adapted control mulberry plants exhibited a typical OJIP transient with F_0 of ~730 a.u. F_M of ~1808 a.u. and the variable fluorescence (F_V) of ~1078 a.u. in WW conditions. But, $[\text{CO}_2]$ enrichment lead to reduction of F_0 (-11%) with concomitant increase in F_M (9%) as well as F_V (18%) in WW conditions than their ambient counterparts. Drought stress significantly increased F_0 in both elevated $[\text{CO}_2]$ ambient $[\text{CO}_2]$ grown plants with parallel decrease in F_M and F_V when compared to their respective WW counterparts.

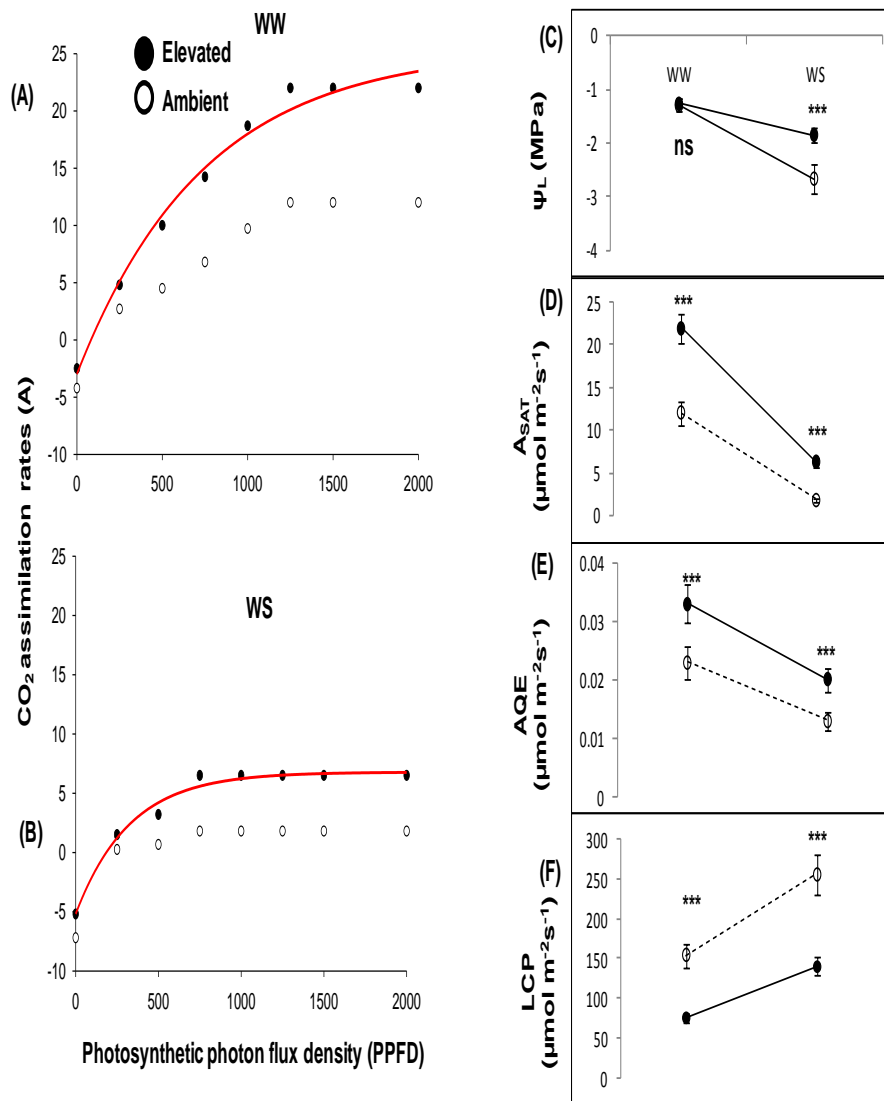


Fig 3.21 Variations in carbon assimilation rates (A) with increasing photosynthetic photon flux density (PPFD), leaf water potential and parameters deduced from A/PPFD curves under well watered (WW) as well as after 30 days of drought (WS) between plants grown under elevated and ambient $[CO_2]$ environments. These measurements were taken on randomly chosen fully matured leaves at 3rd or 4th position from the upper canopy during 10:00-11:30 h and values are \pm SD of three plants ($n = 3$) with statistical significance of *($P < 0.05$), **($P < 0.01$), ***($P < 0.001$) and ns- not significant. E- elevated, A- ambient.

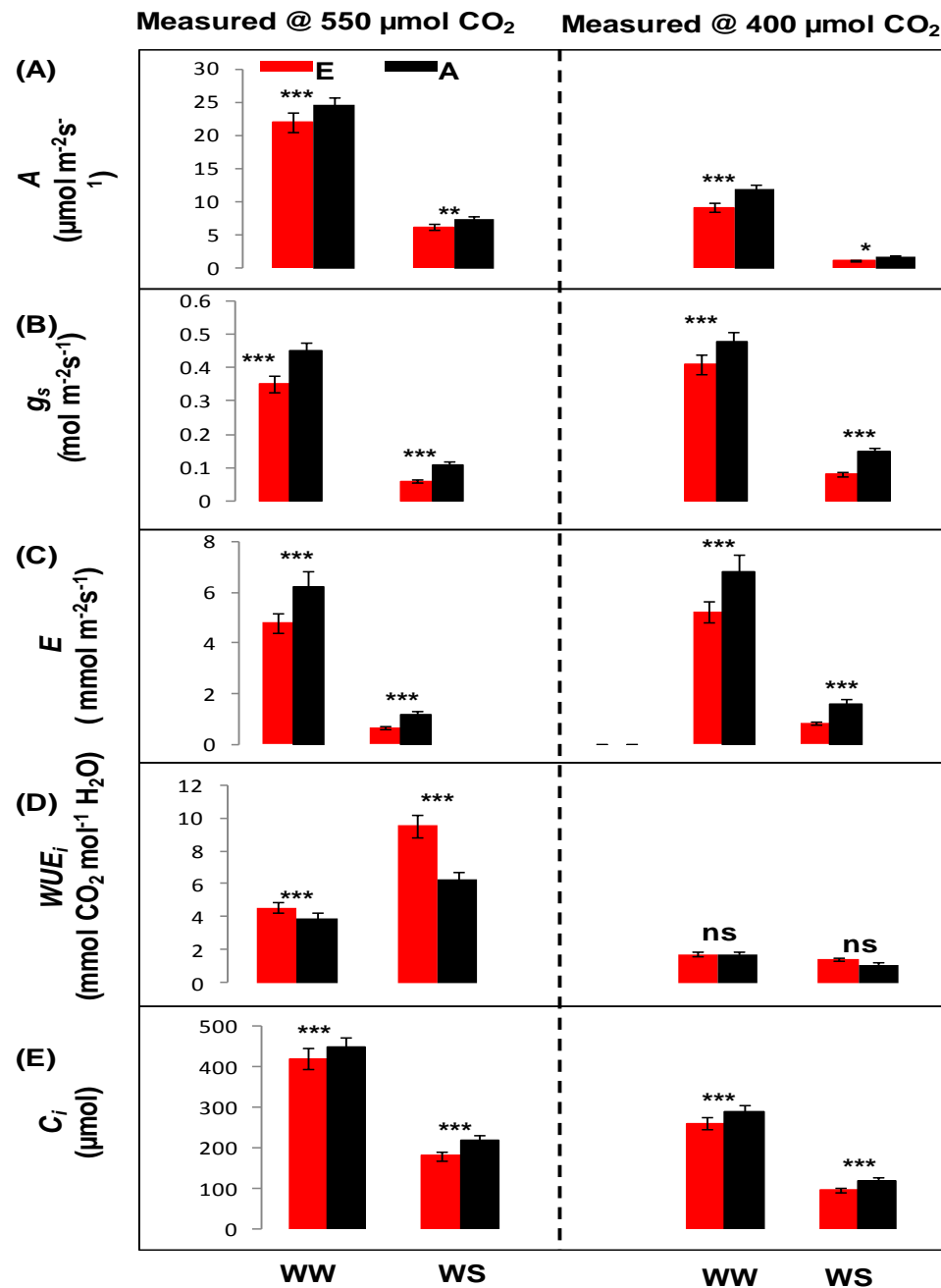


Fig 3.22 Changes in reciprocal instantaneous photosynthetic measurements between elevated and ambient [CO₂] grown plants in well watered (WW) and water stress environments (WS). These measurements were taken on randomly chosen fully matured leaves at 3rd or 4th position from the apex in the upper canopy during 10:00-11:30 h and values are \pm SD of three plants (n = 3) with statistical significance of *(P < 0.05), ***(P < 0.01), *** (P < 0.001) and ns- not significant. E- elevated, A- ambient.

However, plants grown under elevated $[\text{CO}_2]$ environments showed reduced F_M (-2%), which was statistically not significant, and F_0 (-19%) with simultaneous increase in F_V (14%) compared to control plants after 30 days of WS. After 30 days of drought imposition, both elevated and ambient $[\text{CO}_2]$ grown plants showed significantly greater F_0 and rise in fluorescence amplitude at OJ and JI phases; but, the amplitude of fluorescence rise declined at IP phase when compared to their WW counterparts (Fig 3.22 A). Further, OJIP chlorophyll *a* fluorescence transients were double normalized between F_0 and F_M represented as V_{OP} , (Fig 3.22 B), between 50 and 300 μs showed as V_{OK} (Fig. 3C and D) and between 50 μs and 2ms indicated as V_{OJ} (Fig 3.22 C and D) for detailed analysis of the fluorescence kinetics. A positive L-band with a peak at around 150 μs appeared in both elevated $[\text{CO}_2]$ (E), $\Delta V_{OK} = V_{OK \text{ EWS}} - V_{OK \text{ EWW}}$, and ambient $[\text{CO}_2]$ (A), $\Delta V_{OK} = V_{OK \text{ EWS}} - V_{OK \text{ EWW}}$, grown plants after 30 days of WS with respect to their WW counterparts. Similarly, a positive K-band appeared at 300 μs when double normalization was done between O (50 μs) and J (2ms) termed as V_{OJ} in both elevated $[\text{CO}_2]$ ($\Delta V_{OJ} = V_{OJ \text{ EWS}} - V_{OJ \text{ EWW}}$) as well as ambient $[\text{CO}_2]$ ($\Delta V_{OJ} = V_{OJ \text{ AWS}} - V_{OJ \text{ AWW}}$) grown plants after 30 days of water withholding. However, plants grown under current $[\text{CO}_2]$ had increased positive L and K bands amplitude than $[\text{CO}_2]$ enriched plants should suggest that ambient $[\text{CO}_2]$ grown plants were more susceptible to drought stress. In addition to above, plants grown under elevated $[\text{CO}_2]$ atmosphere showed significant variations in parameters derived from OJIP chlorophyll fluorescence transients i.e the JIP-test parameters under WW as well as WS environments when compared to ambient $[\text{CO}_2]$ grown plants. All the data of JIP test parameters from all the experimental conditions were normalized to reference WW ambient $[\text{CO}_2]$ grown plants by giving a numeric value 1 and significant differences between high $[\text{CO}_2]$ and current $[\text{CO}_2]$ environmental conditions in WW as well as WS were represented as a radar plot (Fig 3.23). Drought imposition significantly increased variable fluorescence at step J (V_J) by 7.5 and 8%, at I phase (V_I) by 6% and 3% in elevated and ambient $[\text{CO}_2]$ grown plants respectively than their WW counterparts. Parameter F_V/F_M ($\phi_{P_0} = \text{TR}_O/\text{ABS}$) was

significantly increased in plants grown without water deficit by 12% as well as with water deficit by 16% under increased $[\text{CO}_2]$ than their respective controls.

Similarly, plants grown under $[\text{CO}_2]$ enriched environment exhibited greater increase in ψ_o (8%), ΦE_o (18%), F_v/F_o (15%), TR_o/CSm (21%), ET/CSm (25%), RC/CSm (19%), K_p (18%) and SFI (27%) compared to the ambient CO_2 grown plants. Nevertheless, complete water withholding induced significant reduction in above mentioned parameters in both elevated and ambient $[\text{CO}_2]$ grown plants; but, high $[\text{CO}_2]$ grown plants showed significant increase by 7%, 21%, 28%, 14%, 19%, 16%, 29%, and 35% correspondingly compared to control counterparts. In contrast to above, plants grown under high CO_2 environments showed significant decrease in parameters including ϕD_o (-15% & -14%), F_o/F_M (-16% & -14%), K_n (-9% & -2%), DI_o/RC (-26% & -31%) and DI_o/CSm (-9% & -15%) in WW and WS mulberry plants respectively than their ambient $[\text{CO}_2]$ counter parts. Further, parameters like $PI_{(\text{ABS})}$ (44% and 46%) and $PI_{(\text{CSM})}$ (47% and 45%), tells about the overall performance of the PS-II, were significantly increased in $[\text{CO}_2]$ enriched mulberry plants under without water withholding as well as with water withholding environments than their respective ambient controls. Our results from pipeline models also indicated that ambient $[\text{CO}_2]$ grown plants showed greater photoinhibition when compared to elevated $[\text{CO}_2]$ grown plants (Fig 3.24).

3.3.7 Changes in chlorophyll pigments

There was significant variation in the concentration of chlorophyll pigments between elevated and ambient $[\text{CO}_2]$ grown plants under WW and during WS conditions. Elevated $[\text{CO}_2]$ grown plants exhibited reduced Chl *a* (-15%), Chl *b* (-11%) and total Chl (-14%) than their ambient counterparts. Drought imposition significantly reduced chlorophyll pigment concentration in both elevated (48%) and ambient $[\text{CO}_2]$ (65%) grown plants when compared to their WW counter parts. But, after 30 days of WS, high $[\text{CO}_2]$ grown plants had greater Chl *a* (28%), Chl *b* (34%) and total Chl (32%) content when compared to ambient $[\text{CO}_2]$ grown plants.

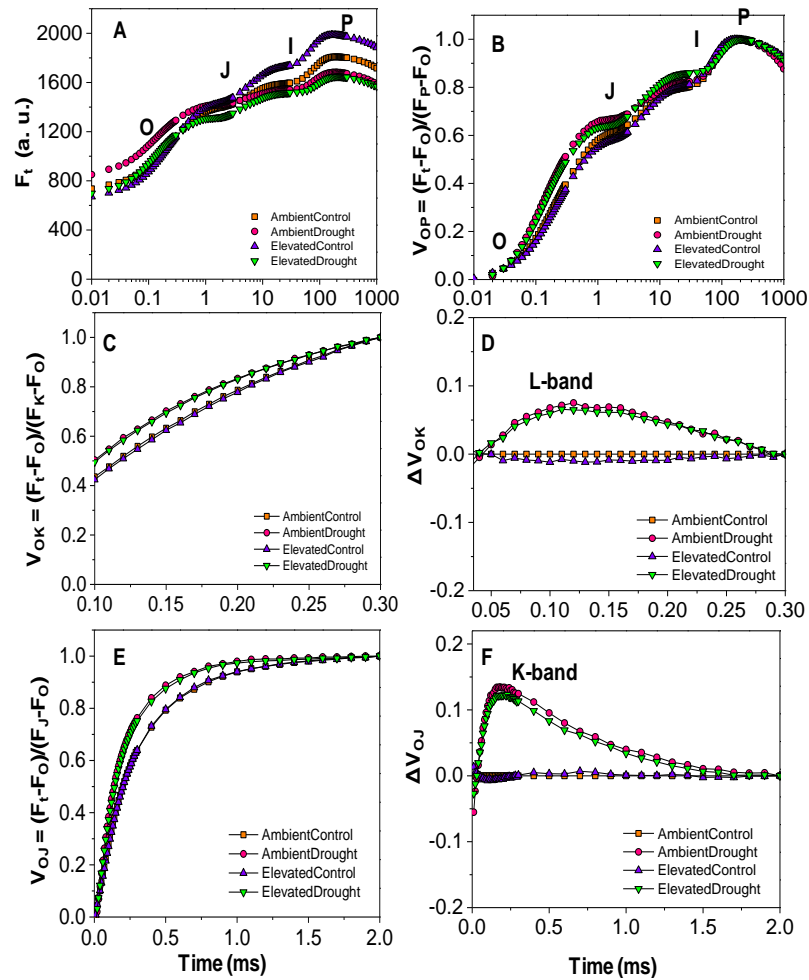


Fig 3.22 Variations in OJIP chl a fluorescence transients, recorded in dark adapted mulberry plants grown in elevated and ambient $[CO_2]$ conditions under control as well as drought environments. (A) Raw chl a fluorescence transient curves exhibiting fluorescence intensity (F_t) recorded between 0.1 and 1000 ms time period (a.u. = arbitrary unit). (B) Chl a fluorescence transients double normalized between the two fluorescence extreme O (F_0) and P (F_M) phases: $V_{OP} = (F_t - F_0)/(F_P - F_0)$. (C) Chl a fluorescence transients double normalized between F_0 and F_K phases: $V_{OK} = (F_t - F_0)/(F_K - F_0)$. (D) Kinetic difference of V_{OK} [$\Delta V_{OK} = (F_t - F_0)/(F_K - F_0)$] showing L-band (0.15 ms). (E) Variable fluorescence transients double normalized between F_0 and F_J phases: $V_{OJ} = (F_t - F_0)/(F_J - F_0)$. (F) Kinetic difference of V_{OJ} [$\Delta V_{OJ} = (F_t - F_0)/(F_K - F_0)$] showing K-band (0.3ms). All these measurements were taken on randomly chosen fully matured leaves at 3rd or 4th position from the upper canopy during 10:00-11:30 h and values are \pm SD of three plants ($n = 3$). E- elevated, A- ambient, C –Well watered, D- drought.

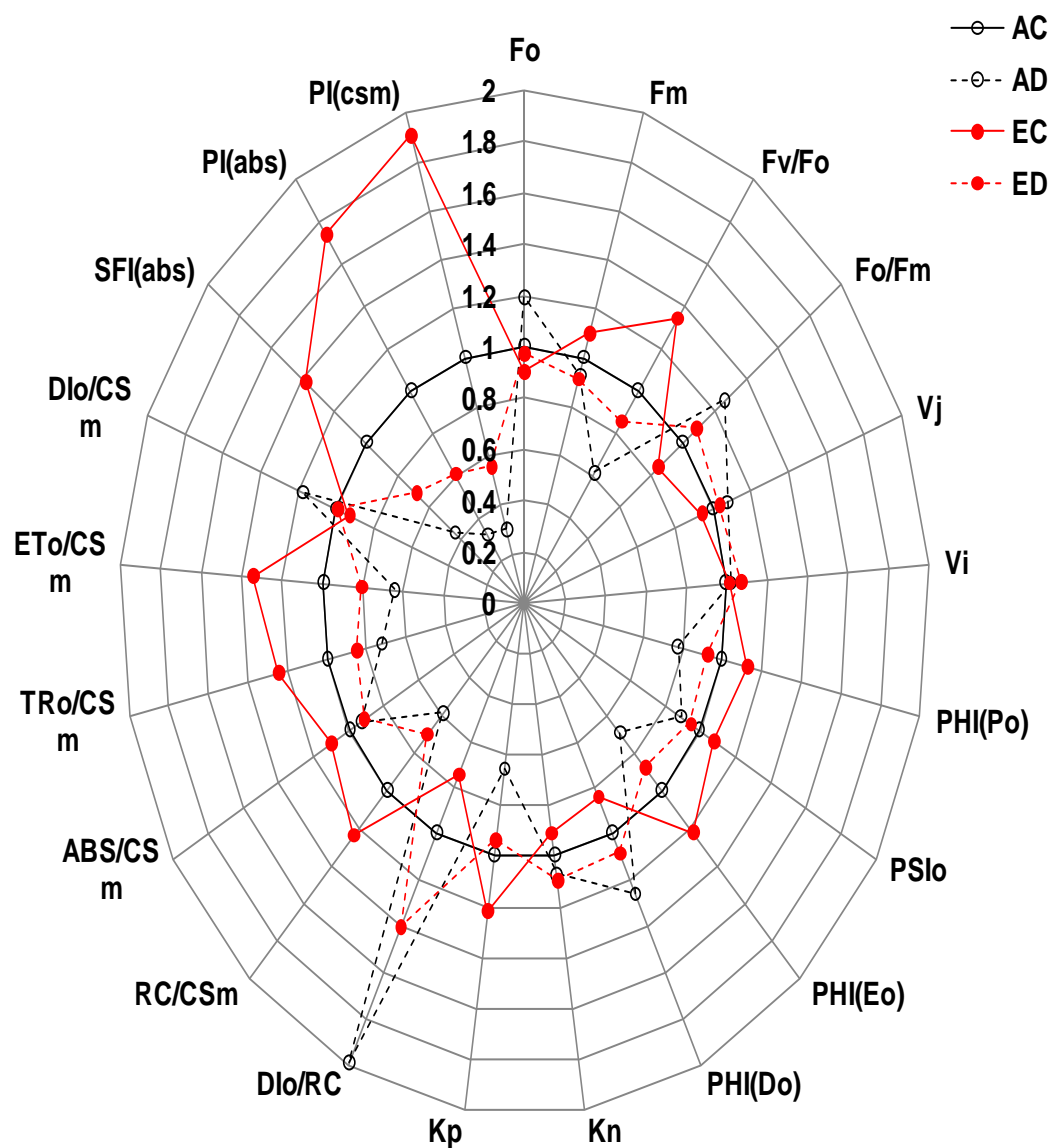


Fig 3.23 Radar plot showing the mean changes of chlorophyll *a* fluorescence JIP-test parameters in mulberry between elevated and ambient [CO₂] grown plants under all the experimental conditions. These measurements were taken on randomly chosen fully mature leaves at 3rd or 4th position from the upper canopy during 11:00-11:30 h and data are mean \pm SD ($n = 3$). C- Well watered, A- Ambient, E- Elevated.

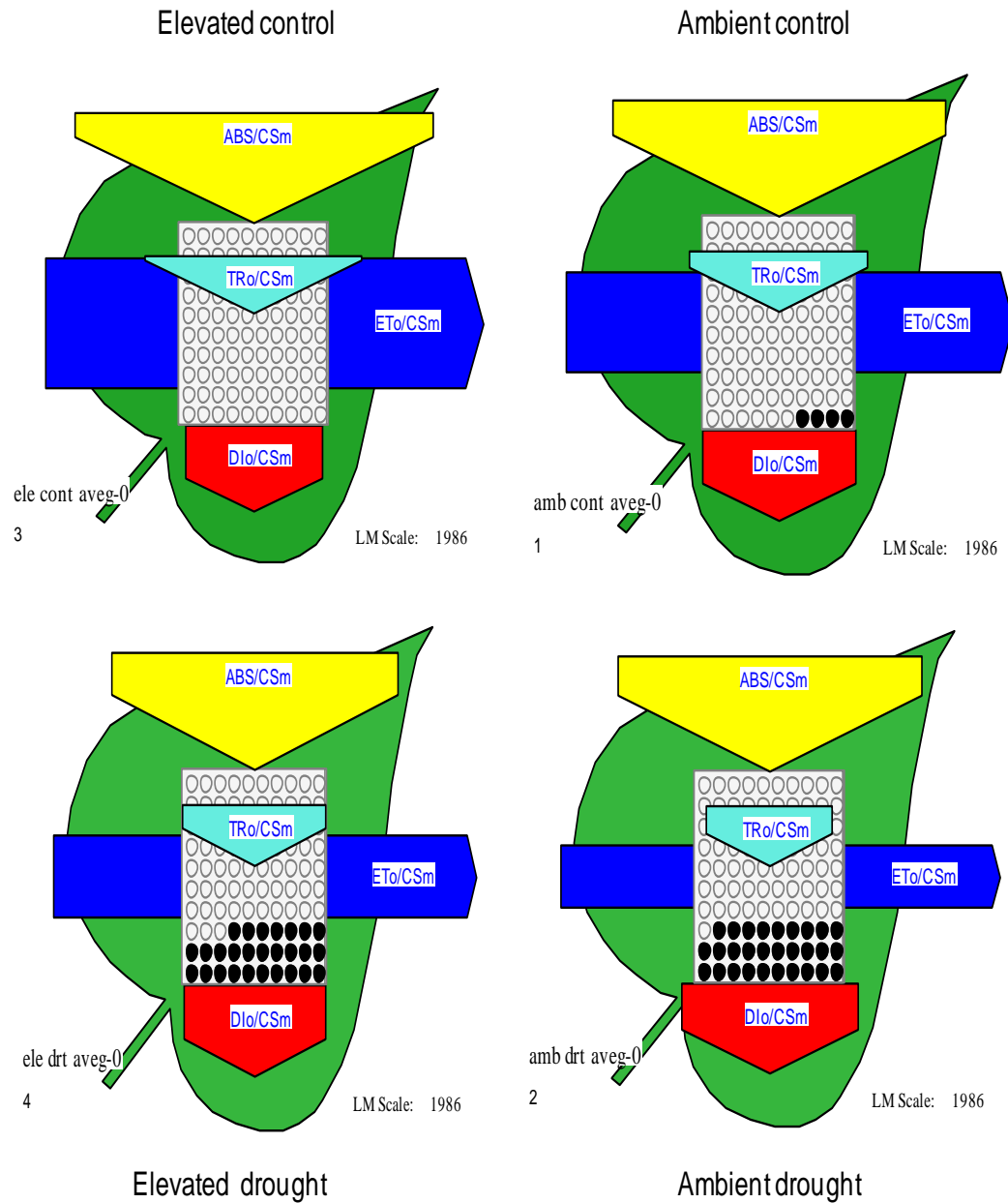


Fig 3.24 pipeline models showing the changes in phonological fluxes and number of open RCs per CSM in mulberry grown under elevated and ambient [CO₂] under WW as well as WS conditions

Table 3.5 Changes in chlorophyll pigments in SRC mulberry grown under both elevated and ambient [CO₂] environments under WW as well as after 30 days of WS

Parameter	Well watered (WW)		Water stress (WS)	
	Elevated	Ambient	Elevated	Ambient
Chlorophyll <i>a</i> (mg g⁻¹ fw)	1.2 (0.036)	1.42 (0.04)	0.632 (0.028)	0.450 (0.04)
Chlorophyll <i>b</i> (mg g⁻¹ fw)	0.67 (0.042)	0.76 (0.047)	0.285 (0.032)	0.186 (0.033)
Total chlorophyll (mg g⁻¹ fw)	1.87 (0.038)	2.18 (0.039)	0.917 (0.034)	0.620 (0.039)

3.4 Objective 4- Investigating the coordinate changes of hydraulic conductance and photosynthesis with particular reference to expression profiles of certain AQPs in short rotation coppice mulberry.

3.4.1 Plant water status

Plants grown under both elevated as well as ambient [CO₂] conditions did not exhibit significant variations in plant leaf water status (Ψ_{pd} , Ψ_{md} and Ψ_X) under control conditions (Fig 3.25). However, drought imposition reduced Ψ_{pd} , Ψ_{md} and Ψ_X significantly in both elevated as well as ambient [CO₂] grown plants compared to their WW counterparts; but, reduction was more in current [CO₂] grown plants compared to [CO₂] enriched mulberry plants. Ψ_{pd} decreased in elevated [CO₂] SRC mulberry plants from -0.5 MPa to -1.4 MPa (-64%), whereas in ambient [CO₂] grown plants it was reduced from -0.62 MPa to -2 MPa (-70%) at 30 DAS. Similarly, Ψ_{md} reduced from -1.2 MPa to -2.1 MPa and -1.4 MPa to -2.8 MPa in elevated as well as ambient [CO₂] grown plants respectively at 30DAS. But, plants grown under [CO₂] enriched environment exhibited 25% more Ψ_{md} compared to their ambient [CO₂] counterparts even under extended drought environments (30DAS). Drought imposition significantly reduced Ψ_X in both elevated and current [CO₂] grown plants, recorded Ψ_X at 30 DAS were -1.4 MPa and -2.2 MPa in [CO₂] enriched as well as control [CO₂] grown plants respectively. Thus, plants grown under increased [CO₂] environments exhibited 36% higher Ψ_X compared to their ambient counterparts under prolonged WS conditions.

3.4.2 Plant hydraulic parameters

Plants grown under elevated [CO₂] environments showed significant variations in plant hydraulic characteristics including K_S , K_L and F under WW as well as WS conditions with respect to their ambient [CO₂] counterparts (Fig 3. 26). Recorded K_S in plants grown under current [CO₂] was $18 \times 10^{-5} \text{ kg m}^{-1} \text{ sec}^{-1} \text{ MPa}^{-1}$, while in [CO₂] enriched mulberry plants it was $14 \times 10^{-5} \text{ kg m}^{-1} \text{ sec}^{-1} \text{ MPa}^{-1}$ under WW conditions. Thus, ambient [CO₂] grown plants showed 22% higher K_S compared to their high [CO₂] counterparts. In

consistent with K_s , parameters including K_L and F were also decreased in elevated $[CO_2]$ grown plants than their ambient $[CO_2]$ counterparts. Observed K_L in plants grown under both ambient and elevated $[CO_2]$ were $13 \text{ mmol m}^{-2} \text{ sec}^{-1} \text{ MPa}^{-1}$ and $10.5 \text{ mmol m}^{-2} \text{ sec}^{-1} \text{ MPa}^{-1}$ respectively under WW conditions. Recorded F in ambient $[CO_2]$ plants was 0.250 kg/hr , whereas in elevated $[CO_2]$ grown plants observed F was 0.175 kg/hr . Therefore, SRC mulberry plants grown under current $[CO_2]$ exhibited greater K_L (26%) and F (30%) compared to the plants grown under $[CO_2]$ enriched environments. Drought imposition induced significant reduction in K_s , K_L and F in both the plants grown under ambient and elevated $[CO_2]$ conditions than their respective WW controls. However, ambient $[CO_2]$ grown plants showed greater reduction in aforementioned hydraulic characteristics (K_s , K_L and F) under prolonged drought conditions (30DAS) than their elevated $[CO_2]$ counterparts. K_s decreased relatively by 55% ($18 \times 10^{-5} \text{ kg m}^{-1} \text{ sec}^{-1} \text{ MPa}^{-1}$ to $8 \times 10^{-5} \text{ kg m}^{-1} \text{ sec}^{-1} \text{ MPa}^{-1}$) and 28% (from $14 \times 10^{-5} \text{ kg m}^{-1} \text{ sec}^{-1} \text{ MPa}^{-1}$ to $10 \times 10^{-5} \text{ kg m}^{-1} \text{ sec}^{-1} \text{ MPa}^{-1}$) in ambient and elevated $[CO_2]$ grown plants respectively at 30DAS when compared to their WW counterparts. Recorded K_L and F at 30 DAS in ambient $[CO_2]$ grown plants were $3.8 \text{ mmol m}^{-2} \text{ sec}^{-1} \text{ MPa}^{-1}$ and 0.125 kg/hr respectively, while in $[CO_2]$ enriched plants observed K_L and F at 30 DAS were $6.5 \text{ mmol m}^{-2} \text{ sec}^{-1} \text{ MPa}^{-1}$ and 0.145 kg/hr correspondingly. Thus, K_L and F were decreased relatively by 70% and 50% respectively in ambient $[CO_2]$ grown plants, whereas in high $[CO_2]$ grown plants K_L and F were reduced by 38% and 17% correspondingly at 30 DAS than their WW counterparts. Nevertheless, mulberry plants grown under increased atmospheric $[CO_2]$ displayed augmented K_L (41%) and F (13%) compared to their control $[CO_2]$ counterparts even under prolonged drier environments.

3.4.3 Correlations of hydraulic characteristics and leaf gas exchange parameters

Photosynthetic leaf gas exchange parameters were (A_{Sat} , g_s and E) positively correlated with plant hydraulic characteristics (K_s , K_L , F and Ψ_{md}) in both elevated and ambient $[CO_2]$ grown mulberry plants under WW as well as WS conditions (Fig 2. 27, 28, . These results clearly demonstrated that changes in photosynthetic leaf gas exchange parameters

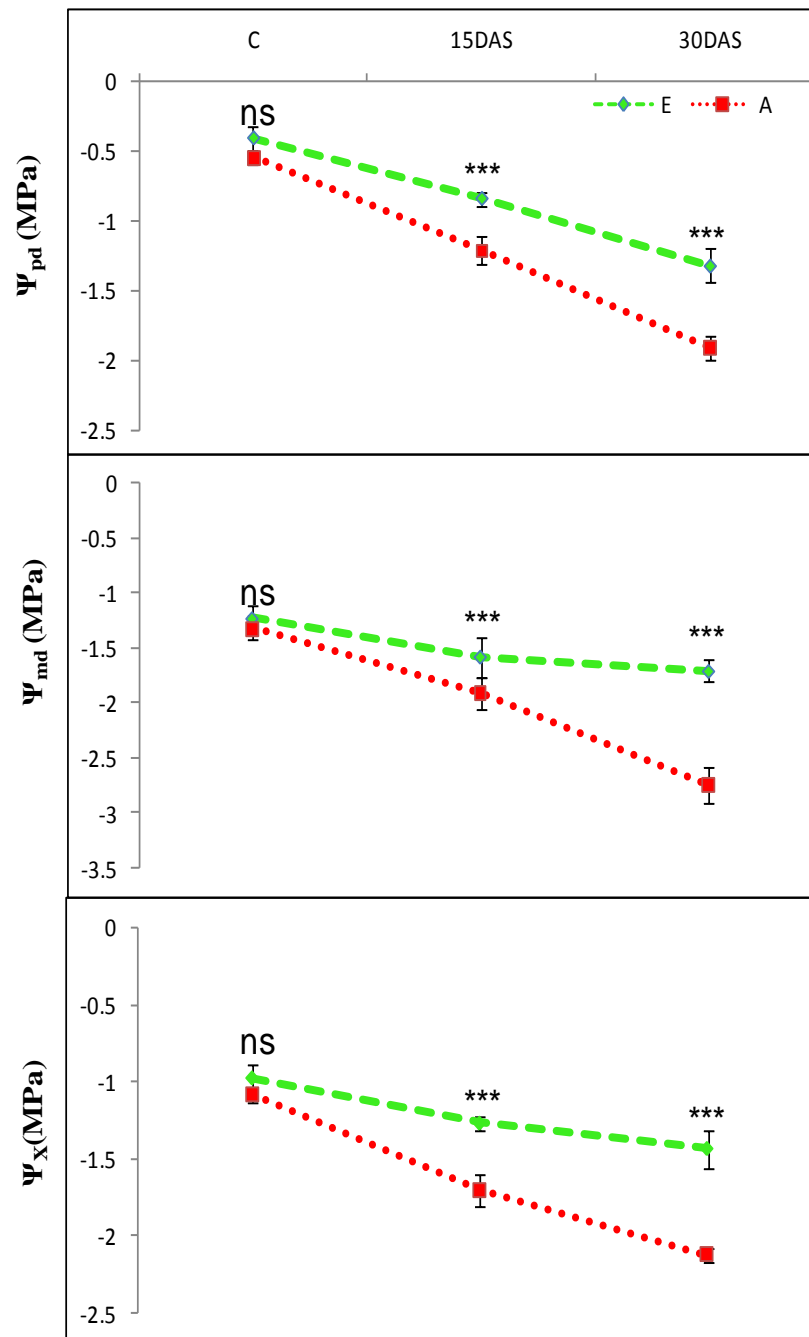


Fig 3.25 Changes in plant water status in SRC mulberry grown in elevated as well as ambient CO₂ environments under WW as well as WS conditions. Results shown in the figures are an average of time points and values are \pm SD of three plants ($n = 3$) with statistical significance of *($P < 0.05$), **($P < 0.01$), ***($P < 0.001$) and ns- not significant.

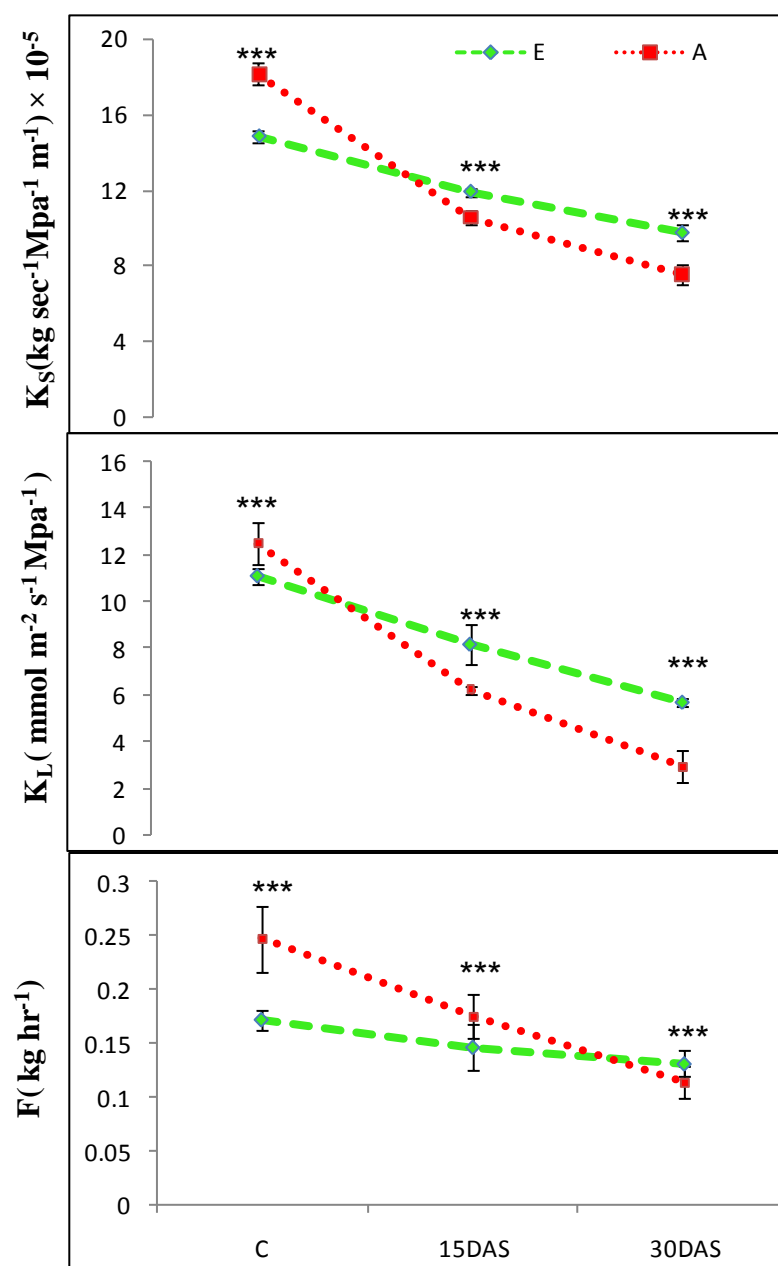


Fig 3.26 Variations in plant hydraulic dynamics in mulberry grown in elevated as well as ambient [CO₂] environments under WW as well as WS conditions. Results shown in the figures are an average of time points and values are \pm SD of three plants (n = 3) with statistical significance of *(P < 0.05), ***(P < 0.001) and ns- not significant.

can proportionally influence the plant hydraulic dynamics or vice versa. Drought imposition significantly reduced photosynthetic leaf gas exchange characteristics including A_{Sat} , g_s and E and hydraulic parameters such as K_s , K_L , F and Ψ_{md} in both elevated as well as ambient $[\text{CO}_2]$ grown plants and reduction was further increased with the progression of stress treatment. However, plants grown under current $[\text{CO}_2]$ exhibited greater reduction in aforementioned parameters at 30 DAS compared to their elevated $[\text{CO}_2]$ counterparts. In addition to above, we also observed that there was a strong positive correlation between K_s and individual A_{Sat} , g_s and E . As K_s was decreasing with the progression of stress treatment, A_{Sat} , g_s and E were gradually decreased in both $[\text{CO}_2]$ enriched as well as control $[\text{CO}_2]$ grown plants. In consistent with K_s , both elevated as well as ambient $[\text{CO}_2]$ grown plants displayed higher photosynthetic performance (A_{Sat}) when plants exhibited increased K_L , F as well as Ψ_{md} and A_{Sat} was decreased linearly when K_L , F and Ψ_{md} were reduced under extended drought environments. Similar trend was observed between g_s Vs K_L , F and Ψ_{md} , E Vs K_L , F and Ψ_{md} in both elevated as well as ambient $[\text{CO}_2]$ grown plants. In contrast to above, plants grown under $[\text{CO}_2]$ enriched environments showed negative correlation between WUE_i and hydraulic characteristics including K_s , K_L , F and Ψ_{md} at 30 DAS.

3.4.4 Expression profiles of aquaporin (AQP) genes under elevated $[\text{CO}_2]$ and drought

Gene specific primers were used for amplifying a 200-300 bp regions from the existing draft genome sequence of the mulberry. After confirming the successful amplification of the target genes, the same primers were used to check the mRNA expression levels of these genes in mulberry grown in elevated as well as ambient CO_2 environment under WW as well as during WS conditions (Fig 3. 31) and the same were used to check their expression levels in mulberry grown in elevated as well as ambient CO_2 environment under WW as well as during WS conditions. Our results from AQPs gene expression studies clearly demonstrated that elevated $[\text{CO}_2]$ significantly influenced the expression profiles of AQPs in WW as well as during WS conditions compared to their control $[\text{CO}_2]$ counterparts (Fig 3.32).

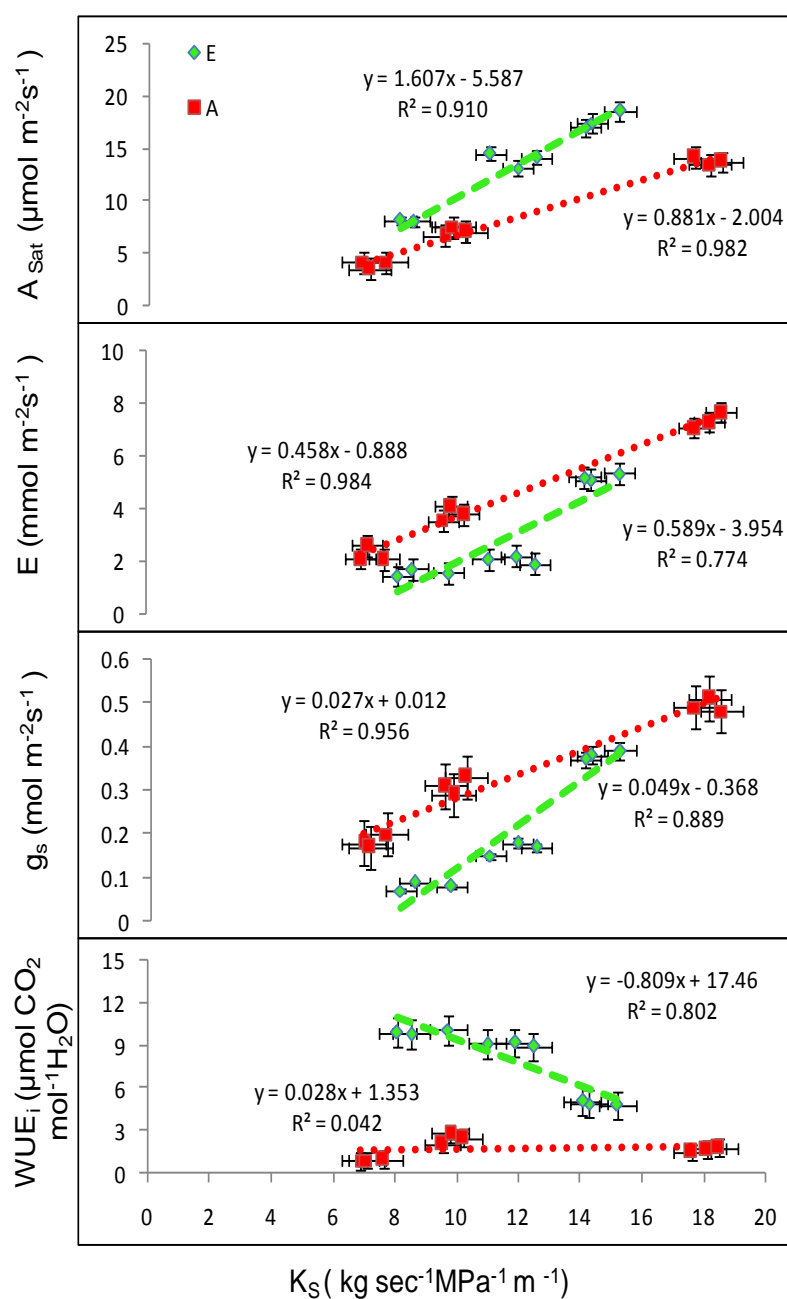


Fig 3.27 Correlation between K_s and photosynthetic leaf gas exchange physiology in mulberry grown in elevated as well as ambient [CO₂] environments under WW as well as WS conditions.

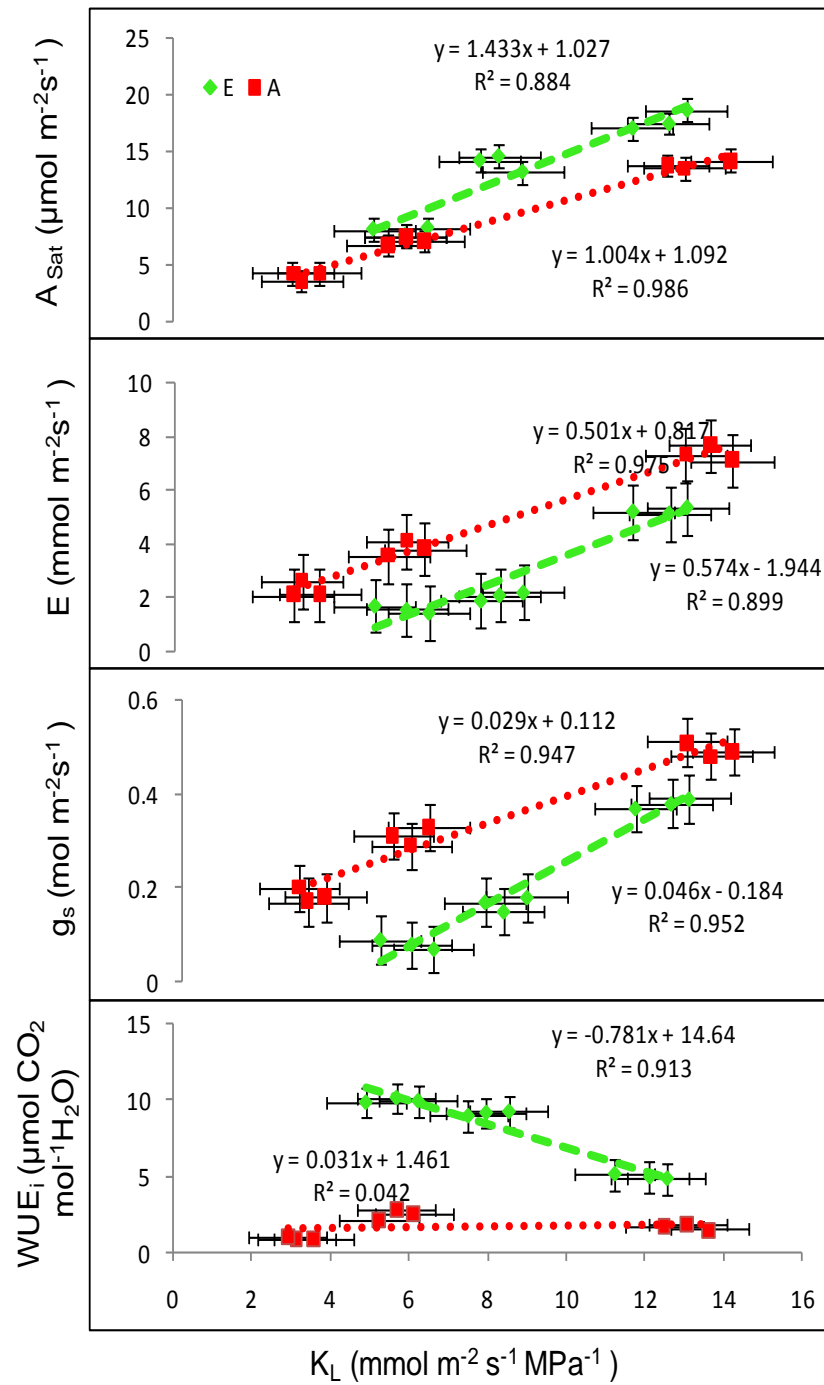


Fig 3.28 Correlation between K_L and photosynthetic leaf gas exchange physiology in mulberry grown in elevated as well as ambient $[\text{CO}_2]$ environments under WW as well as WS conditions.

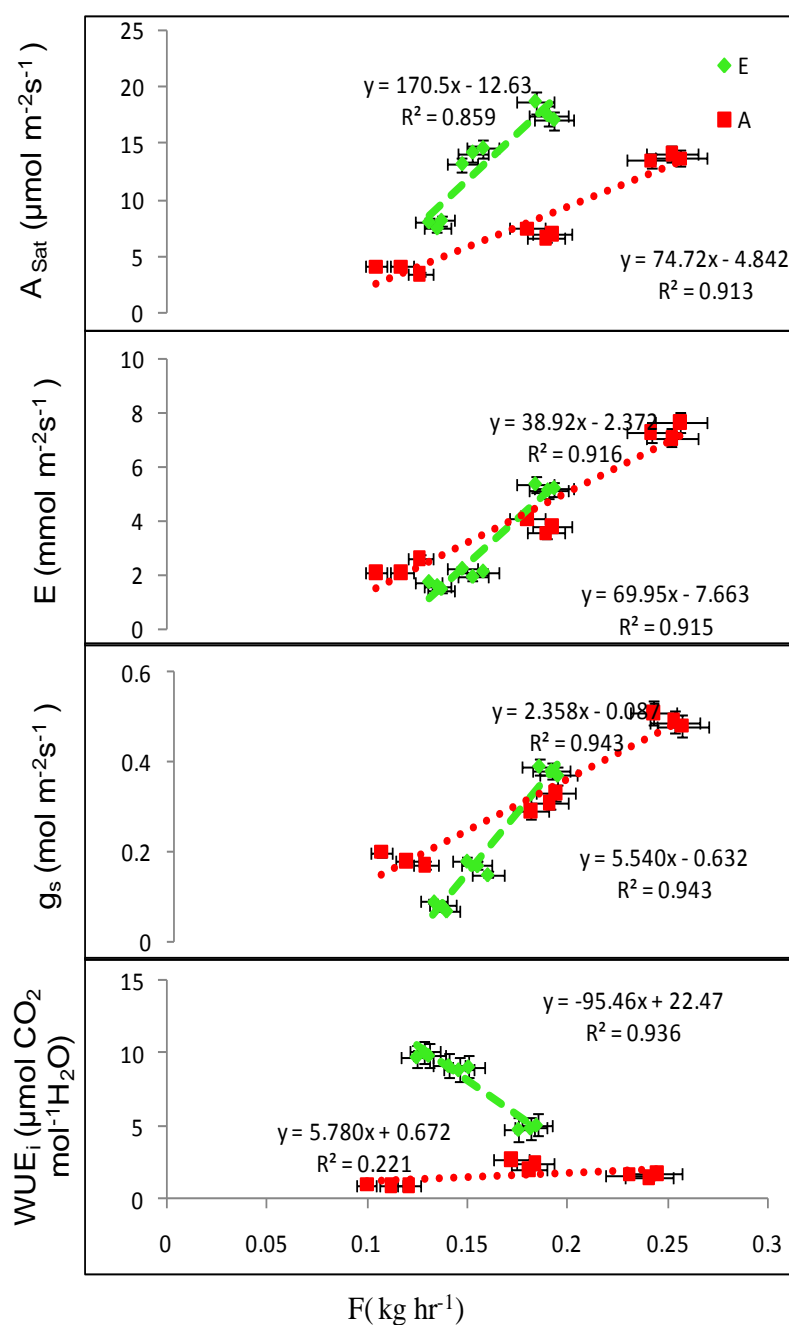


Fig 3.29 Correlation between F and photosynthetic leaf gas exchange physiology in mulberry grown in elevated as well as ambient $[\text{CO}_2]$ environments under WW as well as WS conditions.

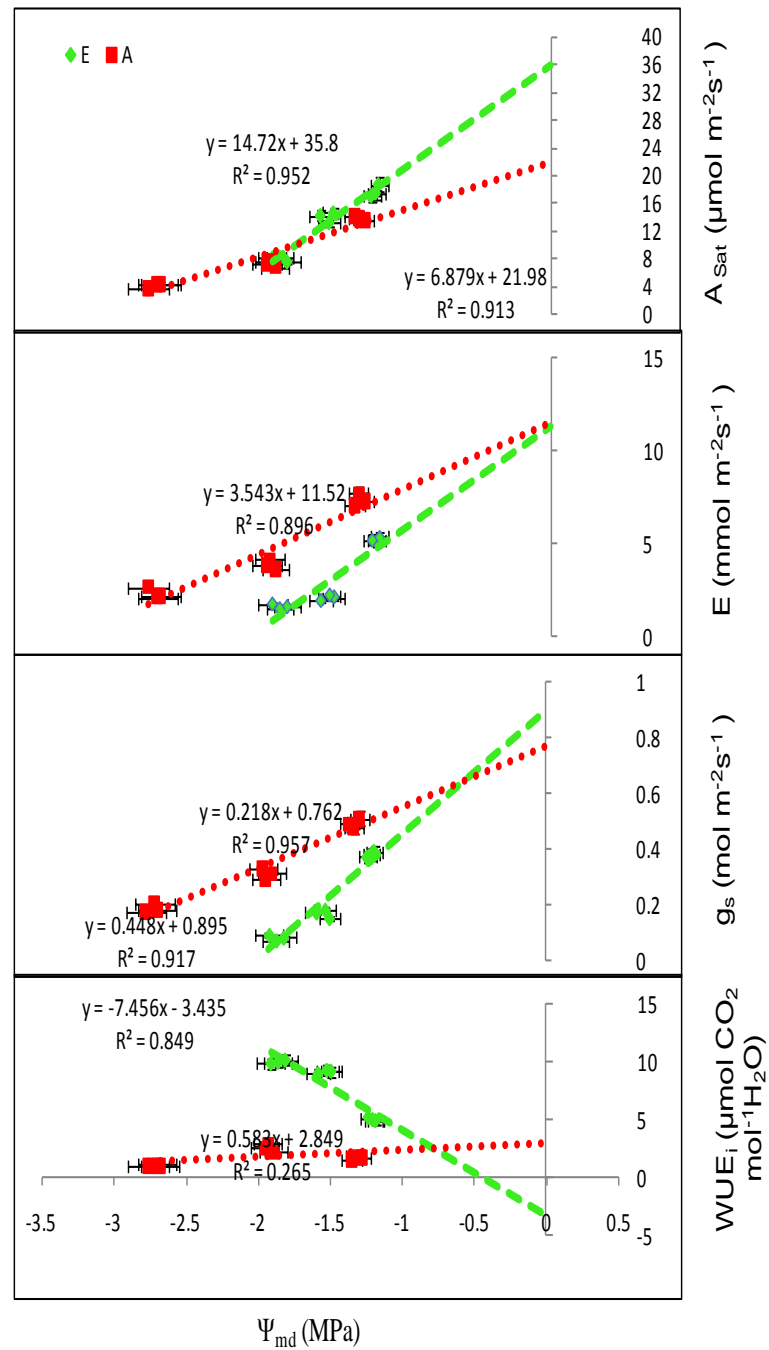


Fig 3.30 Correlation between Ψ_{md} and photosynthetic leaf gas exchange physiology in mulberry grown in elevated as well as ambient $[\text{CO}_2]$ environments under WW as well as WS conditions.

Interestingly, some AQPs showed increased expression levels under WW as well as during WS conditions in ambient [CO₂] grown plants than their elevated [CO₂] counterparts or vice versa. Ambient [CO₂] grown plants showed higher level expression of certain AQP genes including PIP1.1, PIP2.1, PIP2.2, PIP2.7, TIP2.1 and TIP4.1 with concomitant reduction in TIP1.3 and TIP2.3 compared to their high [CO₂] grown plants in WW conditions. However, drought imposition significantly reduced PIP1.1, PIP2.1, TIP2.3 and TIP4.1 at 30DAS despite their higher expressions at 15 DAS than their elevated counterparts. In contrast to above, PIP2.2, PIP2.7, TIP1.3, TIP2.1 and TIP2.3 AQPs were up regulated in [CO₂] enriched mulberry plants even under extended dry environments (30 DAS).

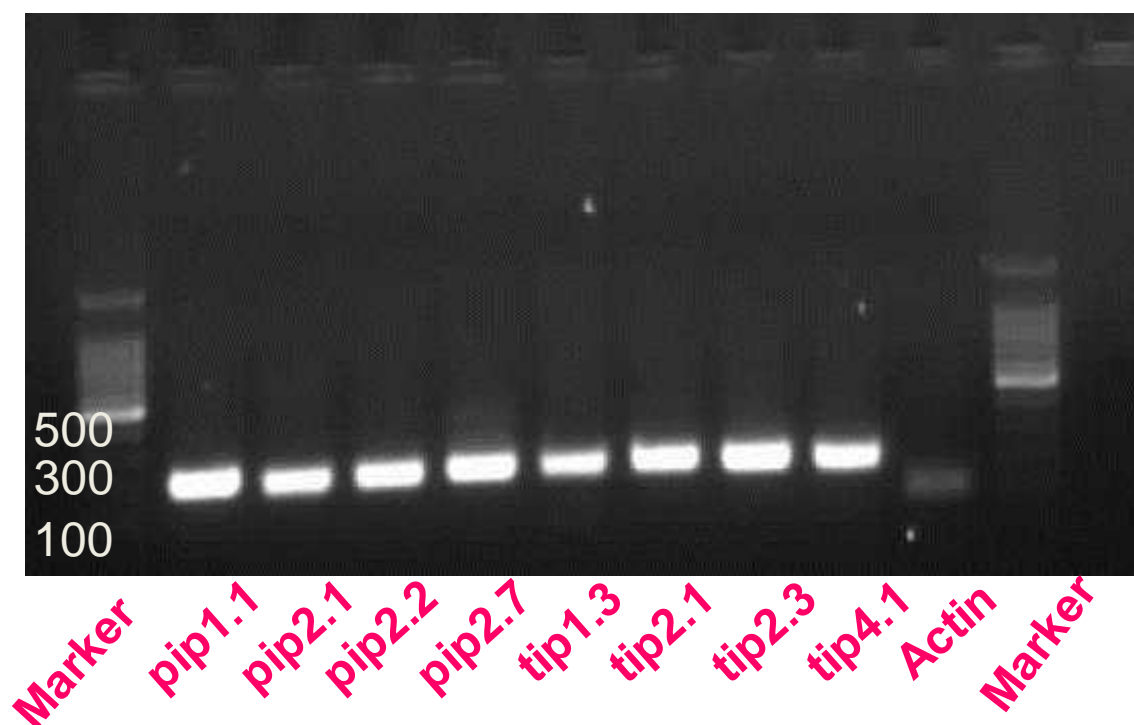


Fig 3. 31 Amplification of designed gene specific primes of both PIPs and TIPs in mulberry.

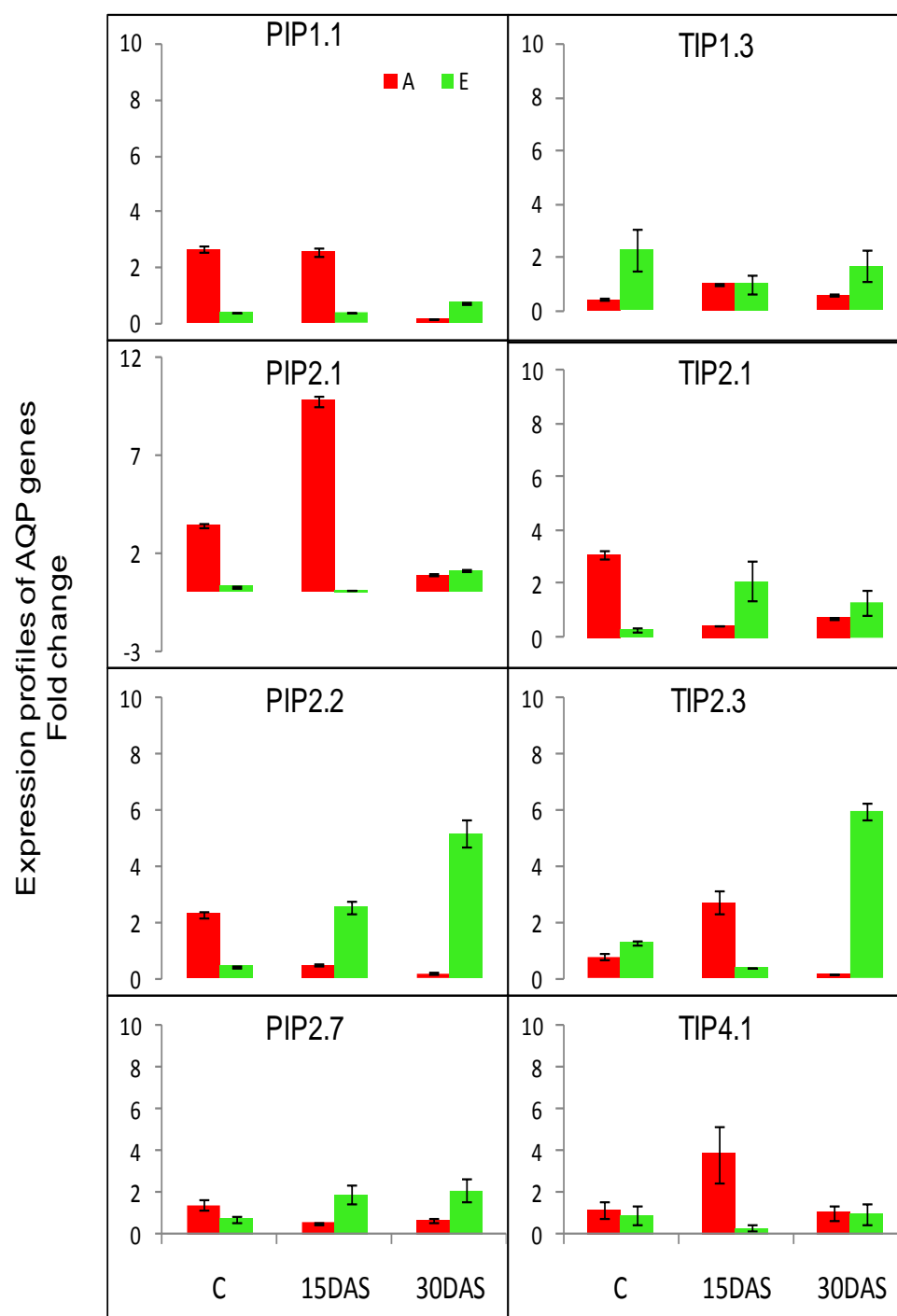


Fig 3.32 Expression profiles of both PIPs and TIPs in mulberry grown in elevated as well as ambient [CO₂] environments under WW as well as WS conditions

Chapter 4

Discussion

4.1 Mulberry plants showed genotypic variations under [CO₂] enriched environment

Mulberry plants showed significant genotypic variations under [CO₂] enriched environment in terms of photosynthetic leaf gas exchange physiology, PS-II efficiency and bio-mass yields. Although both genotypes exhibited positive responses to high [CO₂] environment, S13 showed significant increase of A_{Sat} under both normal as well as [CO₂] enriched environment than K2 inferring possible genotypic variations in RuBP carboxylation associated with increased quantity and/or activity of Rubisco (Darbah et al., 2010; Liberloo et al., 2007). In contrast to A_{Sat} , both genotypes of mulberry grown under high CO₂ environment showed reduced g_s and E which resulted in substantial increase of WUE_i (Onoda et al., 2009; Dang et al., 2008). Studies have demonstrated that in spite of significant reductions in g_s , plants grown under [CO₂] enriched environment showed higher A_{Sat} than their ambient [CO₂] counterparts possibly due to higher C_i (Ainsworth and Long 2005; Rasineni et al., 2011). However, in this study, we observed ascendancy of A_{Sat} in S13 genotype under both elevated and ambient CO₂ conditions, even under reduced C_i , clearly suggest that C_i alone may not be responsible for determining the proportionate changes in A_{Sat} . PS-II efficiency is the most important factor which directly influences the changes in A_{Sat} under any climatic conditions; since, its activity is directly proportional with the production of both ATP and NADPH and these are the vital components to activate most of the enzymes involved in RuBP carboxylation as well as regeneration (Zang et al., 2008). In this study, chlorophyll *a* fluorescence results (discussed more in the following section) clearly demonstrated that improved PS-II efficiency directly correlated with higher A_{Sat} in S13 than in K2 despite the lower C_i . Certain tree species which were grown under elevated CO₂ atmosphere showed reduced photorespiration as evident from the increased AQE with concomitant reduction in LCP (Drake et al., 1997; Bernacchi et al., 2003). Our results from A/Q curves demonstrated that marked rise in AQE and reduced LCP in ES13 compared to EK2 indicates higher Rubisco carboxylation and lower photorespiration.

In the present study, chlorophyll *a* fluorescence analysis emphasized that photosystem-II (PS-II) efficiency differ between the treatments and genotypes. F_v/F_m ($\phi_{Po} = TR_o/ABS$) is the most widely used parameter to understand the PS-II efficiency of plants under any climatic condition, which in turn depends on changes in F_0 and F_m values (Guha et al., 2013). In this study, both ES13 and EK2 showed a decrease in F_0 and an increase in F_m suggesting the efficiency of initial electron donors and final electron acceptors respectively, leading to an increase in F_v/F_m ratio compared to control plants (Mehta et al., 2009). Despite increased F_m values, K2 had lower F_v/F_m than S13 under both elevated and ambient CO_2 atmosphere which was due to higher F_0 values. Greater F_0 value in both AS13 and AK2 indicate an inefficient function of oxygen evolving complex (OEC), which should be associated with inactivation of most of the reaction centers (Strasser, 1997). Higher F_v/F_0 in CO_2 enriched mulberry genotypes (ES13 and EK2) reflects the efficient water splitting complex on the donor side of the PS II resulting in improved photosynthetic electron transport capacity (Kalaji et al., 2011). Significant increase in absorption flux per reaction center (ABS/RC) and cross section (ABS/CS_m) in control S13 and K2 was mostly due to higher chlorophyll content than their respective elevated CO_2 grown plants. Despite an increase in ABS/RC and ABS/CS_m , both AS13 and AK2 showed reduced electron transport capacity per reaction center (ET/RC) and reaction centers per cross section (RC/CS_m), which suggested that most of the reaction centers are inactive. Nevertheless, increased dissipation of the majority of the absorbed light energy in the form of heat was evidenced by an increase in DI/ABS , DI/RC and DI/CS_m (Van Heerden et al., 2003). This infers that most of the absorbed light energy was not used in photochemical reactions; instead it was dissipated in the form of heat energy in order to prevent photo-oxidative damage of the thylakoid membranes as shown by substantial increase in K_n (non photochemical de-excitation constant) in this study (Lin et al., 2009). Considerable increases in TR_o/RC and RC/CS_m could be correlated with the higher ET/TR_o , ET/RC and ET_o/CS_m in both genotypes of mulberry grown under elevated $[CO_2]$, which demonstrates that improved electron transport rate (ETR) is linked with improved overall efficiency of PS-II. This is evident from the greater performance index (PI_{ABS}) of PS-II (Jiang et al., 2009; Rasineni et al., 2011). In the present study,

ES13 showed significant increase in aforementioned parameters than EK2, suggesting that most of the absorbed light energy by ES13 was efficiently used in photochemical quenching (K_p) rather than non photochemical quenching (K_n). Based on our results from chlorophyll a fluorescence JIP-test variables, we believed that PS-II efficiency was much higher in ES13 followed by EK2, AS13 and AK2.

Enhanced photosynthesis under elevated CO_2 atmosphere resulted in higher foliar carbohydrate content, however, most of the assimilated carbon needs to be proportionally exported to potential sinks to avoid end product (especially starch) - associated photosynthetic down regulation (Long et al. 2004). In our study, S13 showed less accumulation of foliar carbohydrates than K2 despite higher A_{Sat} under both elevated as well as ambient $[\text{CO}_2]$, indicating greater carbohydrate mobilization and better sink capacity (Onoda et al., 2009). Increased leaf thickness, due to accumulation of structural and non structural carbohydrates, could be associated with lower SLA in both genotypes grown under elevated CO_2 atmosphere compared to the ambient $[\text{CO}_2]$ counterparts (Sekhar et al., 20014). In addition to above, our results from both non-destructive as well as destructive bio-mass yield showing increased plant height, total number of leaves, leaf size, increased secondary and tertiary branches and dense rooting system in ES13 compared to EK2, could be attributed to their higher sink capacity. Such higher sink capacities could be achieved through continuous mobilization of photosynthates to potential sinks to avoid end-products associated inhibition of photosynthesis. Photosynthetic acclimation is shown to be shown to be associated with reduced accumulation of carbohydrates, which eventually results in superior biomass yields and the same is as shown in the study (Calfapietra et al., 2009; Kumar et al., 2014). These results clearly demonstrated that mulberry showed genotypic variations under anticipated climate changes especially with increased atmospheric $[\text{CO}_2]$ and S13 could be a reasonably suitable genotype for future climate change scenarios in order to mitigate atmospheric $[\text{CO}_2]$ as well as for superior biomass yield. Based on these results, we selected DT S13 genotype for further studies including long term $[\text{CO}_2]$ enrichment as well as drought responses for better understanding of mulberry, a potential bio-energy tree species, under predicted climate change scenarios.

4.2 Short rotation coppice (SRC) mulberry plants exhibited photosynthetic acclimation under long term [CO₂] enrichment

To understand the long term responses, mulberry plants were grown for three years by means of coppice for every 90 days (three months) under elevated [CO₂] environment and these results clearly demonstrated that mulberry plants exhibited reduced photosynthetic performance with increasing [CO₂] exposure time compared to their ambient [CO₂] counterparts. Studies have demonstrated that plants grown under elevated [CO₂] usually stimulates A_{Sat} on an average of 30-60% due to increased Rubisco carboxylation with concomitant reduction in photorespiration (Ainsworth and Long 2005; Ainsworth and Rogers 2007). Similarly, in the present study, SRC mulberry plants grown under elevated [CO₂] exhibited greater A_{Sat} throughout the experimental conditions compared to their ambient controls. However, both elevated and ambient [CO₂] grown plants displayed diminished A_{Sat} after 1095 days (three years) of [CO₂] exposure compared to 365 days (one year), which could be associated with reduced Rubisco activity and/or quantity. Stomatal responses to elevated [CO₂] are highly variable and are mostly dependent on type of species, genotypes, functional groups and environmental conditions (Ainsworth and Rogers 2007). However, many studies have demonstrated that decrease in stomatal conductance (g_s), due to either reduced stomatal density and/or aperture, in high CO₂ environment could be an adaptive mechanism to conserve water to maintain optimum levels of photosynthesis (Long et al., 2004). Our results from SEM studies on topological behavior of stomata indicated that both reduction in stomatal density and stomatal aperture were responsible for lower g_s in SRC mulberry plants grown under [CO₂] enriched environment. In spite of reduced g_s , throughout the experimental period, SRC mulberry plants grown under high [CO₂] environment showed an increase in C_i which could facilitate greater [CO₂] in the vicinity of Rubisco active site leading to increased A_{Sat} compared to their ambient counterparts. Further, reduced g_s was associated with lower E , which in turn was associated with improved WUE_i in elevated [CO₂] grown SRC mulberry plants as observed in our study (Broeckx et al., 2014). However, SRC mulberry plants grown under both elevated as well as ambient [CO₂]

atmosphere showed further reduction in g_s after 1095 days of $[\text{CO}_2]$ exposure compared to 365 days, which might be associated with reduced C_i and A_{Sat} .

In addition to above, many studies have demonstrated that long term growth under elevated $[\text{CO}_2]$ induces photosynthetic acclimation, which is manifested as reduced V_{cmax} , J_{max} and A_{max} (Ainsworth and Long 2004). In consistent with above studies, SRC mulberry plants grown under increased atmospheric $[\text{CO}_2]$ showed reduced V_{cmax} , J_{max} and A_{max} , parameters derived from A/C_i curves, at 365 days after treatment (DAT), which further reduced with the progression of $[\text{CO}_2]$ treatment (at 1095 DAT) compared to ambient $[\text{CO}_2]$ counterparts corroborating the sign of photosynthetic acclimation. Usually, photosynthetic acclimation in $[\text{CO}_2]$ enriched environment is more prevalent under nutrient limiting conditions especially with nitrogen, which induces source to sink imbalance and could be linked to the accumulation of non-structural carbohydrates, especially starch, leading to feedback regulation as well as reduced photosynthetic performance (Sholtis et al., 2004). In the present study, mulberry plants grown under both elevated and ambient $[\text{CO}_2]$ atmosphere showed linear reduction in V_{cmax} , J_{max} and A_{max} with decreasing foliar nitrogen content demonstrating strong positive correlation; however, elevated $[\text{CO}_2]$ grown plants showed greater reduction in V_{cmax} , J_{max} and A_{max} compared to their ambient $[\text{CO}_2]$ counterparts. In addition to above, significant reduction of foliar nitrogen levels in $[\text{CO}_2]$ enriched SRC mulberry plants could be linked with greater accumulation of non-structural carbohydrates (soluble sugars and starch), which due to their reciprocal relationship, promote the sugar signaling associated feedback inhibition, reduced photosynthetic performance (V_{cmax} , J_{max} and A_{max}). Plants grown under $[\text{CO}_2]$ enriched environment showed significant increase in AQE with concomitant reduction in LCP, parameters derived from A/Q curves, compared to their current $[\text{CO}_2]$ grown plants, suggesting reduced photorespiration due to increased Rubisco carboxylation (Drake et al., 1997; Bernacchi et al., 2003). Similarly, in this study, SRC mulberry plants grown under increased atmospheric $[\text{CO}_2]$ showed augmented AQE as well as reduced LCP than their control counterparts, indicating possible reduction in photorespiration. However, both elevated and ambient $[\text{CO}_2]$ grown plants showed reduced AQE with increasing progression of $[\text{CO}_2]$ exposure time (1095 DAT) compared

to the initial stages of experiment (365 DAT), which could be attributed increased photorespiration over carboxylation of Rubisco. This could be the results of reduced Rubisco protein quantity as well as activity due to significant deprivation of foliar nitrogen, which in turn leads to diminished A_{Sat} . Changes in photosystem-II (PS-II) efficiency can proportionally influence the photosynthetic $[\text{CO}_2]$ assimilation rates (A_{Sat}), since the enzymes involved in RuBP carboxylation as well as regeneration requires both ATP and NADPH for their activity (Sekhar et al., 2015 & 2015). Our results from chlorophyll *a* fluorescence measurements using PAM demonstrated that changes in PS-II efficiency and A_{Sat} are positively correlated during the initial period of $[\text{CO}_2]$ exposure (365 DAT), while, upon prolonged $[\text{CO}_2]$ treatment (1095 DAT), significant positive correlation was not observed might be due to further nitrogen dilution. F_v/F_m is the most widely used and reliable diagnostic parameter under any climatic conditions to assess the PS-II efficiency and is known to be influenced by proportionate changes in minimum (F_0) and maximum fluorescence (F_m). In the present study, at 365 DAT, marked rise in F_v/F_m and $\Delta F/F_m'$ in elevated $[\text{CO}_2]$ grown SRC mulberry plants indicated the improved efficiency of PS-II. This could be due to the existence of more number of open PS-II reaction centers, which can facilitate greater light harvesting and energy transduction leading to less photoinhibition compared to ambient $[\text{CO}_2]$ counterparts. However, despite higher total chlorophyll content, ambient $[\text{CO}_2]$ grown plants showed reduced F_v/F_m and $\Delta F/F_m'$ values suggesting that most of the absorbed light energy was not utilized in photochemical quenching, rather dissipated in the form of heat energy. This is evidenced by the significant increase in non-photochemical quenching (NPQ), which further demonstrates the lower sink capacity in ambient $[\text{CO}_2]$ grown plants. On the other hand, plants grown under $[\text{CO}_2]$ enriched environment showed reduced PS-II efficiency at 1095 DAT, which is manifested in the form of lower F_v/F_m with concomitant increase in NPQ compared to control $[\text{CO}_2]$ counterparts. This could be attributed to the reduced sink capacity in these plants due to extensive nitrogen deprivation. In addition to above, many studies have demonstrated that elevated $[\text{CO}_2]$ stimulated plant growth and biomass yield in spite of photosynthetic acclimation. Consistent with above studies, SRC mulberry plants grown under $[\text{CO}_2]$ enriched environment showed increased plant height,

number of leaves, total number of primary as well as auxiliary branches should linked with increased above and below ground bio-mass and carbon sequestration potential compared to control counterparts.

4.3 Elevated [CO₂] ameliorates drought induced negative effects in short rotation coppice (SRC) mulberry even under prolonged dry environments

SRC cultures are gaining greater importance in stabilizing the global climate change by mitigating increased atmospheric [CO₂] proportionally as well as for the production of carbon neutral renewable bio-energy. Many studies have been conducted on SRC cultures to mitigate changing climatic conditions and mostly addressed changes in photosynthetic physiology, biomass yield as well as nutrient relations. However, very little is known about the effects of increased atmospheric [CO₂] and its associated environmental stress factors especially drought on SRC cultures. Our present study describes how DT S13 SRC mulberry cultivar, a potential bio-energy tree, responds to increasing atmospheric [CO₂] and drought individually as well as in their combination with a main focus on changes in photosynthetic physiology and foliar antioxidant systems.

Increased atmospheric [CO₂] significantly influenced the plant morphological, physiological and biochemical characteristics in SRC mulberry under well watered (WW) as well as drought conditions when compared to their respective control plants. Elevated [CO₂] grown mulberry plants were less sensitive to drought stress as indicated by reduced leaf discoloration (chlorosis), wilting, leaf senescence/fall, dehydration (RWC) and higher biomass yields at 30 DAS than their ambient counterparts suggesting that elevated [CO₂] offset the drought induced symptoms in DT S13 cultivar (Hamilton et al., 2008; Darbah et al., 2010; Naudts et al., 2014). Though, increased atmospheric [CO₂] offset drought related symptoms in DT mulberry, genotypic variation might affect the offsetting effects of elevated [CO₂] on drought, and these responses might be differ with a drought sensitive/susceptible (DS) genotype under more severe drought stress conditions. In

addition to above morphological changes, high $[\text{CO}_2]$ grown SRC mulberry plants showed significant increase in A_{Sat} than ambient controls indicating that Rubisco's carboxylation reaction was favored over the oxygenation reaction, facilitating higher $[\text{CO}_2]$ in the vicinity of carboxylation site of Rubisco, which maintains C_i , despite reduced g_s (Ainsworth and Long 2005; Ainsworth and Rogers 2007). Drought showed negative impact in both elevated as well as ambient $[\text{CO}_2]$ grown mulberry plants as manifested reduced A_{Sat} with increasing drought severity, affecting both stomatal and mesophyll conductance (Flexas et al., 2006; Lawlor and Tezara 2009). However, high $[\text{CO}_2]$ grown plants showing better photosynthetic performance (A_{Sat}), through higher C_i , even after 30 days of water withholding demonstrated that elevated $[\text{CO}_2]$ delayed drought induced stress symptoms in SRC mulberry. Our data also showed that $[\text{CO}_2]$ enriched mulberry plants tend to adapt for better water conservation strategy during drier environments via additional reduction in g_s which could be linked with lower transpiration (E) rates leading to substantial increase in WUE_i even after 30DAS. In addition to above, elevated CO_2 grown plants showed significant increase in AQE with concomitant reduction in LCP, parameters derived from A/Q curves, in WW and during WS conditions when compared to their ambient CO_2 counterparts, which further confirms reduced photorespiration (Drake, 1997; Bernacchi et al., 2003). Reciprocal photosynthetic measurements were routinely used in plants grown under elevated CO_2 alone or in combination with one or more abiotic stress factors to check the photosynthetic acclimation and the phenomenon of photosynthetic acclimation, which is known to vary between species, functional groups, genotypes and the type of abiotic stress factors (Darbah et al., 2010). Certain studies showed that elevated CO_2 grown plants showed reduced CO_2 assimilation rates than ambient CO_2 grown plants when measured at common $[\text{CO}_2]$ (Rey and Jarvis 1998), where as others showed that there was no significant difference between elevated and ambient CO_2 grown plants (Darbah et al., 2010) and some studies even showed that elevated CO_2 improved photosynthetic performance when compared to their ambient CO_2 counterparts (Tezara et al., 2002). However, in the present study, reciprocal photosynthetic measurements showed that SRC mulberry plants grown under elevated CO_2 atmosphere showed reduced CO_2 assimilation

rates (P_n) when measured at common $[\text{CO}_2]$ (400 or 550 $\mu\text{mol CO}_2$) compared to ambient CO_2 grown plants under WW and during WS conditions, indicating signs of photosynthetic acclimation. Similarly, there was a significant reduction in g_s in elevated CO_2 grown plants when measured at either 400 or 550 $\mu\text{mol} [\text{CO}_2]$ than control plants under WW and during WS conditions signifying stomatal acclimation. Stomatal acclimation limits mesophyll diffusion of CO_2 due to reduced C_i as well as P_n leading to photosynthetic acclimation (Flexas et al., 2006).

Reduced g_s in CO_2 enriched mulberry plants under both the experimental conditions compared to ambient CO_2 grown plants could be linked with lower E , which results in substantial increase of WUE_i conferring tolerance to longer droughts (Albert et al., 2011b). Changes in PS-II efficiency can proportionally influence the CO_2 assimilation process, since the enzymes involved in RuBP carboxylation and regeneration require both NADPH as well as ATP for their activity (Sreeharsha et al., 2015). Nevertheless, changes in PS-II efficiency in plants grown under elevated CO_2 alone or in combination with drought were highly variable; some studies showed that elevated CO_2 reduces the PS-II efficiency under WW and imposition of WS further exacerbated the negative effects (Kitao et al., 2007; Albert et al., 2011), while others have demonstrated that CO_2 enrichment improved PS-II efficiency and partially ameliorates the negative effects under WW and during WS conditions respectively (Tezara et al., 2002; Li et al., 2008; Zong et al., 2014). In the present study, our results from OJIP chlorophyll a fluorescence measurements demonstrated that elevated CO_2 improved PS-II efficiency under elevated CO_2 conditions and ameliorated the drought-induced photoinhibition even after 30 days of WS in mulberry. F_v/F_m ($\phi_{P_0} = \text{TR}_0/\text{ABS}$) is the most widely used parameter to understand the changes in efficiency of PS-II under different climatic variables and which further depends on changes in F_0 as well as F_m (Sekhar et al., 2014). In this study, elevated CO_2 grown plants under WW conditions showed decrease in F_0 and an increase in F_m , suggesting the efficiency of initial electron donors and final electron acceptors respectively, leading to higher F_v/F_m than ambient control plants (Rasineni et al., 2011). Imposition of WS caused significant reduction of F_v/F_m in both elevated and ambient CO_2 grown mulberry plants; but, the reduction was more in ambient CO_2 grown plants,

which indicate a greater PS-II damage. Our results were consistent with a recent report that showed elevated CO₂ mitigates drought induced photoinhibition as assed by less decrease in Fv/Fm compared to control counterparts (Zintha et al., 2014). Ambient CO₂ grown plants showed significant increase in F₀ under WW conditions, which is further increased during WS conditions when compared to elevated CO₂ counterparts. This might be due to either increased number of inactive RCs leading to slow reduction of primary quinone (Q_A) and/or structural damage leading to less excitation transfer from antenna complex to RCs (Kalaji et al., 2011). In addition to above, double normalization between phase O and K (V_{OK}, 50-300μs) was used to identify the prominent L-band; wherein a positive L-band indicates the less stable connections between PS-II and LHC indicating impairment in excitation energy transfer due to changes in the structural organization of the thylakoid membranes (Guha et al., 2013; Sengupta et al., 2013). In the present study, irrespective of the CO₂ treatment, appearance of positive L-band in SRC mulberry after 30 days of WS indicated that drought negatively affects PS-II efficiency. Similarly, appearance of an accentuated K-band, after 30 days of drought stress, is an indication of reduced efficiency of oxygen evolving complex (OEC) in both elevated and ambient CO₂ grown plants leading to an impairment in electron flow between OEC to RCs as well as towards the electron acceptors of PS-II (Guha et al., 2013). However, certain studies demonstrated that elevated atmospheric temperature can also induce the appearance of K-band (Van Heerden et al., 2007) and drought can even protect OEC against heat-induced damage (Lu et al., 1999). In consistent with above, observation of prominent K- band in both ambient and elevated CO₂ grown mulberry after 30 days of water withholding will indicate indicated that these plants are experiencing higher atmospheric temperatures as the experiments were conducted during severe summer season having midday temperatures of 42°C-46°C. But, in the present study, less prominent L and K bands are observed in plants grown under elevated CO₂ atmosphere compared to control counterparts, which demonstrate that CO₂ fertilization ameliorates both drought as well as heat stress effects towards PS-II damage. Drought significantly increased V_J at 30DAS compared to their respective WW counterparts, which might be associated with the accumulation of the reduced QA pool restricting electron transport

beyond QA (Redillas et al., 2011). In addition to above, significant increase in F_v/F_0 in elevated CO_2 grown plants under WW as well as WS conditions than their controls, reflect the greater efficiency of water splitting complex on the donor side of the PS-II and the rate of photosynthetic quantum conversion at PS-II reaction center (Kalaji et al., 2011). Further, irrespective of the CO_2 treatment, drought imposition induce marked reduction in parameters which reflects the photochemical quenching capacity including ET/RC , ET/TR_0 , RC/CS_m , TR_0/CS_m , ET_0/CS_m , K_P , PI_{ABS} and PI_{csm} with concomitant increase in non-photochemical quenching parameters including DI/ABS , DI/RC , DI/CS_m and K_n compared to WW plants, inferring that drought negatively affects the PS-II efficiency in mulberry (Van Heerden et al., 2007; Guha et al., 2013; Sekhar et al., 2015). Nevertheless, elevated CO_2 grown SRC mulberry showed less decrease in afore mentioned parameters even at 30DAS indicating that CO_2 enriched plants showed better PS-II efficiency.

Effects of elevated $[\text{CO}_2]$ on changes of antioxidant systems in plant tissues depend on plant species, crop variety, developmental stage as well as different abiotic stress factors (Xu et al., 2015). Different studies reported that elevated $[\text{CO}_2]$, under well watered conditions, enhances (Farfan-Vignolo and Asard, 2012; Mishra and Agrawal 2014), decrease (Gillespie et al., 2011), and/or causes no change (Zinta et al., 2014) in the enzyme activities along with corresponding gene expression levels of ROS scavenging enzymes. In this study, under WW conditions, DT mulberry plants grown under high $[\text{CO}_2]$ environment had lower transcript levels and activities of ROS scavenging enzymes providing an evidence that there was a less oxidative load due to higher carboxylation of Rubisco and reduced photorespiration (AbdElgawad et al., 2015). Drought stress, irrespective of $[\text{CO}_2]$ treatment, induced significant increase in transcript levels and enzyme activities of antioxidant systems compared to their respective WW controls in mulberry showing an evidence that ROS signaling mechanisms are activated to protect the plants from oxidative stress (Gill and Tuteja 2010). However, certain studies showed that, elevated $[\text{CO}_2]$ protect plants from oxidative stress and stress mitigation potential under elevated $[\text{CO}_2]$ might originate from either decreased ROS production and/or by increasing the ROS scavenging capacities by increasing antioxidant gene expression

(AbdElgawad et al., 2015). In the present study, mulberry plants grown under CO₂ enriched environment showed both mechanisms including less production of ROS and better antioxidant systems to combat the drought induced oxidative stress. SRC mulberry plants grown under elevated [CO₂] atmosphere showed lower transcript levels as well as activities of ROS scavenging enzymes like SOD, Catalase, GPX, and the enzymes of ascorbate- glutathione cycle (ASC-GSH) including APX, GR, MDHAR during the initial stages of drought (15DAS), suggesting that plants grown under control conditions were primed to respond more quickly to the oxidative stress. Our results are consistent with a recent report which showed excessive gene transcriptional responses related to antioxidant metabolism due to abiotic stress were partly repressed by elevated [CO₂] (Gillespie et al., 2012). In contrast to above, certain studies showed that there were no changes in the activities of antioxidant enzymes except the inhibition of APX (Kumari et al., 2013), reduced SOD, GPX, CAT, GR levels with no effect on other enzymes of ASC-GSH cycle (Li et al., 2014; AbdElgawad et al., 2015), while some reports even showed reduced ASC-GSH cycle associated enzymes with little effect on SOD, GPX and Catalase enzymes (Zinta et al., 2014) during abiotic stress under elevated [CO₂] conditions. These results clearly demonstrated that changes in ROS scavenging enzymes during stressful environmental conditions under elevated [CO₂] differs among various species, type of abiotic stress factor and duration of stress. Nevertheless, in the present study, ambient [CO₂] grown mulberry plants showed down regulation of the protective systems manifested as reduced activities and transcript levels of ROS scavenging enzymes with increasing drought (30 DAS) indicated that these plants are not able to tolerate longer drought periods. Unlike ambient [CO₂] grown plants, high [CO₂] grown plants maintained higher transcript levels and activities of antioxidant enzymes after 30 days of drought (30DAS) showing an effective incessant ROS detoxification to sustain their photosynthetic performance under prolonged drought conditions. Abiotic stress is also known to induce accumulation of proline, a major stress induced osmolyte, and its concentration was directly proportional with stress severity (Reddy et al., 2004). In this study, plants grown under elevated [CO₂] showed lower accumulation of proline even

after 30 DAS compared to ambient [CO₂] grown plants was suggesting that CO₂ enriched plants perceived less oxidative stress.

In addition to above changes, plants grown under elevated [CO₂] triggered greater accumulation of antioxidant compounds like ASA and polyphenols resulting in improved ROS detoxification (Smirnoff and Wheeler 2000; Zvereva and Kozlov 2006; Ghasemzadeh et al., 2010). Nevertheless, changes in antioxidant enzyme activities (ASA-GSH cycle) and ASA levels in mulberry under WW and drought are less correlated. Reduced H₂O₂ as well as MDA levels in elevated [CO₂] grown plants under well watered (WW) as well as during drought conditions, inferred that elevated [CO₂] ameliorate the drought induced ROS accumulation and lipid peroxidation (Salazar-Parra et al., 2012; Xu et al., 2014; Abdelgawad et al., 2015). Moreover, delayed senescence and/or severe stress symptoms (discoloration, wilting and dehydration) in [CO₂] enriched mulberry plants even at 30DAS may possibly be associated with improved antioxidant enzyme activities and greater accumulation of antioxidant compounds (ASA and TPC). In conclusion, our data demonstrate that elevated [CO₂] delayed the onset of drought related stress symptoms in SRC mulberry under prolonged drought treatment (30DAS). Such tree plantations including mulberry are best suitable for SRC forestry based mitigation of increased [CO₂] levels under intermittent prolonged drought conditions, which are projected to prevail in fast changing global climate.

4.4 SRC mulberry exhibited better photosynthetic performance and delayed drought- related symptoms even under prolonged drought conditions due to better hydraulic conductance

In addition to above changes, elevated [CO₂] significantly altered plant hydraulic dynamics under both WW as well as WS conditions with respect to their ambient [CO₂] counterparts. Altered plant water status during WS induces hydraulic signals, which are communicated from root to leaves via xylem, and induce several physiological, biochemical and molecular responses at both roots as well as shoot levels (Sengupta et al., 2013). In the present study, irrespective of the [CO₂] treatment, WS significantly reduced plant leaf water status by causing a gradual decrease in Ψ_{pd} , Ψ_{md} , and RWC when

compared to WW, with increasing progression of stress treatment. However, ambient [CO₂] grown plants showed greater reduction in aforementioned parameters at 30 DAS, suggesting higher level of leaf tissue dehydration; in other words, elevated [CO₂] grown plants were adapted to follow a better water saving strategy, which in turn is linked with maintenance of photosynthesis even at 30 DAS. Further, imposition of WS induce negative effects in SRC mulberry plants, irrespective of the [CO₂] treatment, by closing their stomata as a first level defense mechanism to prevent evapotranspiration, which results in limitations in mesophyll conductance (g_m) as well as photosynthetic performance (A_{Sat}). Reduced A_{Sat} during WS leads to diminished synthesis as well as an increase in depletion of stored carbon reserves, which induces carbon starvation leading to plant mortality (Medrano et al., 2002, Gomes et al., 2008, Sala et al., 2010). However, in the present study, mulberry plants grown under [CO₂] enriched environment displayed increased A_{Sat} in spite of reduced g_s , which could be due to the higher C_i levels, even at 30 DAS. Such maintenance of A_{Sat} could be associated with improved carbohydrate synthesis and less carbon starvation in these plants compared to ambient [CO₂] counterparts. Lower g_s is usually linked with reduced E during WS, which results in substantial increase of WUE_i (A_{Sat}/E) and WUE_i proportionally related to drought tolerance capacity. In our study, SRC mulberry plants grown under high [CO₂] exhibited significantly higher WUE_i even under extended drought environment due to both reduced E as well as improved A_{Sat} which might be the reason for showing better tolerance against prolonged drought treatments.

Water movement in plants is known to be regulated by variations in hydraulic conductance through soil-root-shoot-leaf, which in turn determines the leaf turgor status (Ψ_{pd} , Ψ_{md} , and RWC) and photosynthetic performance (Costa et al., 2004). In the present study, WS induced significant reduction in hydraulic conductivity parameters including F , Ψ_x , K_s and K_L , which indicates the conflicts of water movement from soil to leaf to atmosphere in SRC mulberry plants grown under both elevated and ambient [CO₂] atmosphere when compared to their control WW plants. Nevertheless, [CO₂] enriched mulberry plants showed comparatively lesser reduction in F , Ψ_x , K_s and K_L their ambient [CO₂] counterparts even at 30 DAS. This suggests that high [CO₂] grown plants exhibited

greater hydraulic safety, which could possibly be associated with maintenance of better photosynthetic performance under extended drought conditions. Certain studies have demonstrated that variations in water transport under WS environments in stem and leaf are inversely related to the formation of xylem embolism and reduced hydraulic conductivity parameters including F , Ψ_X , K_S and K_L during drought environments, the result of greater xylem embolism or vice versa (Nolfet al., 2015). In this study, we have observed significant decrease in F , Ψ_X , K_S and K_L at 30 DAS in SRC mulberry plants grown under ambient $[CO_2]$, which indicates that these plants are possibly more vulnerable to xylem embolism leading to early hydraulic failure as well as plant mortality under prolonged water deficit environments (30 DAS).

Furthermore, stomatal closure as well as hydraulic failure were highly variable in plants under WS environment; in some instances, early stomatal closure facilitate pre-empting the drought induced xylem cavitation and hence prevents plant mortality under prolonged dry environments (Cochard et al., 2002, Brodribb and Holbrook 2003, Chen et al., 2010). In contrast to above, some studies have demonstrated that plant mortality during extended drought environments was more pronounce due to early stomatal closure and hydraulic failure (Brodribb and Holbrook 2003, Nardini et al., 2003). However, in the present study, mulberry plants grown under $[CO_2]$ enriched environment showed reduced g_s as well as E , leading to better water conservation as well as greater hydraulic safety as demonstrated by the increased F , Ψ_X , K_S and K_L at 30 DAS with respect to their control counterparts. In addition to above, better water relations (improved F , Ψ_X , K_S and K_L) observed in $[CO_2]$ enriched SRC mulberry plants even under extended drought environments could be due to better rooting volume (Guha et al., 2010a).

Many studies have demonstrated that variations in expression profiles of AQPs can affect the plant hydraulic dynamics, photosynthetic performance and plant survivability under different abiotic stress factors (Fetter et al., 2004; Galmes et al., 2007, Benabdellah et al., 2009). In the present study, elevated $[CO_2]$ significantly influenced the expression profiles (both up and down regulation), of AQPs under WW as well as during WS conditions corroborating their potential roles in plant survivability under future climatic conditions. Studies have demonstrated that reduced expression levels of

PIP1 induces mesophyll conductance limitations (g_m) to CO_2 in tobacco, which in turn was linked with diminished photosynthetic performance compared to their wild types (Flexas et al., 2006) and studies also demonstrated that increased expression of PIP1 in *Arabidopsis* stimulated photosynthetic performance even under unfavorable conditions (Aharon et al., 2003). In contrast to above, over expression of PIP2 in *Arabidopsis* did not show any effect on g_m (Tournaire-Roux et al., 2003); but, it improved water permeability in *xenopus oocytes* (Biela et al., 1999). Further, coexpression of PIP1 and PIP2 enhanced the water permeability many folds in *xenopus oocytes* compared to individual PIP2 expression supports the notion of cooperative effects (Fetter et al., 2004; Zelazny et al., 2007). In the present study, SRC mulberry plants grown under elevated $[CO_2]$ showed reduced PIP 1.1 under WW as well as WS conditions could be possibly associated with increased limitations in mesophyll conductance (g_m) and photosynthetic acclimation. Unlike PIP1, drought imposition significantly increased expression levels PIP2 isoforms, except PIP2.1, including PIP2.2 and PIP2.7 in $[CO_2]$ enriched mulberry plants causing improved transcellular water permeability and hydraulic conductivity. Consistent with PIPs, increased expression levels of TIPs, another group of MIPs, confer resistance to different abiotic stress factors (Wang et al., 2013). Studies with increased expression levels TIP1 in *Arabidopsis* showed significant increase in tolerance to WS by minimizing transpirational water loss compared to their wild types (Martinez-Ballesta and Carvajal 2014). Further, over expression of TIP2 controls the transpiration rates under different stress conditions in *Solanum lycopersicum* resulting in better CO_2 uptake and better water as well as nutrient use efficiency (Martinez-Ballesta and Carvajal 2014). But, under certain circumstances, improved expression levels of some AQPs aggravate the stress symptoms leading to plant mortality implicating various roles of AQPs in plant community against different abiotic stress factors (Afzal et al., 2016). However, SRC mulberry plants grown under increased atmospheric $[CO_2]$ showed increased abundance of TIP 1 (TIP1.1) and TIP 2 (TIP 2.1 and TIP 2.3) compared to their ambient counterparts even at 30 DAS demonstrates their key roles in water conservation and CO_2 uptake.

Chapter 5

Summary and Conclusions

Mulberry showed significant genotypic variations in terms of photosynthetic performance and bio-mass yielding capacity under elevated $[\text{CO}_2]$ environment ($550 \mu\text{mol mol}^{-1}$). Genotypes including the drought tolerant (DT) Selection-13 (S13) and the drought susceptible (DS) Kanva-2 (K2) showed positive responses towards increased atmospheric $[\text{CO}_2]$ when compared to their ambient $[\text{CO}_2]$ counterparts ($400 \mu\text{mol mol}^{-1}$). However, S13 genotype showed comparatively better response towards increased atmospheric $[\text{CO}_2]$ than K2 genotype. There was a significant increase in light saturated photosynthetic rates (A_{Sat}) and apparent quantum efficiency (AQE) in elevated $[\text{CO}_2]$ grown S13 (ES13) plants, indicating higher Rubisco carboxylation efficiency compared to K2. Improved water use efficiency (WUE_i) in ES13 was due to reduced stomatal conductance (g_s) and transpiration rates (E).

Elevated CO_2 significantly increased chlorophyll *a* fluorescence characteristics including maximum quantum yield of primary photochemistry (F_v/F_m) and performance index (PI_{ABS}) suggesting improved photosystem-II efficiency in both genotypes compared to the ambient $[\text{CO}_2]$ grown. In spite of superior photosynthetic performance observed in ES13, accumulation of soluble and insoluble sugars (starch) were significantly low compared to elevated $[\text{CO}_2]$ grown K2 (EK2), demonstrating higher sink capacity in ES13 and better bio-mass yields. Thus, S13 could be a potential genotype for mulberry- based short rotation coppice (SRC) forestry to mitigate increasing atmospheric $[\text{CO}_2]$ as well as for the production of carbon neutral renewable bio-energy.

Mulberry plants grown for 3years under elevated $[\text{CO}_2]$ showed reduced photosynthetic performance compared to their ambient $[\text{CO}_2]$ grown plants indicating the sign of photosynthetic acclimation and once again emphasizing the role of long-term Vs short term $[\text{CO}_2]$ enrichment studies. SRC mulberry plants grown under high $[\text{CO}_2]$ showed significant increase in light saturated photosynthetic rates (A_{Sat}), intercellular $[\text{CO}_2]$ (C_i), instant water use efficiency (WUE_i), apparent quantum efficiency (AQE) throughout the experimental period when compared to the ambient $[\text{CO}_2]$ grown plants. In contrast to above, high $[\text{CO}_2]$ grown plants showed reduction in stomatal conductance (g_s) and transpiration rates (E). Further, plants grown under $[\text{CO}_2]$ enriched environment

showed reduced *in vivo* maximum Rubisco carboxylation (V_{cmax}), maximum electron transport rate (J_{max}) and light and CO_2 saturated photosynthetic rates (A_{max}) compared to their ambient $[\text{CO}_2]$ grown plants indicating the occurrence of photosynthetic acclimation. We also observed significant foliar nitrogen dilution, leading to accumulation of foliar carbohydrates (due to their reciprocal relationship), which induced sugar signaling associated photosynthetic acclimation. Despite photosynthetic acclimation, plants grown under elevated $[\text{CO}_2]$ atmosphere displayed greater above and below ground bio-mass when compared to their control counterparts due to their growth $[\text{CO}_2]$. Increased bio-mass yields could be due to the higher carbon sequestration potential in elevated $[\text{CO}_2]$ grown mulberry plants. Our results clearly demonstrated that alterations in coppice management practices i.e reduced coppice duration is the best strategy to mitigate increased atmospheric $[\text{CO}_2]$ and generate CO_2 neutral renewable bio-energy.

Our results from interactive studies ($\text{CO}_2 \times$ drought) demonstrated that elevated $[\text{CO}_2]$ is able to ameliorate drought induced negative responses in short rotation coppice (SRC) mulberry, a potential bio-energy tree, when compared to the ambient $[\text{CO}_2]$ counterparts. Growth in $[\text{CO}_2]$ enriched environment stimulated photosynthetic performance in well watered (WW) as well as during water stress (WS) with significant increases in light saturated photosynthetic rates (A_{Sat}), water use efficiency (WUE_i), intercellular $[\text{CO}_2]$, and photosystem–II efficiency (F_v/F_M and $\Delta F/F_M'$) with concomitant reduction in stomatal conductance (g_s) and transpiration (E) compared to ambient CO_2 (A) grown plants. Reduced levels of proline, H_2O_2 and malondialdehyde (MDA) and higher contents of antioxidants including ascorbic acid and total phenolics in WW and WS in $[\text{CO}_2]$ enriched plants clearly demonstrated lesser oxidative damage. Further, ambient $[\text{CO}_2]$ grown plants showed higher transcript abundance and antioxidative enzyme activities under WW as well as during initial stages of WS (15 days). However, with increasing drought imposition (30 days), ambient $[\text{CO}_2]$ grown plants showed down regulation of antioxidant systems compared to their respective elevated $[\text{CO}_2]$ grown plants.

In addition to above, elevated $[\text{CO}_2]$ grown mulberry plants showed significant reduction in net photosynthetic rates (P_n), stomatal conductance (g_s), transpiration rates and intercellular $[\text{CO}_2]$ when measured at common $[\text{CO}_2]$ (400 or 550 μmol) in all the experimental conditions, which indicated the occurrence of photosynthetic acclimation. Elevated $[\text{CO}_2]$ plants showed substantial increase in instant water use efficiency (WUE_i) despite reduced P_n after 30 days of WS, which suggests that these plants are well adapted for water conservation. Analysis of OJIP chl *a* fluorescence kinetics revealed that WS negatively affects the photosystem-II (PS-II) performance in both elevated as well as ambient $[\text{CO}_2]$ grown plants, as evident from the prominent L and K bands. However, greater amplitude of positive K and L bands in ambient $[\text{CO}_2]$ grown plants indicates less energy connectivity among PS-II units and inefficient electron flux movement from oxygen evolving complex (OEC) towards PS-II acceptor side in these plants. Further, significant increase in parameters including F_v/F_m , ET/CSm and $\text{PI}_{(\text{ABS})}$ with concomitant reduction of DI_0/RC and DI_0/CSm in $[\text{CO}_2]$ enriched plants under WW as well as during WS demonstrated more photochemical quenching.

Delayed drought related symptoms in SRC mulberry grown under elevated $[\text{CO}_2]$ conditions even under prolonged drought conditions were mostly due to less constrains in water movement when compared to ambient $[\text{CO}_2]$ counterparts. Hydraulic conductance quantifies the efficiency of water transport in plants from soil to atmosphere via root-shoots-leaves. We observed significant reduction in hydraulic conductivity characteristics including sap flow rate (F) and hydraulic conductance in stem (K_s) as well as leaf (K_L) during WS in both elevated and ambient $[\text{CO}_2]$ grown mulberry plants compared to their WW counterparts. However, $[\text{CO}_2]$ enriched plants maintained increased F , K_s and K_L when compared to the ambient $[\text{CO}_2]$ grown plants even at 30 DAS attributed to the better hydraulic safety should linked with less vulnerable to embolism. Further, we also observed strong positive correlation in both elevated and ambient $[\text{CO}_2]$ grown mulberry plants between photosynthetic leaf gas exchange parameters (A_{sat} , g_s and E) and hydraulic characteristics (F , K_s and K_L). But, WUE_i was negatively correlated with F , K_s and K_L . Better hydraulic conductivity in mulberry plants grown under elevated $[\text{CO}_2]$ even under extended drought environment (30 DAS) was possibly due to higher

expression of certain aquaporins including PIPs and TIPs compared to their ambient [CO₂] counterparts. Our data provide evidence that under future increased atmospheric CO₂ conditions, SRC mulberry would be able to sustain enhanced photosynthetic potential and also mitigate the drought induced oxidative stress. Our results in this study also demonstrates that mulberry is a potential bio-energy tree crop, which is best suitable for SRC forestry-based mitigation of increased [CO₂] levels even under intermittent drought conditions, which are projected to prevail in the fast changing global climate.

Chapter 6

Literature Cited

Publications

- AbdElgawad H, Farfan-ignolo ER, De Vos D, Asard H** (2015) Elevated CO₂ mitigates drought and temperature-induced oxidative stress differently in grasses and legumes. *Plant Sci* 231:1-10
- Aebi H** (1984) Catalase in vitro. *Methods Enzymol* 105:121-126
- Afzal Z, Howton TC, Sun Y, Shahid Mukhtar M** (2016) The Roles of Aquaporins in Plant Stress Responses. *J. Dev. Biol* 4(1): 9.
- Aharon R, Shahak Y, Wininger S, Bendov R, Kapulnik Y, Galili G** (2003) Over expression of plasma membrane aquaporin in transgenic tobacco improves plant vigor under favorable conditions but not under drought or salt stress. *Plant Cell* 15: 439-484.
- Ainsworth EA, Long S** (2005) What have we learned from 15 years of free-air CO₂ enrichment (FACE)? A meta-analytic review of the responses of photosynthesis, canopy properties and plant production to rising CO₂. *New Phytol.* 165:351–372
- Ainsworth EA, Rogers A** (2007) The response of photosynthesis and stomatal conductance to rising [CO₂]: mechanisms and environmental interactions. *Plant Cell Environ.* 30:258–270
- Albert KR, Mikkelsen TN, Michelsen A, Ro-Poulsen H, Van der Linden L** (2011) Interactive effects of drought, elevated CO₂ and warming on photosynthetic capacity and photosystem performance in temperate heath plants. *J Plant Physiol.* 168:1550–1561
- Albert KR, Ro-Poulsen H, Mikkelsen TN, Michelsen1 A, Van der Linden L, Beier C** (2011) Interactive effects of elevated CO₂, warming, and drought on photosynthesis of *Deschampsia flexuosa* in a temperate heath ecosystem. *J Exp. Bot.* 62:4253-4266
- Alexandersson E, Frayse L, Sjoval-Larsen S, Sofia G, Fellert M, Kaelsson M, et al.** (2005) Whole gene family expression and drought stress regulation of aquaporins. *Plant Mol. Biol.* 59: 469-484.
- Arnon DI** (1949) Copper enzymes in isolated chloroplasts. polyphenol oxidase in *Beta vulgaris*. *Plant Physiol.* 24: 1-15
- Aronsson P, Perttu K** (2001) Willow vegetation filters for wastewater treatment and soil remediation combined with biomass production. *Forestry Chronicle* 77: 293–299
- Bates LS, Walderen RP, Teare ID** (1973) Rapid determination of free proline for water stress studies. *Plant Soil* 39:205-207

- Benabdellah L, Ruiz-Lozano JM, Aroca R** (2009) Hydrogen peroxide effects on root hydraulic properties and plasma membrane regulation in *Phaseolus vulgaris*. *Plant Mol. Biol.* 70: 647-661
- Bernacchi CJ, Calfapietra C, Davey PA, Wittig VE, Scarascia-Mugnozza GE, Raines CA, Long SP** (2003) Photosynthesis and stomatal conductance responses of poplars to free-air CO₂ enrichment (PopFACE) during the first growing cycle and immediately following coppice. *New Phytol.* 159: 609–621
- Biela A, Grote K, Otto B, Hoth S, Hedrich R, Kaldenhoff R** (1999) The *Nicotiana tabacum* plasma membrane aquaporin NtAQP1 is mercury-insensitive and permeable for glycerol. *Plant J.* 18: 565–570
- Bradford MM** (1976) A Rapid and Sensitive Method for the Quantitation of Microgram Quantities of Protein Utilizing the Principle of Protein-Dye Binding. *Anal. Biochem.* 72: 248-254
- Brodersen CR, McElrone AJ, Choat B, Shackel KA, Matthews MA** (2013) In vivo visualization of drought-induced embolism spread in *Vitis vinifera*. *Plant Physiol.* 162: 1-10.
- Brodrribb TJ, Holbrook NM** (2003) Stomatal closure during leaf dehydration correlation with other leaf physiological traits. *Plant Physiol.* 132: 2166-2173
- Brodrribb TJ, Cochard H** (2009) Hydraulic failure defines the recovery and point of death in water stressed *Conifers*. *Plant Physiol.* 149: 575-584
- Broeckx LS, Fichot R, Verlinden MS, Ceulemans R** (2014) Seasonal variations in photosynthesis, intrinsic water-use efficiency and stable isotope composition of poplar leaves in a short-rotation plantation. *Tree Physiol.* 34: 701–715
- Calfapietra C, Gielen B, Karnosky D, Ceulemans R, Scarascia Mugnozza G** (2010) Response and potential of agroforestry crops under global change, *Environ. Pollut.* 158: 1095-1104
- Ceulemans R, Deraedt W** (1999) Production physiology and growth potential of poplar under short-rotation forestry culture. *Forest Ecology and Management* 121: 9–24
- Chaitanya KV, Jutur PP, Sundar D, Reddy AR** (2003) Water stress effects on photosynthesis in different mulberry cultivars. *Plant Growth Regul.* 40: 75-80
- Chen WJ, Zhang Q, Li SX, Cao FK** (2010) Gas exchange and hydraulics in seedlings of *Hevea Brasiliensis* during water stress and recovery. *Tree Physiology* 30: 876-885

- Cochard H, Coll L, Le Roux X, Améglio T** (2002) Unraveling the effects of plant hydraulics on stomatal closure during water stress in walnut. *Plant Physiol.* 128: 282–290
- Costa ESF, Shvaleva A, Maroco PJ, Almeida HM, Chaves MM, Pereira SJ** (2004) Responses to water stress in two *Eucalyptus globulus* clones differing in drought tolerance. *Tree Physiol.* 24: 1165-1172.
- Dandin SB, Jayaswal J, Giridhar K** (2003) Handbook of sericulture technologies, Central Silk Board, Bangalore, India. pp. 35–55
- Dang QL, Maepea JM, Parker WH** (2008) Genetic variation of ecophysiological responses to CO₂ in *Picea glauca* Seedlings. *The Open Forest Sci. J.* 1: 68-79
- Darbah JN, Sharkey TD, Calfapietra C, Karnosky DF** (2010) Differential response of aspen and birch trees to heat stress under elevated carbon dioxide. *Environ Pollut.* 158:1008–1014
- Darbah JNT, Kubiske ME, Nelson N, Kets K, Riikonen J, Sober A, Rouse L, Karnosky DF** (2010) Will photosynthetic capacity of aspen trees acclimate after long-term exposure to elevated CO₂ and O₃? *Environ. Pollut.* 158: 983-991
- Dhindsa RS, Plumb-Dhindsa P, Thorpe TA** (1981) Leaf senescence: correlated with increased levels of membrane permeability and lipid peroxidation, decreased levels of superoxide dismutase and catalase. *J. Exp. Bot.* 32:93-101
- Dixon M, Downey A** (2013) PSY1 Stem Psychrometer manual. Available: <http://www.ictinternational.com/content/uploads/2014/05/PSY1-stem-psychrometer-manual-ver.-4.4.pdf>
- Domec JC, Schäfer K, Oren R, Kim HS, McCarthy HR** (2010) Variable conductivity and embolism in roots and branches of four contrasting tree species and their impacts on whole-plant hydraulic performance under future atmospheric CO₂ concentration. *Tree Physiol.* 30: 1001–1015
- Drake BG, Miquel AGM, Long SP** (1997) More efficient plants: A consequence of rising atmospheric CO₂? *Annu .Rev. Plant Physiol.* 48: 609–639
- Duan H, Duursma RA, Huang G, Smith RA, Choat B, O'Grady AP, Tissue DT.** (2014) Elevated [CO₂] does not ameliorate the negative effects of elevated temperature on drought-induced mortality in *Eucalyptus radiata* seedlings. *Plant Cell Environ.* 37:1598–1613

- Dyson T** (2005) On development, demography and climate change: The end of the world as we know it? *Population and Environ.* 27: 117-149
- Ellsworth DS, Reich PB, Naumburg ES, Koch GW, Kubiske ME, Smith SD** (2004) Photosynthesis, carboxylation and leaf nitrogen responses of 16 species to elevated pCO₂ across four free-air CO₂ enrichment experiments in forest, grassland and desert. *Glob Change Biol* 10:2121–2138
- Farfan-Vignolo ER, Asard H** (2012) Effect of elevated CO₂ and temperature on the oxidative stress response to drought in *Lolium perenne* L. and *Medicago sativa* L. *Plant Physiol Biochem.* 59:55-62
- Fetter K, Van Wilder V, Moshelion M, Chaumont F** (2004) Interactions between plasma membrane aquaporins modulate their water channel activity. *The Plant Cell Online* 16: 215-228
- Flexas J, Bota J, Galmes J, Medrano H, Ribas-Carbo M** (2006) Keeping a positive carbon balance under adverse conditions: responses of photosynthesis and respiration to water stress. *Physiol. Plant.* 127:343–52
- Franks PJ, Adams MA, Amthor JS, Barbour MM et al.,** (2013) Sensitivity of plants to changing atmospheric CO₂ concentration: from the geological past to the next century. *New Phytol.* 197: 1077-1094
- Fu J, Huang B** (2001) Involvement of anti-oxidant and lipid peroxidation in the adaptation of two cool season grasses to localized drought stress. *Environ. Exp. Bot.* 45:105-114
- Galmes J, Medrano H, Flexas J** (2007) Photosynthetic limitations in response to water stress and recovery in Mediterranean plants with different growth forms. *New Phytol.* 175: 81–93
- Ghasemzadeh A, Jaafar HZE, Rahmat A** (2010) Elevated carbon dioxide increases contents of flavonoids and phenolic compounds and antioxidant activities in Malaysian young ginger (*Zingiber officinale* Roscoe.) varieties. *Molecules* 15:7907–7922
- Gill SS, Tuteja N** (2010) Reactive oxygen species and antioxidant machinery in abiotic stress tolerance in crop plants. *Plant Physiol. Biochem.* 48:909-930
- Gillespie KM, Rogers A, Ainsworth EA** (2011) Growth at elevated ozone or elevated carbon dioxide concentration alters antioxidant capacity and response to acute oxidative stress in soybean (*Glycine max*). *J. Exp. Bot.* 62:2667-2678

- Gillespie KM, Xu F, Richter KT, McGrath JM, Markelz RC, Ort DR, Leahey, Ainsworth EA** (2012) Greater antioxidant and respiratory metabolism in field grown soybean exposed to elevated O₃ under both ambient and elevated CO₂. *Plant Cell Environ.* 35:169–184
- Gomes FP, Oliva MA, Mielke MS, De Almeida A-AF, Leite HG, Aquino LA** (2008) Photosynthetic limitations in leaves of young Brazilian green dwarf coconut (*Cocos nucifera* L. *nana*) palm under well-watered conditions or recovering from drought stress. *Environ. Exp. Bot.* 62: 195-204
- Goor F, Jossart JM, Ledent JF** (2000) ECOP: an economic model to assess the willow short rotation coppice global profitability in a case of small scale gasification pathway in Belgium. *Environ. Model. & Software* 15: 279–292
- Griffith OW, Meister A** (1979) Potent and specific inhibition of glutathione synthesis by buthionine sulfoximine (s-n-butyl homocysteine sulfoximine). *J. Biol. Chem.* 254:7558–7560
- Guha A, Rasineni GK, Reddy AR** (2010) Drought tolerance in mulberry (*Morus* spp.): A physiological approach with insights to growth dynamics and leaf yield production. *Exp. Agric.* 46: 471-488
- Guha A, Sengupta D, Reddy AR** (2013) Polyphasic chlorophyll *a* fluorescence kinetics and leaf protein analyses to track dynamics of photosynthetic performance in mulberry during progressive drought. *J. Photoch. Photobiol. B: Biol.* 119: 71-83
- Guha A, Reddy AR** (2012) Leaf functional traits and stem wood characteristics influencing biomass productivity of mulberry (*Morus* spp. L) genotypes grown in short-rotation coppice system. *Bioenerg Res.* 6:547–563
- Guha A, Reddy AR** (2013) Leaf functional traits and stem wood characteristics influencing biomass productivity of mulberry (*Morus spp.* L) genotypes grown in short-rotation coppice system. *Bioenergy Res.* 6: 547-563
- Guha A, Sengupta D, Reddy AR** (2010) Physiological optimality, allocation trade-offs and antioxidant protection linked to better leaf yield performance in drought exposed mulberry. *J Sci. Food Agr.* 90: 2649-2659
- Hamilton EW, Heckathorn SA, Joshi P, Wang D, Barua D** (2008) Interactive effects of elevated CO₂ and growth temperature on the tolerance of photosynthesis to acute heat stress in C3 and C4 species. *J. Integr. Plant Biol.* 50: 1375–1387

- He N, Zhang C, Qi X, Zhao S, Tao Y, Yang G et al.,** (2013) Draft genome sequence of the mulberry tree *Morus notabilis*. *Nat. Commun.* 4: 2445
- Heilman PE, Ekuan G, Fogle D** (1994) Above- and below-ground biomass and fine roots of 4-year-old hybrids of *Populus trichocarpa* *Populus deltoides* and parental species in short rotation culture. *Can. J. Forest Res.* 24: 1186–1192
- Hu WJ, Yuan Q, Wang Y, Cai R, Deng X, Wang J, Zhou S, et al.,** (2012) Overexpression of a wheat aquaporin gene, *TaAQP8*, enhances salt stress tolerance in transgenic tobacco. *Plant Cell Physiol.* 53: 2127–2141
- Hubbard RM, Ryan MG, Stiller V, Sperry JS** (2001) Stomatal conductance and photosynthesis vary linearly with plant hydraulic conductance in *Ponderosa* pine. *Plant Cell Environ.* 24: 113–121
- IPCC (2013)** Climate change 2013: The physical science basis. Contribution of working group I to the fifth assessment report of the intergovernmental panel on climate change. Cambridge University Press, Cambridge, New York
- Jiang HX, Tang N, Zheng JG, Chen LS** (2009) Antagonistic actions of boron against inhibitory effects of aluminum toxicity on growth, CO₂ assimilation, ribulose-1,5-bisphosphate carboxylase/oxygenase and photosynthetic electron transport probed by the JIP-test, of *Citrus grandis* seedlings. *BMC Plant Biol.* 9: 102
- Kalaji HM, Govindjee, Bosa K, Kościelniak J, Żuk-Golaszewska K** (2011) Effects of salt stress on photosystem II efficiency and CO₂ assimilation of two Syrian barley landraces. *Environ. Exp. Bot.* 73: 64-72
- Kaldenhoff R, Ribas-Carbo M, Sans JF, Lovisolo C, Heckwolf M, Uehlein N** (2008) Aquaporins and plant water balance. *Plant Cell Environ.* 31: 658–666
- Karaba NN, Sheshshayee MS, Udaykumar M** (2008) *Biotech News: Options for improvement- mulberry*, Vol III, No 5
- Karacic A, Verwijst T, Weih M** (2003) Above-ground woody biomass production of short-rotation *Populus* plantations on agricultural land in Sweden. *Scandinavian J. Forest Res.* 18: 427–437
- Kitao M, Lei TT** (2007) Circumvention of over-excitation of PSII by maintaining electron transport rate in leaves of four cotton genotypes developed under long-term drought. *Plant Biol.* 9: 69-76.

- Kumar S, Chaitanya BSK, Ghatty S, Reddy AR** (2014) Growth, reproductive phenology and yield responses of a potential biofuel plant, *Jatropha curcas* grown under projected 2050 levels of elevated CO₂. *Physiol. Plant.* 152: 501-519
- Kumari S, Agrawal M, Tiwari S** (2013) Impact of elevated CO₂ and elevated O₃ on *Beta vulgaris* L.: pigments, metabolites, antioxidants, growth and yield. *Environ. Pollut.* 174: 279-288
- Lawlor DW, Tezara W** (2009) Causes of decreased photosynthetic rate and metabolic capacity in water deficient leaf cells: a critical evaluation of mechanisms and integration of processes. *Ann. Bot.* 103:561–79
- Lemus R, Lal R** (2005) Bioenergy crops and carbon sequestration. *Crit. Rev. in Plant sci.* 24: 1-21
- Lewis JD, Smith RA, Ghannoum O, Logan BA, Phillips NG, Tissue DT** (2013) Industrial-age changes in atmospheric [CO₂] and temperature differentially alter responses of faster-and slower-growing eucalyptus seedlings to short-term drought. *Tree Physiol.* 33: 475–488
- Li QM, Liu BB, Wu Y, Zou ZR** (2008) Interactive effects of drought stresses and elevated CO₂ concentration on photochemistry efficiency of cucumber seedlings. *J. Integr. Plant Biol.* 10:1307-1317
- Li X, Ahammed G, Zhang Y, Zhang G, Sun Z, Zhou J, Zhou Y, Xia X, Yu J, Shi K** (2014) Carbon dioxide enrichment alleviates heat stress by improving cellular redox homeostasis through an ABA-independent process in tomato plants. *Plant Biol.* 17:81-89
- Liberloo M, Calfapietra C, Lukac M, Godbold DL, Luo ZB, Polle A, Hoosbeek MR, Ceulemans R** (2006) Woody biomass production during the second rotation of a bio-energy *Populus* plantations increases in a future high CO₂ world. *Glob. Change Biol.* 12: 1094-1106
- Liberloo M, Tulva I, Raim O, Kull O, Ceulemans R** (2007) Photosynthetic stimulation under long –term CO₂ enrichment and fertilization is sustained across a closed populus canopy profile (EUROFACE). *New Phytol.* 173: 537-549
- Liberloo M, Lukac M, Calfapietra C, Hoosbeek MR, Gielen B, Miglietta F, Scarascia-Mugnozza GE, Ceulemans R** (2009) Coppicing shifts CO₂ stimulation of poplar productivity to above-ground pools: a synthesis of leaf to stand level results from the POP/EUROFACE experiment. *New Phytol.* 182: 331–346

- Lin ZH, Chen LS, Chen RB, Zhang FZ, Jiang HX, Tang N** (2009) CO₂ assimilation, ribulose-1,5-bisphosphate carboxylase/oxygenase, carbohydrates and photosynthetic electron transport probed by the JIP-test, of tea leaves in response to phosphorus supply. *BMC Plant Biol.* 9: 43
- Liu N, Dang QL, William H, Parker WH** (2006) Genetic variation of *Populus tremuloides* in ecophysiological responses to CO₂ elevation. *Can. J. Bot.* 84: 294-302
- Livak KJ, Schmittgen TD** (2001) Analysis of relative gene expression data using real-time quantitative PCR and the $2^{-\Delta\Delta C_T}$ method. *Methods* 25: 402-408
- Long SP, Ainsworth EA, Rogers A, Ort DR** (2004) Rising atmospheric carbon dioxide: plants face the future. *Ann. Rev. of Plant Biol.* 55: 591–628
- Long SP, Bernacchi CJ** (2003) Gas exchange measurements, what can they tell us about the underlying limitations to photosynthesis? Procedures and sources of error. *J. Exp. Bot.* 54: 2393-2401
- Lu C, Zhang J** (1999) Effects of water stress on photosystem II photochemistry and its thermostability in wheat plants. *J. Exp. Bot.* 50: 1199-1206
- Lu L, Tang Y, Xie J, Yuan Y** (2009) The role of marginal agricultural land-based mulberry planting in biomass energy production. *Renew. Energ.* 34: 1789–1794
- Machii H, Koyama A, Yamanouchi H** (2000) Mulberry breeding, cultivation and utilization in Japan. In: *Mulberry for Animal Production. FAO Electronic Conference*, Feed Resources Group (AGAP), FAO, Rome, Italy
- Martinez-Ballesta MDC, Carvajal M** (2014) New challenges in plant aquaporin biotechnology. *Plant Sci.* 217: 71-77.
- Martorell S, Espejo AD, Medrano H, Ball MC, Choat B** (2014) Rapid hydraulic recovery in *Eucalyptus pauciflora* after drought, linkage between stem hydraulics and leaf gas exchange. *Plant Cell Environ.* 37: 617-626
- Martre P, Morillon R, Barrieu F, North GB, Nobel PS, Chrispeels MJ** (2002) Plasma membrane aquaporins play a significant role during recovery from water deficit. *Plant Physiol.* 130: 2101-2110
- Matsumoto T, Lian HL, Su WA, Tanaka D, Liu CW, Iwasaki I, Kitagawa Y** (2009) Role of the aquaporin PIP1 subfamily in the chilling tolerance of rice. *Plant Cell Physiol.* 50: 216–229

- Maxwell K, Johnson GN** (2000) Chlorophyll fluorescence—a practical guide. *J Exp Bot.* 51: 659-668
- Medrano H, Escalona JM, Bota J, Gulias J, Flexas J** (2002) Regulation of photosynthesis of C3 plants in response to progressive drought, stomatal conductance as a reference parameter. *Ann. Bot.* 89: 895-905
- Mehta P, Jajoo A, Mathur S, Bharti S** (2009) Chlorophyll a fluorescence study revealing effects of high salt stress on Photosystem II in wheat leaves. *Plant physiol. Biochem.* 48: 16–20
- Mishra AK, Agrawal SB** (2014) Cultivar specific response of CO₂ fertilization on two tropical mung bean (*Vignaradiata*L.) cultivars: ROS generation, antioxidant status, physiology, growth, yield and seed quality. *J. Agron. Crop Sci.* 20: 273-289
- Mitchell CP, Stevens EA, Watters MP** (1999) Short rotation forestry – operations, productivity and costs based on experience gained in the UK. *Forest Eco Manag.* 121: 123–136
- Murshed R, Lopez-Lauri F, Sallanon H** (2008) Micro plate quantification of enzymes of the plant ascorbate-glutathione cycle. *Anal. Biochem.* 383:320-322
- Nardini A, Salleo S, Raimondo F** (2003) Changes in leaf hydraulic conductance correlate with leaf vein embolism in *Cercis siliquastrum* L. *Trees* 17: 529–534
- NASA.** (2014). Global Climate Change: Vital Signs of the Planet. Available at: <http://climate.nasa.gov/400ppmquotes> [accessed December 4, 2014].
- Naudts K, Van Den Berge J, Farfan E, Rose P, AbdElgawad H, Ceulemans, Janssens IA, Asard H, Nijs I** (2014) Future climate alleviates stress impact on grassland productivity through altered antioxidant capacity. *Environ. Exp. Bot.* 99: 150–158
- Nolf M, Creek D, Duursma R, Holtum J, Mayr S, Choat B** (2015) Stem and leaf hydraulic properties are finely coordinated in three tropical rain forests tree species. *Plant Cell Environ.* 38: 2652–2661
- Nowak RS, Ellsworth ES, Smith SD** (2004) Functional responses of plants to elevated atmospheric CO₂: do photosynthetic and productivity data from FACE experiments support early predictions? *New Phytol.* 162: 253–280
- Olaetxea M, Mora V, Bacaicoa E, Garnica M, Fuentes M, Casanova E, Zamarreno AM, Iriarte JC, Etayo D, Ederra I, Gonzalo R, Baigorri R, Garcia-Mina JM** (2015)

- Abscissic acid regulation of root hydraulic conductivity and aquaporin gene expression is crucial to the plant shoot growth enhancement caused by rhizospherehumic acids. *Plant Physiol.* 169: 2587-96
- Omaye ST, Turnbull JD, Sauberilich HE** (1979) Selected methods for the determination of ascorbic acid in animal cells, tissues and fluids. *Methods Enzym.* 62: 3-11
- Onoda Y, Hirose T, Hikosaka K** (2009) Does leaf photosynthesis adapt to CO₂-enriched environments? An experiment on plants originating from three natural CO₂ springs. *New Phytol.* 182: 698-709
- Papanastasis VP, Yiakoulaki MD, Decandia M, Dini-Papanastasi O** (2008) Integrating woody species into livestock feeding in the Mediterranean areas of Europe. *Anim Feed Sci. Tech.* 140: 1–17
- Parent B, Hachez C, Redondo E, Simonneau T, Chaumont F, Tardieu F** (2009) Drought and abscissic acid effects on aquaporin content translate into changes in hydraulic conductivity and leaf growth rate: a trans-scale approach. *Plant Physiol.* 149: 2000–2012
- Postarie O, Tournaire-Roux C, Grondin A, Boursiac Y, Morillon R, Schaffner AR, Maurel C** (2010) A PIP1 aquaporin contributes to hydrostatic pressure-induced water transport in both the root and rosette of *Arabidopsis*. *Plant Physiol.* 152:1418–1430
- Pou A, Medrano H, Flexas J, Tyerman SD** (2013) A putative role for TIP and PIP aquaporins in dynamics of leaf hydraulic and stomatal conductance in grapevine under water stress and re-watering. *Plant, Cell Environ.* 36: 828–843
- Prentice IC, Farquhar GD, Fasham MJR, Goulden ML, Heimann M, Jaramillo VJ, Kheshgi HS, LeQuere C, Scholes RJ, Wallace DWR, et al.** (2001) The carbon cycle atmospheric carbon dioxide. In: Houghton JT, Ding Y, Griggs DJ, Noguer M, Van der Linder PJ, Dai X, Maskell K, Johnson CA, eds. *Climate Change 2001: The scientific Basis. Contribution of working group I to the Third assessment report of the Intergovernmental Panel on Climate Change.* Newyork: Cambridge University Press
- Quirk J, McDowell NG, Leake JR, Hudson PJ, Beerling DJ** (2013) Increased susceptibility to drought-induced mortality in *Sequoia sempervirens* (cupressaceae) trees under cenozoic atmospheric carbon dioxide starvation. *Am. J. Bot.* 100: 582-591
- Ramanjulu S, Sreenivasalu N, Giridhara Kumar S, Sudhakar C** (1998) Photosynthetic characteristics in mulberry during water stress and re-watering. *Photosynthetica* 35: 259-263

- Rasineni GK, Guha A, Reddy AR** (2011) Elevated atmospheric CO₂ mitigated photoinhibition in a tropical tree species, *Gmelina arborea*. J. Photoch. Photobiol. B: Biol. 103: 159-165
- Rasineni GK, Guha A, Reddy AR** (2011) Responses of *Gmelina arborea*, a tropical deciduous tree species, to elevated atmospheric CO₂: Growth, biomass productivity and carbon sequestration efficacy. Plant Sci. 181: 428–438
- Reddy AR, Chaitanya KV, Vivekanandan M** (2004) Drought induced responses of photosynthesis and antioxidant metabolism in higher plants. J. Plant Physiol. 161: 1189–1202
- Reddy AR, Rasineni GK, Ragavendra AS** (2010) The impact of global elevated CO₂ concentration on photosynthesis and plant productivity. Current Sci. 99: 46-57
- Redillas MCFR, Strasser RJ, Jeong JS, Kim YS, Kim J-K.** 2011. The use of JIP test to evaluate drought-tolerance of transgenic rice overexpressing *OsNAC10*. Plant Biotech. Report 5: 169-175
- References:**
- Rey A, Jarvis PG** (1998) Long-term photosynthetic acclimation to increased atmospheric CO₂ concentration in young birch (*Betula pendula*) trees. Tree Physiol. 18: 441–450
- Sala A, Piper F, Hoch G** (2010) Physiological mechanisms of drought induced tree mortality are far from being resolved. New Phytol. 186: 274-281
- Salazar-Parra C, Aguirreolea J, Sánchez-Díaz M, JoséIrigoyen J, Morales F** (2012) Climate change (elevated CO₂, elevated temperature and moderate drought) triggers the antioxidant enzymes response of grapevine cv. Tempranillo, avoiding oxidative damage. Physiol. Plant. 144: 99-110
- Sekhar KM, Rachapudi VS, Mudulkar S, Reddy AR** (2014) Persistent stimulation of photosynthesis in short rotation coppice mulberry under elevated CO₂ atmosphere. J. Photochem. Photobiol. B: Biol. 137: 21–30
- Sekhar KM, Rachapudi VS, Reddy AR** (2015) Differential responses in photosynthesis, growth and biomass yields in two mulberry genotypes grown under elevated CO₂ atmosphere. J. Photochem. Photobiol. B: Biol. 151: 172-179

- Sengupta D, Guha A, Reddy AR** (2013) Interdependence of plant water status with photosynthetic performance and root defence responses in *Vigna radiate* (L.) Wilczek under progressive drought stress and recovery. *J. Photochem. Photobiol. B: Biol.* 127: 170-181
- Sengupta S, Majumder AL** (2014) Physiological and genomic basis of mechanical-functional trade-off in plant vasculature. *Front. Plant Sci.* 5:224.
- Sharkey TD, Bernacchi CJ, Farquhar GD, Singsaas EL** (2007) Fitting photosynthetic carbon dioxide response curves for C3 leaves. *Plant Cell Environ.* 30: 1035–1040
- Sholtis JD, Gunderson CA, Norby RJ, Tissue DT** (2004) Persistent stimulation of photosynthesis by elevated CO₂ in a sweetgum (*Liquidambar styraciflua*) forest stand. *New Phytol.* 162: 343-354
- Smirnoff N, Wheeler GL** (2000) Ascorbic acid in plants: biosynthesis and function. *Cr Rev Plant Sci.* 19: 267–290
- Solomon S, Qin D, Manning RB et al.,** (2007) Technical summary. In: Solomon S, Qin D, Manning M, Chen Z, Marquis M, Averyt KB, Tignor M, Miller HL, eds. *Climate Change 2007: The physical Science Basis. Contribution of working group I to the Fourth annual assessment report of the Intergovernmental Panel on Climate Change.* Newyork: Cambridge University Press
- Sperry JS, Pockman WT** (1993) Limitation of transpiration by hydraulic conductance and xylem cavitation in *Betula occidentalis*. *Plant Cell Environ* 16:279–287
- Sreeharsha RV, Sekhar KM, Reddy AR** (2015) Delayed flowering is associated with lack of photosynthetic acclimation in Pigeon pea (*Cajanuscajan* L.) grown under elevated CO₂. *Plant Sci.* 231:82–93
- Stankovic MS** (2011) Total phenolic content, flavonoid concentration and Antioxidant activity of *Marrubium peregrinum* L. extracts. *Kragujevac J. Sci.* 33: 63-72
- Strasser RJ** (1997) Donor side capacity of Photosystem II probed by chlorophyll a fluorescence transients. *Photosynth. Res.* 52: 147-155
- Strasser RJ, Srivastava A, Govindjee** (1995) Polyphasic chlorophyll-a fluorescence transient in plants and cyanobacteria. *J. Photoch. Photobiol. B: Biol.* 61: 32-42
- Streck C, Scholz SM** (2006) The role forest in global climate change: where we come and where we go. *International Affairs* 82: 861-879

- Suga S, Maeshima M** (2004) Water channel activity of radish plasma membrane aquaporins heterologously expressed in yeast and their modification by site directed mutagenesis. *Plant Cell Physiol.* 45: 823–830
- Teng N, Wang J, Chen T, Wu X, Wang Y, Lin J** (2006) Elevated CO₂ induces physiological, biochemical and structural changes in leaves of *Arabidopsis thaliana*. *New Phytol.* 172: 92–103
- Tezara W, Mitchell V, Driscoll SP, Lawlor DW** (2002) Effects of water deficit and its interaction with CO₂ supply on the biochemistry and physiology of photosynthesis in sunflower. *J Exp Bot.* 53:1781–91
- Tournaire-Roux C, Sutka M, Javot H, Gout E, Gerbeau P, Luu DT, Bligny R, Maurel C** (2003) Cytosolic pH regulates root water transport during anoxic stress through gating of aquaporins. *Nat.* 425: 393-397
- Urli M, Porte AJ, Cochard H, Guengant Y, Burlett R, Delzon S** (2013) Xylem embolism threshold for catastrophic hydraulic failure in angiosperm trees. *Tree Physiol.* 33: 672-683
- Van Heerden PDR, Swanepoel JW, Kruger GHJ** (2007) Modulation of photosynthesis by drought in two desert scrub species exhibiting C3- mode CO₂ assimilation. *Environ. Exp. Bot.* 61: 124–136
- Van Heerden PDR, Tsimilli-Michael M, Krüger GHJ, Strasser RJ** (2003) Dark chilling effects on soybean genotypes during vegetative development: Parallel studies of CO₂ assimilation, chlorophyll-a fluorescence kinetics O-J-I-P and nitrogen fixation, *Physiol. Plant.* 117: 476-491
- Wang LL, Chen PA, Zhong QN, Liu N, Wu MX, Wang F, et al.,** (2014) The *Thellungiella salina* tonoplast aquaporin *TsTIP1;2* functions in protection against multiple abiotic stresses. *Plant Cell Physiol.* 55: 148-161
- Wang P, Duan W, Takabayashi A, Endo T, Shikanai T, Ye JY, Mi H** (2006) Chloroplastic NAD(P)H dehydrogenase in tobacco leaves functions in alleviation of oxidative damage caused by temperature stress. *Plant Physiol.* 141: 465-474
- Wang W, Yang X, Zhang S, Sun Y** (2013) The root cortex cell hydraulic conductivity is enhanced with increasing chromosome ploidy in wheat. *Plant Physiol. Biochem.* 68: 37–43
- Warren JM, Norby RJ, Wullschleger SD** (2011) Elevated CO₂ Enhances leaf senescence during extreme drought in a temperate forest. *Tree Physiol.* 31: 117-130

- Watling JR, Press MC, Quick WP** (2000) Elevated CO₂ induces biochemical and ultra structural changes in leaves of C₄ cereal sorghum. *Plant Physiol.* 123: 1143–1152
- Weih M** (2004) Intensive short rotation forestry in boreal climates: present and future perspectives. *Can. J. Forest Res.* 34: 1369–1378
- Wullschleger S, Tschaplinski T, Norby R** (2002) Plant water relations at elevated CO₂ - implications for water-limited environments. *Plant Cell Environ.* 25: 319-331
- Xu Z, Jiang Y, Zhou G** (2015) Response and adaptation of photosynthesis, respiration, and antioxidant systems to elevated CO₂ with environmental stress in plants. *Front Plant Sci.* 6:701
- Xu ZZ, Shimizu H, Ito S, Yagasaki Y, Zou CJ, Zhou GS, Zheng YR** (2014) Effects of elevated CO₂, warming and precipitation change on plant growth, photosynthesis and peroxidation in dominant species from North China grassland. *Planta.* 239:421-435
- Zelazny JE, Borst JW, Muylaert M, Batoko H, Hemminga MA, Chaumont F** (2007) FRET imaging in living maize cells reveals that plasma membrane aquaporins interact to regulate their subcellular localization. *Proc. Natl. Acad. Sci. U. S. A* 104: 12359–12364
- Zhang DY, Chen GY, Gong ZY, Chen J, Yong ZH, Zhu JG, XU DQ** (2008) Ribulose-1,5-bisphosphate regeneration limitation in rice leaf photosynthetic acclimation to elevated CO₂. *Plant Sci.* 175: 348–355
- Zinta G, AbdElgawad H, Domagalska MA, Vergauwen L, Knapen D, Nijs I, Janssens IA, Beemster GT, Asard H** (2104) Physiological, biochemical, and genome wide transcriptional analysis reveals that elevated CO₂ mitigates the impact of combined heat wave and drought stress in *Arabidopsis thaliana* at multiple organizational levels. *Glob. Change Biol.* 20:3670–3685
- Zong YZ, Wang WF, Xue QW, Shangguan ZP** (2014) Interactive effects of elevated CO₂ and drought on photosynthetic capacity and PSII performance in maize. *Photosynthetica* 52: 63-70
- Zvereva EL, Kozlov MV** (2006) Consequences of simultaneous elevation of carbon dioxide and temperature for plant-herbivore interactions: a meta-analysis. *Glob. Change Biol.* 12: 27–41